

DYE DECOLOURIZATION BY IMMOBILIZED LACCASE AND
IMPACT OF AUXILIARY CHEMICALS ON DYE
DECOLOURIZATION

by

PAUL-PHILIPPE CHAMPAGNE

A thesis submitted to the
Department of Chemical Engineering
in conformity with the requirements for
the degree of Doctor of Philosophy

Queen's University
Kingston, Ontario, Canada

June 2009

Copyright © Paul-Philippe Champagne, 2009

Abstract

Textile dyes are molecules designed to impart a permanent colour to textile fabrics. They pose an environmental problem because they are toxic and they decrease the aesthetic value of rivers and lakes. Current technologies for dye removal cannot remove all classes of dyes and two or more technologies are usually combined to achieve satisfactory decolourization efficiencies. Lignin-degrading enzymes like laccases are potential technologies for dye decolourization and decolourization with immobilized laccase has been intensively investigated. The majority of those studies however have focused on dye disappearance and several reported that significant dye adsorption had occurred during the dye removal, making the role of the enzyme unclear. Moreover, textile wastewaters contain auxiliary chemicals that can impact enzymatic dye decolourization and very few studies have evaluated the impact of those substances on laccase. This research evaluated the feasibility of treating dye-contaminated textile wastewaters with an immobilized laccase system. The first sub-objective was to examine the decolourization of Reactive blue 19 (an anthraquinone dye) by *Trametes versicolor* laccase immobilized on controlled porosity carrier (CPC) silica beads and the second was to analyze the kinetic effects of a non-ionic surfactant Mergol, sodium sulfate, and sodium chloride on laccase decolourization of Reactive blue 19. Decolourization of Reactive blue 19 by immobilized laccase was mainly enzymatic although dye adsorption occurred. Decolourization led to less toxic by-products from azo and

indigoid dyes whereas increased toxicity was observed for anthraquinone dyes. The feasibility of immobilizing laccase on poly(methyl methacrylate) (PMMA) through its sugar residues with a simple procedure was demonstrated and the mass of enzyme immobilized compared well with other commercial acrylic supports. The decolorization of Reactive blue 19 by laccase was inhibited by the non-ionic surfactant, Merpol by substrate depletion. A model describing this inhibition was developed and was validated by a saturated equilibrium binding experiment. While sodium sulfate (ionic strength) had no effect on either ABTS oxidation or dye decolourization, sodium chloride inhibited laccase during dye decolourization and the type and nature of the inhibition depended on the substrate. With ABTS, the inhibition was hyperbolic non-competitive whereas it was parabolic mixed with Reactive blue 19.

Acknowledgements

I am expressing my deepest gratitude to my supervisor Dr. Juliana Ramsay since this research thesis would not have been possible without her guidance and support. Her perpetual enthusiasm in research has motivated me. I would like to express my special thanks to my advisor Dr. Michael Nesheim for his support, guidance, patience and invaluable advice. He has been a constant source of inspiration throughout my thesis. I am very grateful to Dr. Ronald Neufeld for being very generous with his time and advice to my research. I would also like to thank my colleagues Zhiyong, Jade, Bozhi and Eric for making the time I spent in Kingston memorable. I would like to also thank the Natural Sciences and Engineering Research Council of Canada (NSERC) and Ontario Premier's Research Excellence Award which have funded my research.

I would like to deeply thank my family, my mother Marie-Rose, my father Paul, my brothers Max and Marc-André for their unconditional love, support and encouragement. Last but certainly not least, I would like to express my most sincere thanks and gratitude to Nicole for her love, enthusiastic and energetic support throughout my research and the writing of this thesis.

Statement of originality

I hereby certify that all of the work described within this thesis is the original work of the author except for three experiments. The radio-iodination of laccase in chapter three was conducted by Mr. Paul Kim in Dr. Michael Nesheim's laboratory in the Department of Biochemistry at Queens. The Microtox assays in chapter five for the toxicity analysis of the dyes was conducted by Ms Denise Kuperschmid-Moy under my supervision. Finally, the specific area analysis of the porous silica and PMMA was determined at the Centre for Manufacturing of Advanced Ceramics and Nanomaterials at Queens.

Any published (or unpublished) ideas and/or techniques from the work of others are fully acknowledged in accordance with the standard referencing practices.

Paul-Philippe Champagne

June, 2009

Table of Contents

Abstract	i
Acknowledgements	iii
Statement of originality	iv
Table of Contents	v
List of Tables	x
List of Figures	xii
1 Introduction	1
2 Literature review	5
2.1 Classification of dyes	5
2.2 Current technologies for dye decolourization	8
2.3 Dye decolourization by white rot fungi	12
2.4 Dye decolourization in white rot fungal bioreactors	20
2.5 Dye decolourization by immobilized lignin-degrading enzymes	24
2.6 Objectives of research project	33
2.7 Enzyme kinetics fundamentals	35

Bibliography	52
---------------------	-----------

Chapter 3:

Rb19 decolourization by immobilized laccase	68
3.1 Abstract	68
3.2 Introduction	69
3.3 Materials and Methods	71
3.4 Results	76
3.5 Discussion	81
3.6 Conclusion	84
Bibliography	85

Chapter 4:

Dye decolourization and toxicity	89
4.1 Abstract	89
4.2 Introduction	90
4.3 Materials and methods	91
4.4 Results	94
4.5 Discussion	100
4.6 Conclusion	103
Bibliography	103

Chapter 5:

Immobilization of laccase on PMMA	107
5.1 Abstract	107

5.2	Introduction	108
5.3	Materials and methods	109
5.4	Results	113
5.5	Discussion	115
5.6	Conclusion	117
Bibliography		118
Chapter 6:		
Decolourization inhibition by substrate depletion		122
6.1	Abstract	122
6.2	Introduction	123
6.3	Materials and methods	125
6.4	Results	129
6.5	Discussion	140
Bibliography		142
Chapter 7:		
Effects of pH and salts on dye decolourization		145
7.1	Abstract	145
7.2	Introduction	146
7.3	Material and methods	147
7.4	Results	151
7.5	Discussion	159
7.6	Conclusions	165

Bibliography	166
Chapter 8:	
Conclusions	169
Chapter 9:	
Contributions	171
9.1 Decolourization of Reactive blue 19 by laccase immobilized on CPC-silica beads	171
9.2 Immobilization of laccase on PMMA	171
9.3 Effect of Merspol on the decolourization of Reactive blue 19 by laccase . . .	172
9.4 Effect of Sodium chloride and ionic strength on the decolourization of Re- active blue 19 by laccase	172
Chapter 10:	
Recommendations	174
10.1 To investigate the influence of the nature of the enzyme support on enzy- matic dye decolourization	174
10.2 Immobilization of laccase on porous PMMA beads	175
10.3 Characterize laccase kinetic in real textile wastewaters	175
10.4 Study the impacts of factors like salts and pH on the interaction of Merspol and Reactive blue 19	176
Appendix A:	
Statistical analysis of the dissociation constants	177

Appendix B:

Derivation of enzyme rate equations	179
B.1 Rate equation for the general mixed inhibition	179
B.2 Derivation of the rate equation for the parabolic mixed inhibition	181

Appendix C:

Calculation of reaction rates	184
C.1 Initial rates	184
C.2 Calculation of average reaction rates and of rate constants from the immobilized laccase reactor	184

List of Tables

2.1	Classification of Colourants	6
2.2	Dye decolourization in fungal bioreactors	21
2.3	Dye decolourization in fungal bioreactors	22
2.4	Dye decolourization with immobilized lignin-degrading enzymes	29
2.5	Dye decolourization with immobilized lignin-degrading enzymes	30
2.6	Dye decolourization with immobilized lignin-degrading enzymes	31
2.7	Dye decolourization with immobilized lignin-degrading enzymes	32
3.1	Comparison of Reactive blue 19 decolourization with active and inactive immobilized laccase	81
4.1	Dye structures and their maximum wavelength of absorption	95
4.2	Decolourization of dyes by free and immobilized laccase.	97
4.3	Toxicity of initial and decolourized dye solutions by free and immobilized laccase	99
5.1	Effect of temperature, pH and initial laccase concentration laccase immobilization on PMMA-hydrazide beads	115
5.2	Comparative table of masses immobilized laccase with commercial acrylic-based carriers	116

6.1	Effect of Merspol on ABTS oxidation and the decolourization of Reactive blue 19 by laccase	139
7.1	The effect of pH on the oxidation kinetics of ABTS	151
7.2	The effect of pH on the oxidation kinetics of Reactive blue 19	152
7.3	Estimation of the kinetic paramaters from the proposed models for the oxidation of ABTS and for the decolourization of Reactive blue 19	162

List of Figures

2.1	Acid red 27 (Amaranth)	7
2.2	Reactive blue 19 (Remazol Brilliant Blue R)	8
2.3	Acid blue 74 (Indigo carmine)	8
2.4	Catalytic cycle of lignin-peroxidase	14
2.5	Catalytic cycle of Mn(II)-peroxidase	15
2.6	Catalytic cycle of laccase	17
2.7	Lineweaver-Burk and Eadie Hofstee plots	45
2.8	Mixed type enzyme inhibition	46
2.9	Lineweaver-Burk plots of the competitive, non-competitive and uncompetitive inhibitions	48
2.10	General partial mixed inhibition (hyperbolic)	50
2.11	Replots of Lineweaver-Burk slopes or intercepts for the detection of non-linear inhibition	53
2.12	Inhibition with 2 inhibitor binding sites affecting the binding of the substrate	54
3.1	Chemical structure of Reactive blue 19	70
3.2	Schematic of Immobilized laccase setup	74
3.3	Decolourization of Reactive blue 19 by laccase immobilized on CPC-silica beads	77

3.4	Decolourization of Reactive blue 19 in a packed bed by immobilized laccase after 4 months of storage	78
3.5	Effect of laccase immobilization on the pH profile of ABTS oxidation and the decolourization of Reactive blue 19	79
3.6	Effect of ethanolamine pretreatment on Reactive blue 19 adsorption on laccase immobilized on CPC-silica particles	80
5.1	Effect of initial laccase concentration on its mass immobilized on PMMA-hydrazide pellets.	114
6.1	Structure of Reactive blue 19 and ABTS	126
6.2	Effect of Merspol on the rate of ABTS oxidation and Reactive blue 19 decolourization by laccase	130
6.3	Effect of Merspol on ABTS oxidation by laccase	131
6.4	Spectrophotometric analysis of ABTS, Reactive blue 19, with and without Merspol	133
6.5	Saturation equilibrium of Reactive blue 19 and Merspol binding	134
6.6	Inhibition of laccase decolourization of Reactive blue 19 by Merspol	136
6.7	Kinetic scheme for the inhibition of dye decolourization by substrate depletion	137
7.1	The effect of pH on the oxidation kinetics of ABTS and on the decolourization of Reactive blue 19	153
7.2	Effect of ionic strength on the oxidation of ABTS and Reactive blue 19	154
7.3	Effect of sodium chloride on the oxidation of ABTS and Reactive blue 19 by laccase	155

7.4	Non-linear dependence of slopes from the Lineweaver-Burk plots for ABTS and Reactive blue 19	156
7.5	Proposed scheme hyperbolic inhibition of laccase for the oxidation of ABTS	157
7.6	Proposed scheme for parabolic inhibition of laccase for the decolourization of Reactive blue 19	158
7.7	Hyperbolic inhibition model fitting for the ABTS oxidation	160
7.8	Parabolic inhibition model fitting for the decolourization of Reactive blue 19	161
B.1	General partial mixed inhibition (hyperbolic)	180
B.2	Parabolic two-site mixed inhibition	182
C.1	Progress curve:Decolourization of Reactive blue 19 by laccase monitored at 592.	185
C.2	Concentration profile of Reactive blue 19 decolourization by immobilized laccase.	185
C.3	Table of measured concentrations, calculated 1-reactor volume removal efficiency in (%) with time	186

Chapter 1

Introduction

Textiles dyes are poly-aromatic molecules that give a permanent color to materials like textile fabrics (Vandevivere *et al.*, 1998; of public works and government services Canada, 2001). Approximately 50,000 tons of dyes per year is lost to the environment worldwide (Lewis, 1999) and Canada releases 500 tons per year mainly in the St-Lawrence River (Maguire, 1992). Dyes can create an environmental problem since they resist biodegradation, and several of them and/or their degradation products are toxic (Moawad *et al.*, 2003). Environmental regulatory agencies in several countries are adopting stringent regulations for the discharge of coloured effluents from textile and dyestuff manufacturers. The cities of Kingston and Toronto (Ontario, Canada) modified their municipal by-laws in 2000 to prohibit the discharge of coloured effluents to the municipal sewage (City of Kingston, 2000; City of Toronto, 2000).

Textile wastewaters must be treated since residual dyes are toxic. Studies have shown that several dyes, in particular azo dyes, are mutagenic as parent molecules or when they are metabolized (Moawad *et al.*, 2003; Bakshi and Sharma, 2003). As a result, the use of certain azo dyes in Germany in consumer goods was banned in 1996 (Reid, 1996;

ETAD, 1996). Auxiliary chemicals such as solvents, detergents, dispersants and wetting agents that are used to aid in the dyeing process add to the treatment complexity of textile wastewaters (Wang *et al.*, 2002). Substances like soaps and dispersants often disrupt nitrogen removal by nitrifying bacteria in activated sludge processes (Bohm, 1994; Vandevivere *et al.*, 1998). Although manufacturers have made considerable efforts to improve dye fixation, the reduction achieved in residual dye concentration in waste effluents has not been sufficient (Pierce, 1994). The widespread and increasing use of reactive dyes constitutes a major part of the problem because these water-soluble dyes pass through the activated sludge process untreated and are discharged into rivers (Pierce, 1994; Vandevivere *et al.*, 1998). The discharge of textile dyes into rivers or lakes is the most visible sign of water pollution since several are visible at a low concentration of 0.005 ppm (mg/l) (O'Neill *et al.*, 1999).

No single conventional technology can remove all types of dyes because their molecular structure and chemical properties vary widely and may be complex. Current technologies such as coagulation, ozonation and activated carbon can efficiently remove only restricted classes of dyes (Dubrow *et al.*, 1996; Hassan and Hawkyard, 2002; Matsui, 1996). Dyes adsorb to membrane of cells in conventional activated sludge and are poorly degraded. This creates large volumes of sludge, and complicates subsequent disposal operations (Dubrow *et al.*, 1996; Robinson *et al.*, 2001). A combination of physical, chemical and biological processes is most efficient for dye decolourization but can be expensive (Hai *et al.*, 2007; Robinson *et al.*, 2001). Therefore, a more efficient and cost-effective treatment is needed.

White rot fungi degrade lignin, a resistant bio-polymer, with their extracellular lignin-degrading enzymes (LDEs), lignin peroxidase (LiP), Manganese dependent peroxidase (MnP) and laccase (phenol oxidase), when nutrient limitation triggers a secondary metabolic phase

(Cameron *et al.*, 2000; Leonowicz *et al.*, 2001; Pointing, 2001). They degrade also a wide range of persistent organic pollutants including textile dyes (Spadaro and Renganathan, 1994; Wong and Yu, 1999; Heinfling *et al.*, 1998; Reyes *et al.*, 1999; Nyanhongo *et al.*, 2002; Champagne and Ramsay, 2005). Fungal reactors have been developed for dye decolourization (Schliephake *et al.*, 1993; Yang and Yu, 1996a,b). The challenge in designing such reactors for wastewater treatment is maintaining an adequate enzyme concentration for high dye decolourization efficiencies; lignin-degrading enzymes are not continuously secreted during the secondary phase and are digested by extracellular proteases as part of the nitrogen turnover of fungi (Dosoretz *et al.*, 1990; Staszczak *et al.*, 2000). In addition, fungi in reactors entangle with the impeller, increase the medium viscosity, and consequently impede oxygen transfer because of their excessive growth and adhesion to surfaces (Zhang *et al.*, 1999; Moreira *et al.*, 2003). Using immobilized enzymes to maintain an adequate enzyme concentration in a reactor is more easily achieved than controlling fungal growth and avoids the increase of medium viscosity and the need of nutrient addition.

This research project aims at investigating dye decolourization by immobilized laccase and to analyze the impacts of auxiliary chemicals (textile wastewater components) like surfactants and salts on enzymatic dye decolourization.

In chapter two, an overview of the the current technologies for dye removal will be introduced. Dye decolourization by white rot fungi and their enzymes will be reviewed. This chapter will be concluded by a review of enzyme kinetics fundamentals so that the reader has the tools necessary to understand the logic behind the models developed in chapter 6 and 7 and how they were derived.

The goal of chapter three was to characterize the decolourization of Reactive blue 19, a model anthraquinone dye, by *Trametes versicolor* laccase immobilized on porous silica

beads and quantify the contribution of dye adsorption to dye decolourization. In chapter four, the application of immobilized laccase in decolourization was broadened to other textile dyes and their toxicity before and after enzyme treatment was evaluated. The fifth chapter focused on the feasibility of immobilizing of laccase on poly(methyl methacrylate) (PMMA).

Finally, chapter six and seven focus on the impact of auxiliary chemicals on dye decolourization. In Chapter six, the effects of the non-ionic surfactant Merpol on the kinetics of Reactive blue 19 decolourization was analyzed by steady-state kinetic analysis and a model was accordingly developed. In the final chapter, the effects of pH, sodium sulfate and sodium chloride on the kinetics of the oxidation of ABTS and on the decolourization of Reactive blue 19 by laccase was analyzed and models were also developed. The conclusions, contributions, and recommendations will be presented in chapter eight, nine, and ten respectively.

Chapter 2

Literature review

2.1 Classification of dyes

Dye classification is published in the Colour Index (C.I.) (Christie, 2001; Waring and Hallas, 1990). The C.I. name of a dye indicates how it is applied to material, its hue (colour), and its number specifies the chronological order of its commercial introduction (Christie, 2001). The CI classification is shown in Table 2.1 (O'Neill *et al.*, 1999). The most common chemical classes include the azo (-N=N-) and carbonyl (C=O) (including anthraquinones).

2.1.1 Azo dyes

Azo dyes like Acid red 27 (Figure 2.1) are the most important class of dyes and constitute approximately 50 % of commercial dyes and 60 to 70 % of dyes used in traditional textile applications. They are characterized by their azo bond(s) (-N=N-) which is generally attached to 2 aromatic radicals. The aromatic ring and the azo bond form the chromogen (Christie, 2001; Waring and Hallas, 1990). Azo dyes as colourants can provide a complete

Table 2.1: Classification of Colourants

Table 2. Application classes of dyes and their chemical type (after Kirk-Othmer,¹¹ copyright© John Wiley & Sons Inc, 1993, reprinted by permission of John Wiley & Sons Inc)

<i>Class</i>	<i>Substrates</i>	<i>Method of application</i>	<i>Chemical types</i>
Acid	Nylon, wool, silk, paper, inks, and leather	Usually from neutral to acidic dyebaths	Azo including premetallised anthraquinone, triphenylmethane, azine, xanthene, nitro, and nitroso
Azoic components and compositions	Cotton, rayon, ^a cellulose acetate, ^b and polyester ^b	Fibre impregnated with coupling component and treated with a solution of stabilised diazonium salt	Azo
Basic	Paper, polyacrylonitrile-modified nylon, ^c polyester, and inks	Applied from acidic dyebaths	Diazacarbocyanine, cyanine, hemicyanine, diazahemicyanine, diphenylmethane, triarylmethane, azo, azine, xanthene, acridine, oxazine, and anthraquinone
Direct	Cotton, rayon, ^a paper, leather, and nylon	Applied from neutral or slightly alkaline baths containing additional electrolyte	Azo, phthalocyanine, stilbene, and oxazine
Disperse	Polyester, polyamide, acetate, acrylic, and plastics	Fine aqueous dispersions often applied by high temperature-pressure or lower temperature carrier methods; dye may be padded on cloth and baked on or thermofixed	Azo, anthraquinone, styryl, nitro, and benzodifuranone
Fluorescent brighteners	Soaps and detergents, all fibres, oils, paints, and plastics	From solution, dispersion, or suspension in a mass	Stilbene, pyrazoles, coumarin, and naphthalimides
Food, drug and cosmetic	Foods, drugs, and cosmetics		Azo, anthraquinone, carotenoid, and triarylmethane
Mordant	Wool, leather, and anodised aluminium	Applied in conjunction with chelating Cr salts	Azo and anthraquinone
Natural	Food	Applied as mordant, vat, solvent, or direct and acid dyes	Anthraquinone, flavonols, flavones, indigoids, chroman
Oxidation bases	Hair, fur, and cotton	Aromatic amines and phenols oxidised on the substrate	Aniline black and indeterminate structures
Pigments	Paints, inks, plastics, and textiles	Printing on the fibre with resin binder or dispersion in the mass	Azo, basic, phthalocyanine, quinacridone, and indigoid
Reactive	Cotton, wool, silk, and nylon	Reactive site on dye reacts with functional group on fibre to bind dye covalently under influence of heat and pH (alkaline)	Azo, anthraquinone, phthalocyanine, formazan, oxazine, and basic
Solvent	Plastics, gasoline, varnish, lacquer, stains, inks, fats, oils, and waxes	Dissolution in the substrate	Azo, triphenylmethane, anthraquinone, and phthalocyanine
Sulfur	Cotton and rayon ^a	Aromatic substrate vatted with sodium sulfide and re-oxidised to insoluble sulfur-containing products on fibre	Indeterminate structures
Vat	Cotton, rayon, ^a and wool	Water-insoluble dyes solubilised by reducing with sodium hydrosulfite, then exhausted on fibre and re-oxidised	Anthraquinone (including polycyclic quinones), and indigoids

^a Rayon now referred to as viscose.

^b Azoics no longer used on polyester and cellulose acetate.

^c Should read basic-dyeable nylon.

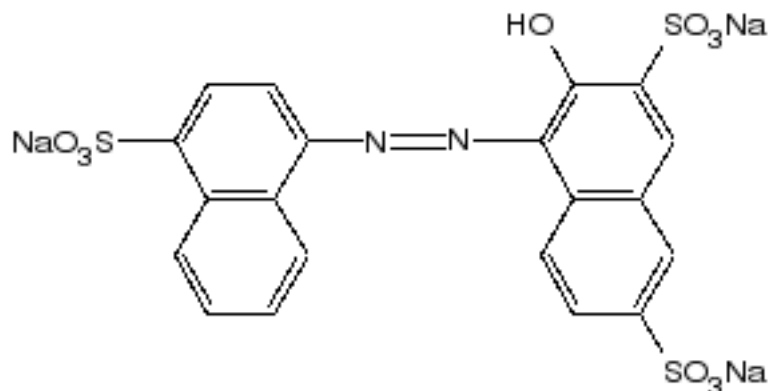


Figure 2.1: Acid red 27 (Amaranth)

range of hues. However, they are more important commercially in the yellow, orange and red colours (Christie, 2001).

2.1.2 Anthraquinone dyes

The anthraquinone dyes form the most important subclass of the carbonyl dyes. The basic structure of anthraquinone dye includes three membered rings where two carbonyl groups are located on the middle ring (quinone moiety) (Figure 2.1.2), and the two outer rings aromatic. Anthraquinones can provide the entire range of hues but are more used for their violet, blue and green shades (Christie, 2001).

2.1.3 Ingoid dyes

The first indigoïd dyes were produced from the plant *Indigofera tinctoria* by Chinese, Indians and Indonesians through a fermentation process. These dyes form the oldest class of naturally derived dyes. They are recognized for the wide variety of bright blue shades.

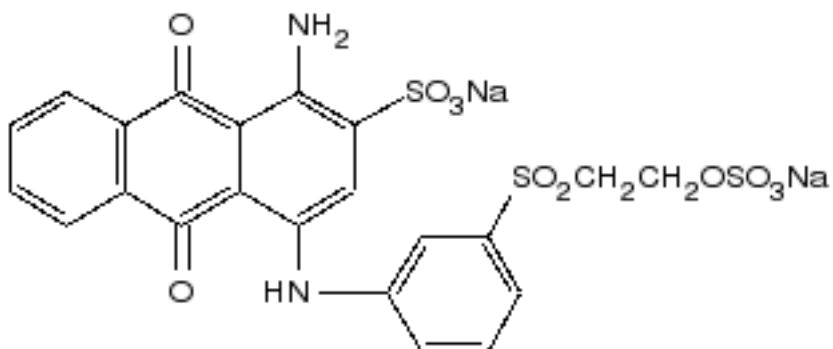


Figure 2.2: Reactive blue 19 (Remazol Brilliant Blue R)

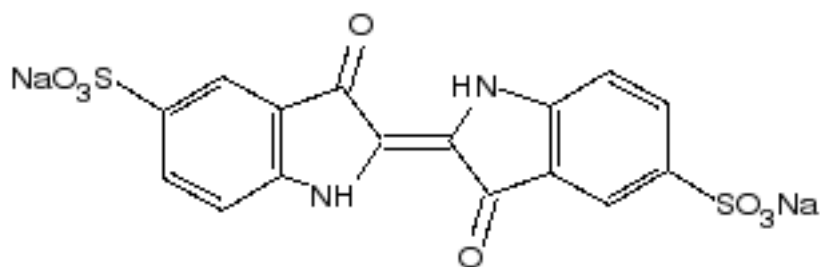


Figure 2.3: Acid blue 74 (Indigo carmine)

Nowadays, they are synthesized and used to dye denim jeans and jackets. Acid blue 74 or indigo carmine (Figure 2.1.3) is a common dye of this class (Christie, 2001).

2.2 Current technologies for dye decolourization

There is currently no single technology that can decolorize all types of dyes (Talarposhti *et al.*, 2001). Dye decolourization can occur chemically, physically or biologically. Dyes can be physically removed by adsorption onto activated carbon for example where no molecular degradation occurs. In dye degradation, the chromophore (the portion of the

molecule responsible for color) has been modified through chemical reactions. Biological decolourization can occur through sorption to cellular membrane or by biochemical degradation from biocatalysts. In this thesis, dye decolourization means dye degradation.

2.2.1 Activated carbon

Activated carbon is used to remove mainly acidic dyes but not reactive dyes (Reife and Freeman, 1996; Robinson *et al.*, 2001). High removal efficiencies are not reproducible if the sorbent is reused and/or the wastewater characteristics change (Robinson *et al.*, 2001). Although a growing number of reports on the development of low cost activated carbon are being published (Kim *et al.*, 2008; Hameed *et al.*, 2008; Nunes *et al.*, 2009), it is mostly used for effluents with low dye concentrations or is used as a polishing step (Reife and Freeman, 1996).

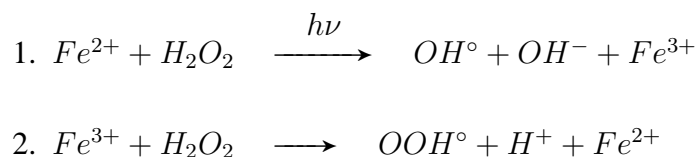
2.2.2 Flocculation and electro-coagulation

In flocculation, colloids and/or particulates agglomerate as their electrostatic charges are neutralized by flocculants (e.g., lime, alum, ferric salts or poly-electrolytes). In electro-coagulation, an electrical current generates flocculants from the anode (Dubrow *et al.*, 1996; Robinson *et al.*, 2001). These processes have been used to remove dyes and pigment aggregates from textile wastewaters (Essadki *et al.*, 2008; Zidane *et al.*, 2008). The density of an aggregate can be controlled to enhance its settling or flotation (Kang, 2007). The optimal concentration of flocculant depends on the static charge of the dye molecule (Robinson *et al.*, 2001) and must be determined for each dye for efficient removal. However, these technologies tend to produce large volumes of sludge (suspended solids) and

therefore require adequate space and capacity for disposal (Dubrow *et al.*, 1996; Robinson *et al.*, 2001).

2.2.3 Fenton's reagent

Fenton's reagent combines hydrogen peroxide, H_2O_2 , and ferrous iron (Fe^{2+}) in solution and can decolorize a variety of dyes (Sun *et al.*, 2009; Ay *et al.*, 2009; Alshamsi *et al.*, 2007). The reaction occurs through the following mechanism,



and hydroxyl and peroxy radicals generated can oxidize the dye. Fenton's reagent is adequate for toxic wastewaters that inhibit growth of the microbial consortium in the sludge. However, the large volume of suspended solids that is generally produced through flocculation requires space and capacity (Robinson *et al.*, 2001; Vandevivere *et al.*, 1998; Slokar and Majcen Le Marechal, 1998).

2.2.4 Ozonation

Several studies reported the successful decolourization of dye solution by ozonation (Khadhraoui *et al.*, 2009; Wu *et al.*, 2008). Ozone is a strong oxidizing agent compared to chlorine and hydrogen peroxide and can degrade a wide range of dyes. Ozonation is mostly used in the later stage of the treatment process since it is less efficient in treating high-strength raw textile wastewaters (Lu *et al.*, 2009) which need additional treatment to achieve an acceptable level of decolourization. The half-life of the ozonide radical (O_3^-) ranges from seconds to

hours depending on the quality of the water and is generally decreased by organics compounds present in the wastewater (von Gunten, 2007). Conditions such as pH must be tightly controlled because hydroxide anions catalyze the decomposition of ozone (Hoigné, 1998). This technology is however applied to effluents with high dye concentrations only because the capital costs to setup an ozonation facility are substantially higher than other technologies (Robinson *et al.*, 2001; Vandevivere *et al.*, 1998).

2.2.5 Activated sludge dye decolourization

Treatment of textile effluents by activated sludge has been achieved almost exclusively under anaerobic conditions especially for azo dyes (Knapp and Newby, 1995; Bromley-Challenor *et al.*, 2000). The toxicity of auxiliary chemicals and dyes to the activated sludge also renders textile wastewater treatment difficult (Talarposhti *et al.*, 2001). Conventional activated sludge can remove basic and direct dyes mainly through adsorption to the cellular membrane and shown to be effective (Chu and Chen, 2002; Shaul *et al.*, 1991). It is inefficient for effluents containing large quantities of reactive and acid dyes diluted with domestic sewage (Vandevivere *et al.*, 1998; Willmott *et al.*, 1998). A small minority of bacterial species can aerobically decolorize a restricted number of dyes. A few species of actinomycetes were shown to efficiently decolorize and mineralize textile dyes (Ball *et al.*, 1989; Zhou and Zimmermann, 1993). Extra-cellular peroxidases produced by the bacteria were shown to mediate decolourization (Paszczynski *et al.*, 1992) and the degradation pathway was determined (Goszczynski *et al.*, 1994).

2.2.6 Anaerobic dye decolourization

Several bacterial species can decolorize azo dyes under anaerobic conditions. Complete mineralization of azo dyes, Disperse blue 79 and Acid orange 10, by *Bacillus fusiformis* from a dye-contaminated soil (Kolekar *et al.*, 2008) and by a bacterial consortium (Barragán *et al.*, 2007) was recently demonstrated. Decolourization begins by a strict anaerobic reductive cleavage of the azo linkage and produces colorless aromatic amines that are potential carcinogens (Mason *et al.*, 1978; Liu *et al.*, 2007). Other researchers have added an aerobic oxidation step to degrade and mineralize the amines (Libra *et al.*, 2003; O'Neill *et al.*, 2000; Supaka *et al.*, 2004). The dye molecule is reduced by either azoreductase (Libra *et al.*, 2003), or by unspecific cytoplasmic enzymes, which act as azoreductases (Russ *et al.*, 2000). Although significant progress has been made, more species that can completely mineralize textiles dyes need to be isolated.

2.3 Dye decolourization by white rot fungi

White rot fungi have been studied for nearly three decades and new species are being shown to decolourize various textile dyes with their lignin-degrading enzymes (LDEs) (Cripps *et al.*, 1990; Champagne and Ramsay, 2005; Bhatti *et al.*, 2008). Lignin peroxidases (LiP), Mn-dependent peroxidases (MnP) and laccases are secreted when fungi are limited in carbon, nitrogen, and sulfur and/or phosphorous sources (secondary metabolism) (Kirk and Farrell, 1987; Cameron *et al.*, 2000; Leonowicz *et al.*, 2001). Tien and Kirk (1983) reported the first dye decolourization by *Phanerochaete chrysosporium*. Wesenberg *et al.* (2003) surveyed 29 white rot fungi capable of dye decolourization. Since then, several investigators have evaluated the decolourization of commercial dyes by new species (Asgher

et al., 2008a; dos Santos *et al.*, 2004; Levin *et al.*, 2004; Mendonça *et al.*, 2008; Robinson and Nigam, 2008). Dye decolourization capabilities vary with the fungal or enzyme species (Chagas and Durrant, 2001; Nyanhongo *et al.*, 2002). Cripps *et al.* (1990) issued the first report demonstrating the major role of lignin peroxidase in *P. chrysosporium* cultures decolourizing Orange II, Trapeolin O and Azure B. Manganese peroxidase (MnP) and laccase were the main enzymes detected in decolourizing cultures of *Trametes versicolor* (ATCC 20869) (Swamy and Ramsay, 1999b) and the contribution of each enzyme to dye decolourization depended on the dye (Champagne and Ramsay, 2005). MnP was eight times more efficient than laccase in decolourizing the azo dye Acid red 27 but did not decolorize Reactive blue 19, an anthraquinone dye. On the other hand, laccase efficiently decolourized the anthraquinone dye. More recently, the central roles of laccase and manganese peroxidase in decolorizing cultures of *Pleurotus ostreatus* (Faraco *et al.*, 2009) and *Shizophyllum commune* IBL-6 (Bhatti *et al.*, 2008) respectively, were demonstrated.

2.3.1 Main lignin-degrading enzymes

Lignin peroxidase (E.C. 1.11.1.14)

Lignin peroxidase (LiP) was detected for the first time in cultures of *Phanerochaete chrysosporium* (Tien and Kirk, 1983). It is a monomeric N- and O-glycosylated protein expressed in several iso-forms. LiP contains one iron in a protoporphyrin IX (heme) as a prosthetic group and its molecular weight varies from 38 and 47 kDa. The enzyme is basic having an iso-electric point between 3 and 5 depending on the iso-form (reviewed by Leonowicz *et al.* (2001)). It requires hydrogen peroxide (H_2O_2) to catalyze a reaction that occurs through a cycle illustrated in Figure 2.4. Hydrogen peroxide oxidizes the iron center of the heme to generate an oxoferryl iron ($Fe(IV)=O$) and an oxidizing equivalent as a radical (compound

1. $Enz-heme[Fe(III)]_{(PX)} + H_2O_2 \rightarrow (Enz-heme^{\bullet+})[O = Fe(IV)]_{(Compound\ I)} + H_2O$
2. $(Enz-heme^{\bullet+})[O = Fe(IV)]_{(Compound\ I)} + RH \rightarrow Enz-heme[O = Fe(IV)]_{(compound\ II)} + H^+ + R^{\bullet}$
3. $Enz-heme[O = Fe(IV)]_{(compound\ II)} + RH \rightarrow Enz-heme[Fe(III)]_{(PX)} + H^+ + R^{\bullet}$

PX = native or resting enzyme Enz = enzyme

Figure 2.4: Catalytic cycle of lignin-peroxidase (Adapted from Banci (1997))

D). The enzyme intermediates, compound I and II, oxidize by one electron two substrates to return to the resting state (PX).

Through this catalytic cycle, liP catalyzes C-C and C-O cleavages in side chains of lignin-like compounds leading in general to the depolymerization of dimers and oligomers (de Jong *et al.*, 1994; Spadaro and Renganathan, 1994; Tien *et al.*, 1986). These reactions can involve the oxidation of small molecular weight substrates like veratryl alcohol (VA) (3,4-dimethoxy phenol) to veratraldehyde where an aryl cation radical intermediate is generated. The latter is highly reactive and can subsequently oxidize lignin subunits. Furthermore, veratryl alcohol can also reverse the deactivation of the enzyme caused by an excess hydrogen peroxide (Wariishi and Gold, 1989; Chung and Aust, 1995).

The vast majority of decolourization studies with liP were conducted with azo dyes and this may suggest that liP decolorizes these dyes more efficiently than the other classes of dyes (Cripps *et al.*, 1990; Young and Yu, 1997; Podgornik *et al.*, 1999; Verma and Madamwar, 2002). However, other investigators have reported the decolourization of triphenyl methane dyes (Ollikka *et al.*, 1993; Cripps *et al.*, 1990) and methylene blue (Ferreira-Leitão *et al.*, 2007). Spadaro and Renganathan (1994) analyzed the decolourization of the azo dye, Disperse Yellow 3, by *P. chrysosporium* liP and proposed a degradation pathway.

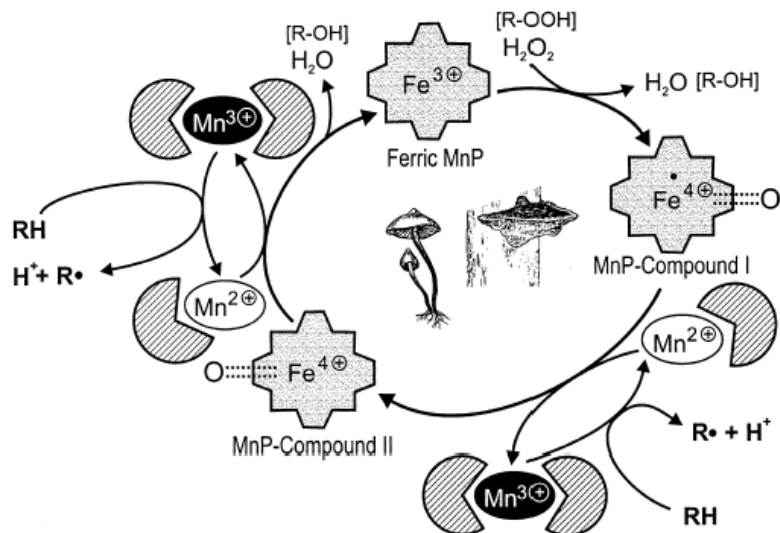


Figure 2.5: Catalytic cycle of Mn(II)-peroxidase (Hofrichter, 2002)

Redox mediators can be used for dyes not directly degraded by the enzyme. For instance, veratryl alcohol is required to decolorize Reactive Blue 19 (anthraquinone) (Christiana *et al.*, 2005).

Manganese peroxidase (E.C. 1.11.1.13)

Manganese peroxidase (MnP) is a glycoprotein containing an iron protoporphyrin group IX as a prosthetic group. Its molecular weight varies from 40 to 46 kDa. Its iso-electric point varies from 2.9 to 7.0 depending on the source species of the enzyme and iso-form (reviewed by Leonowicz *et al.* (2001)). For *T. versicolor*, the optimum pH of MnP can vary from 3.5 to 5 depending on its iso-form (Johansson and Nyman, 1993). The catalytic cycle of MnP shown in Figure 2.5 resembles that of lIP but Mn²⁺ is the preferred electron donor that reduces compound I and II back to the resting state.

Mn^{3+} can oxidize the aromatic rings of the lignin subunits or other substrates once it is chelated to organic acids produced by fungi (e.g., oxalate, malonate). Very few phenolic substrates can reduce MnP compound II to the native ferric state because of the steric hindrance at the active site (Boominathan and Reddy, 1992). Like liP, MnP is also deactivated by excess hydrogen peroxide (Wariishi *et al.*, 1988).

The dye decolorization capability of MnP varies from one species to another and depends on the iso-enzyme and reaction conditions (Li *et al.*, 2009). In general, MnP requires organic acids to decolorize dyes (Young and Yu, 1997). However, Heinfling *et al.* (1998) showed that *P. chrysosporium* MnP decolorized little to none of the azo dyes Reactive blue 38, Reactive violet 5, Reactive black 5, Reactive orange 96, Reactive red 198, and Reactive blue 15 whereas MnP from *Bjerkandera adusta* decolorizes all these dyes in the presence and in absence of Mn^{2+} . Shrivastava *et al.* (2005) showed that *Pleurotus ostreatus* MnP decolorized brominated and methylated sulfophthalein dyes less efficiently than their non-substituted analogs because of steric hindrance.

Laccase (E.C. 1.10.3.2)

Laccase is a multi-copper glycoprotein and its molecular weight varies from 54 to 383 kDa depending on the fungal species (Baldrian, 2006). The enzyme contains four coppers (Cu^{2+}) with one near the active (type 1 (T1) copper) and a buried cluster of three coppers with one type 2 (T2) and two type 3 (T3) coppers (Figure 2.6). The T1 copper extracts electrons from the reducing substrate and transfers it to the tri-nuclear T2/T3 copper cluster where molecular oxygen is reduced to water at T2 copper and T3 coppers act as electron reservoirs (Claus, 2003, 2004; Bertrand *et al.*, 2002; Bukh *et al.*, 2006). The

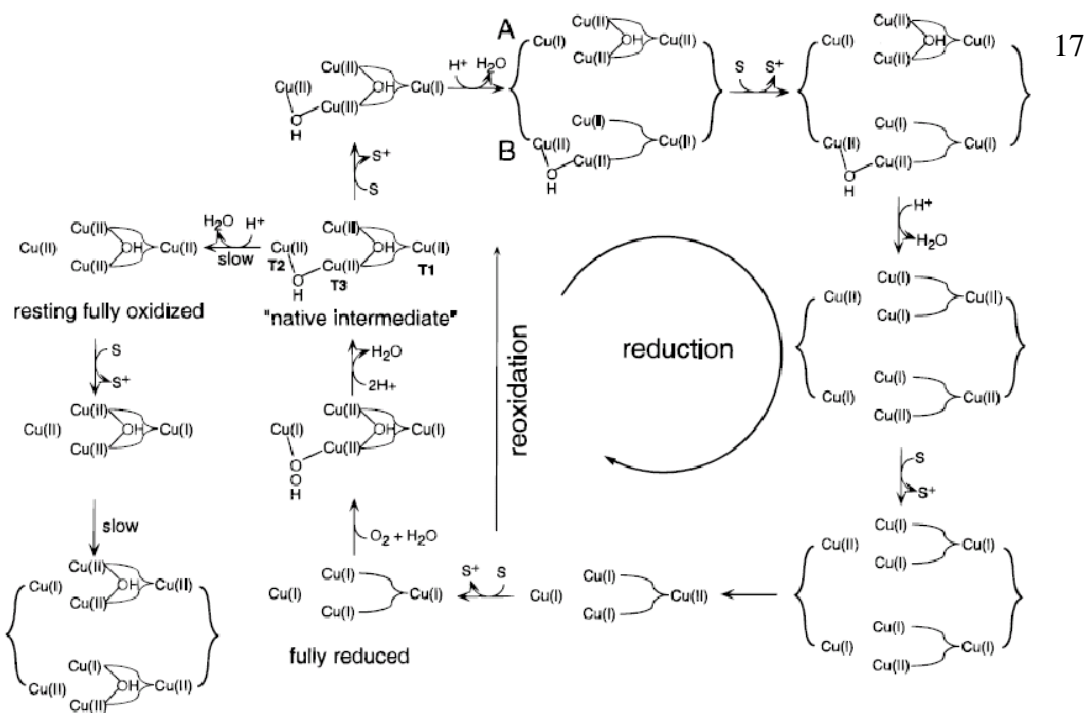


Figure 2.6: Catalytic cycle of laccase (reviewed in Solomon *et al.* (1996))

enzyme catalyzes the oxidation of phenolic compounds and anilines (Xu, 1996). Laccase is almost exclusively in a native intermediate oxidized state in aqueous solution (four Cu^{2+}) (Solomon *et al.*, 1996).

The oxidation of the substrate limits the overall catalytic turnover as the reduction of oxygen is relatively fast (Solomon *et al.*, 1996; Bukh *et al.*, 2006). Laccases efficiently decolorize anthraquinone dyes and dyes containing phenolic moieties and are less efficient at decolorizing azo dyes than peroxidases. Electron mediators like hydroxybenzotriazole (HOBT), various phenolic compounds (Reyes *et al.*, 1999; Michniewicz *et al.*, 2008; Hu *et al.*, 2009; Murugesan *et al.*, 2009) or few anthraquinones dyes (Wong and Yu, 1999) can broaden the range of dyes decolourized by the enzyme. The dye decolourization capability of a laccase depends on its species and strain, and on the structure of the dye. Nyanhongo *et al.* (2002) demonstrated that laccases from four white rot fungal species (*T.hirsuta*, *T.modesta*, *T.versicolor* and *Sclerotium rolfsii*) decolourized anthraquinone,

azo, indigo, and triarylmethane dyes at different rates and extent. Although Peralta-Zamora *et al.* (2003) reported that *T. versicolor* laccase (strain CCT-4521) decolourized Reactive blue 19 only in presence of HOBT, laccase from *T.versicolor* (ATCC 20869) decolourized the anthraquinone dye without a redox mediator (Champagne and Ramsay, 2005; Reyes *et al.*, 1999). Thus, generalized trends for predicting the capability of an enzyme to decolorize a target dye are not always valid.

2.3.2 Factors influencing dye decolourization by white rot fungi

Nutrients requirements

White rot fungi require nutrient-limiting conditions to secrete the lignin-degrading enzymes and to decolourize textile dyes. Few species like *Pycnoporus cinnabarinus* are exceptions since they can decolourize coloured effluents during its growth phase with their constitutively produced laccase (Schliephake *et al.*, 1993). Although nutrient limitation is necessary, minimal amount of carbon and nitrogen sources are needed. Swamy and Ramsay (1999c) determined that at least 0.5-g/l glucose was necessary for dye decolourization by *Trametes versicolor*; however, excess ammonium cultures inhibited the decolourization (Swamy and Ramsay, 1999b). Cultures growing with high amounts of carbon and nitrogen instead (prior to the secondary metabolism) resulted in higher enzyme production and increased decolourization rates (Chao and Lee, 1994).

Glucose is the mostly used carbon source for dye decolourization by white rot fungi. Since it is not abundant in wastewater streams and can be expensive for large-scale treatment, more economical carbon sources are being sought. Kapdan *et al.* (2000) conducted dye decolourization with *Coriolus versicolor* using molasses, starch and fructose and showed

that color removal was not as efficient as with glucose and the decolourization extent varied. The carbon to nitrogen ratio also affects the enzyme secretion during dye decolourization (Asgher *et al.*, 2008b) and can be adjusted to minimize the secretion of proteases that digest the lignin-degrading enzymes as part of the nitrogen metabolic turnover of fungi (Dosoretz *et al.*, 1990; Staszczak *et al.*, 2000).

Influence of the dye molecular structure on biodegradability

The molecular structure of the dye impacts the rate of dye decolourization and few scientists attempted to formulate general rules to predict the degradability of dyes. Pasti-Grigsby *et al.* (1992) studied the influence of aromatic substitution patterns on the bio-degradability of sulfonated azo dyes with *Streptomyces* sp. and *P. chrysosporium*. Molecules including a *para* or *ortho* hydroxyl group and at least one *ortho* electron-releasing substituent relative to the azo bond (-N=N-) on an aromatic ring were rapidly decolourized by *Streptomyces* sp peroxidase. However, purified *P. chrysosporium* liP and MnP degraded all dyes including those without those molecular features. It was hypothesized that the liP and MnP capabilities to degrade a wider range of molecules was due to their higher redox potential relative to that of the dyes. Kandelbauer *et al.* (2004) reported a similar correlation between molecular structure and degradability with *Trametes modesta* laccase. Although there are ample reports on dye decolourization using purified enzymes, the trends on peroxidase and laccase reactivity towards a specific class of dyes still have to be validated for a greater number of dyes.

2.4 Dye decolourization in white rot fungal bioreactors

Few investigations have evaluated dye decolourization in fungal bioreactors for the design of continuous decolourization processes. Successful uses of such bioreactors are summarized in Tables 2.2 and 2.3. *P. chrysosporium* is the most studied species for decolourization in bioreactors. In general, decolourization extents reported were reproducible and no external intervention was needed over a period of 9 to 12 days, after which, decolourization efficiency would decrease with the enzyme activity. Rodriguez Couto *et al.* (2000) suggested that unstable enzyme production in an aged culture was due to the secretion of extracellular proteases.

Table 2.2: Dye decolourization in fungal bioreactors

Bioreactor type	Species	Dyes	Operation mode efficiency (%) *	Decolourization	References
	<i>P. cinnabarinus</i>	natural pigments	continuous	88 % (HRT = 3h)	Schliephake <i>et al.</i> (1993)
	<i>P. chrysosporium</i> (ATCC 24725)	Dispersed red 533	Batch & continuous	Batch: 85 % (1-2d) Continuous: 87 - 95 % (HRT=2 d)	Yang and Yu (1996a,b)
Packed bed	<i>P. chrysosporium</i> (ATCC24725)	Poly R-478	Continuous	55 % (HRT=24 h)	Palma <i>et al.</i> (1999)
	<i>P. chrysosporium</i> (ATCC 24725)	Poly R-478	Batch & continuous	Batch: 70 % (24 h)	Rodriguez Couto <i>et al.</i> (2000)
	unidentified fungal species (strain F29)	Orange II (azo dye)	Continuous	95 % (3.5 d) over 2 months	Zhang <i>et al.</i> (1999)

Table 2.3: Dye decolourization in fungal bioreactors. HRT means hydrolic retention time

Bioreactor type	Species	Dyes	Operation mode efficiency (%) *	Decolourization	References
Fluidized bed	unidentified fungal species (strain F29)	Orange II	Fed-batch - continuous	Fed-batch:95-98 % cycles over 30 days)	Zhang <i>et al.</i> (1999)
Airlift	<i>P. chrysosporium</i> (ATCC 24725)	Azo,sulfonated dyes and pigments	Fed-batch	90 % (HRT=24 h)	Shahvali <i>et al.</i> (2000)
Rotating biological contactor	<i>T. versicolor</i> (ATCC 20869)	Carpet dye mixture	Batch	71 % (5-10h)	Ramsay and Goode (2004)
	<i>Coriolus versicolor</i>	Everzol turquoise G,phthalocyanine dye	55 % (2h)	Kapdan <i>et al.</i> (2000)	

Sustained enzyme production is an essential requirement for a stable decolourization process. It depends on the oxygen transfer and nutrient feeding rate (Couto *et al.*, 2004; Shahvali *et al.*, 2000; Swamy and Ramsay, 1999a; Li and Jia, 2008). However, good oxygen transfer rate is hampered by the tendency of the fungal mycelium to excessive growth, adhesion to surfaces, which increases oxygen demand and the medium viscosity (Moreira *et al.*, 2003). To maximize the operation time of fungal bioreactor, Zhang *et al.* (1999) were able to operate a dye decolourizing fluidized bed reactor for two months by cleaning screens and removing excess mycelia in the reactor each week in order to maintain operation. Eventually, the reactor was plugged and the decolourization efficiency decreased. Decolourization resumed once the excess mycelia was removed.

The use of rotating biological contactors (RBCs) for white rot fungi is relatively recent, as few investigations have reported its use for the decolourization of dyes (Kapdan *et al.*, 2000; Ramsay and Goode, 2004; Guimaraes *et al.*, 2005; Nilsson *et al.*, 2006). Kapdan *et al.* (2000) showed that the rotational speed, the biofilm thickness and the carbon source concentration impacted on the decolourization efficiency with *C. versicolor* (MUCL). Thicker biofilms when nutrient concentration was high increased the mass transfer resistance to nutrient transfer and to enzyme secretion.

Dye decolourization in fungal bioreactors needs additional investigations to determine efficient strategies to sustain a continuous enzyme production and control the growth of the mycelium as they are essential for a stable dye decolourization process.

2.5 Dye decolourization by immobilized lignin-degrading enzymes

Maintaining a stable enzyme concentration for dye decolourization with white rot fungi is challenging. Intermittent feeding and appropriate maintenance must be provided and this may not always be possible in a wastewater treatment process. For example, addition of high glucose concentrations to provided high enzyme production is not cost effective (Kapdan *et al.*, 2000) and more economical and suitable carbon sources are required. While fungal bioreactors are being developed, the potential of immobilized enzyme reactors is being seriously examined (Tables 2.4, 2.5, 2.6, and 2.7). Immobilized peroxidase from *S. spontaneum* decolorized six azo, anthraquinone and triphenyl methane dyes (Shaffiqu *et al.*, 2002) and *T. modesta* laccase immobilized on alumina decolourized 41 commercial azo, triphenyl methane, indigoid and heterocyclic dyes. Of these dyes, 36 were degraded from 65 % to 100 % and five dyes were adsorbed and not degraded (Kandelbauer *et al.*, 2004).

Dye adsorption to the enzyme support is frequent particularly when the material is polar or charged and may enhance the rate of color removal (Kandelbauer *et al.*, 2004; Peralta-Zamora *et al.*, 2003; Zille *et al.*, 2003; Rekuć *et al.*, 2009a). Peralta-Zamora *et al.* (2003) showed that IRA-400 ionic exchange resin had the highest adsorption capacity for the anthraquinone dye, Reactive blue 19, when compared with imidazol-modified silica and montmorillonite. *T. versicolor* laccase on amberlite IRA-400, an anionic-exchange resin, decolourized Reactive blue 19 with the highest rates compared to when the enzyme was immobilized on the other supports. In addition, IRA-400-laccase decolourized the dye

with and without hydroxybenzotriazole (HOBT), a redox mediator, but the free enzyme required the mediator to decolorize the anthraquinone dye. The authors concluded that decolourization with immobilized laccase occurred mainly through dye adsorption since the rates of decolourization with and without the redox mediator were identical. Zille *et al.* (2003) demonstrated that 90 % of the Reactive black 5 decolourization by *T. hirsuta* laccase immobilized on alumina was due to adsorption. Moreover, adsorption was still occurring even after loss of laccase activity. On the other hand, dye adsorption did not occur during decolourization with a plant peroxidase immobilized on polyethylene, a hydrophobic material (Shaffiqu *et al.*, 2002).

There are fewer investigations on dye decolourization with immobilized peroxidases most likely because hydrogen peroxide is required. Hydrogen peroxide must be carefully added to the decolourization process or generated in situ to avoid enzyme deactivation and achieve a stable decolourization process (Kim *et al.*, 2005; Conesa *et al.*, 2002; Torres *et al.*, 2003). *Saccharum spontaneum* peroxidase immobilized on polyethylene decolourized 15 batches of Procion green HE-4BD. Careful addition of hydrogen peroxide to the reactor favoured an enzyme half-life of 60 h (Shaffiqu *et al.*, 2002). When *Bjerkandera* sp MnP decolourized the azo dye, Orange II, in a membrane reactor, 49 % of its initial activity was lost in two hours and it was more sensitive to increased loading rates of hydrogen peroxide (López *et al.*, 2004). However, decolourization was operated under optimized H₂O₂ and MnP feeding rates for eight days with a stable decolourization efficiency of 96 %.

So far, the disappearance of dyes in defined solutions has been the main focus in the vast majority of dye decolourization studies and more investigations must be conducted in the context of a textile wastewater since some components may affect dye decolourization and/or the enzyme. The application of dyes to fabrics requires auxiliary chemicals (dyeing

aids) such as solvents, detergents, and wetting agents which are present in textile effluents (Smith, 1986). Non-ionic surfactant like alcohol ethoxylates, alkylphenol ethoxylates, and ionic ethoxylate surfactants such as alkylsulfates, and alkylether sulfates constitute a major portion of the pollutants (González *et al.*, 2008). Abadulla *et al.* (2000) demonstrated that *Thirsuta* laccase was mildly inhibited by textile surfactants such as Univadine PA (anionic), Tinegal MR (cationic) but not by Albegal FFA (non-ionic) and the immobilization of the enzyme on alumina did not eliminate the inhibition. Although, surfactants generally tend to denature proteins (Madaeni and Rostami, 2008; Otzen *et al.*, 2009), reversed micelles can stabilize enzymes in the organic phase for enzyme catalysis (Yang and Robb, 2005; Wang *et al.*, 2008b) or even allow protein refolding at their water core (Hagen *et al.*, 2006).

Few studies have provided any information on how dye auxiliary chemicals may affect decolourizing enzymes. This may be due to (1) the complex nature of colloidal interactions which may exist between the enzyme, the dye molecule(s), and auxiliary chemicals and (2) the scarce information on the composition of the dye effluent and the nature of its constituents, which are usually undisclosed for proprietary processes. Stable immobilized enzymes will deactivate with time and this must be considered in the design of an enzymatic process (Aitken, 1993).

Reyes *et al.* (1999) showed that *Coriolus gallica* laccase immobilized on agarose retained 85 % of its activity after 10 batch decolourizations of a synthetic dye effluent containing Direct blue 200, Direct red 80, Direct black 28, sodium sulfate, sodium carbonate, soap and dispersants. However, a laccase reactor retained only 14 % of its initial decolourization activity after decolourizing ten batches of an industrial effluent and further investigation did not provide information on the cause of the activity loss. Zille *et al.* (2003) showed that free laccase from the same species was two times more stable at high ionic strength (30

g/l NaCl) than when immobilized on alumina when decolorizing 40 ppm Reactive black 5 (azo dye) in a real textile wastewater. The authors suggested that the enzyme and the dye at high salt concentration form stable aggregates; the aggregation is favoured because sodium chloride neutralizes the enzyme and dye net charges. The aggregates would prevent the denaturation of the enzyme. Finally, this study demonstrates that predicting enzyme stability is not always intuitive because of the numerous possible interactions between different dyes and the enzymes.

2.5.1 Laccase immobilization and influence of the support material on the stability of decolourization

The most important criteria for good immobilized enzyme activity are the mechanical properties (rigidity and durability), physical form (granules, sheets, inner tube walls, etc), resistance to chemical and microbial attacks, material hydrophilicity, price, and availability (Mosbach *et al.*, 1976). Laccase has been immobilized on gels like Sepharose (agarose), Sephadex (dextran), cellulose-based materials (Duran *et al.*, 2002; Rekuć *et al.*, 2008) and allowed good activity retention since these materials are highly hydrophilic. However these gels tend to may compress or expand and cannot be used in packed bed reactors (Rekuć *et al.*, 2009b). Laccases can also be immobilized on inorganic supports like alumina (Kandelbauer *et al.*, 2004; Zille *et al.*, 2003), and silica (Peralta-Zamora *et al.*, 2003; Zhu *et al.*, 2007). Satisfactory laccase activities were achieved by first activating the material surface with 3-aminopropyltriethoxysilane (APTES) to introduce amines and cross-link the enzyme to the surface with glutaraldehyde (Duran *et al.*, 2002). However, these materials tend to be brittle and therefore mechanical agitation must be limited. More recently, laccase was immobilized on acrylic supports like poly(butyl acrylate-co-ethyleneglycol dimethacrylate)

(Bryjak *et al.*, 2007), poly(glycidyl methacrylate-co-ethyleneglycol dimethacrylate) (Arica *et al.*, 2009), commercial acrylic carriers like Dilbeads and Sepabeads (Kunamneni *et al.*, 2008) and very high laccase activities were reported. Acrylic carriers have good mechanical and chemical stability and can be made highly hydrophilic (Mosbach *et al.*, 1976).

The stability of a decolourization process depends on the properties of the enzyme support. Beads made of brittle materials, like as alumina or silica, erode when mechanically agitated and this results in enzyme loss (Kandelbauer *et al.*, 2004). Wang *et al.* (2008a) showed that dye decolourization by laccase encapsulated in alginate-gelatin-PEG (polyethylene glycol) beads depended strongly on the composition of the blend; using alginate alone gave the lowest decolourization efficiency and enzyme stability. A bead blend of alginate/gelatin and PEG improved enzyme stability and dye decolourization efficiency. The investigation confirms that a support material must be chosen to maximize enzyme activity and its mechanical properties and will dictate the configuration of the reactor (e.g. packed bed reactor vs continuous stirred tank reactor).

Table 2.4: Dye decolourization with immobilized lignin-degrading enzymes

Enzyme	Source	Immobilization method	Dyes	Decolourization efficiency	References
Laccase	<i>Coriolopsis gallica</i> (UMH8260)	Covalent on activated agarose-CNBr	Reactive blue 198 - Dye effluent	70 %	Reyes <i>et al.</i> (1999)
Laccase	<i>Trametes modesta</i>	Covalent on Al_2O_3	Lanaset Blue R (anthraquinone) Acid blue 74 (indigoid) Crystal violet (triphenyl-methane dye) Phenyl azo dye	100 % (10-12 h) 99 % 98 % 99 %	Kandelbauer <i>et al.</i> (2004)
Laccase	<i>Trametes versicolor</i> (CT-4521)	Covalent on silica	Reactive blue 19 (anthraquinone) Remazol black B (azo) Reactive orange 122 (azo) Reactive red 251 (type n.a.)	45 % (0.5 h) 9 % 55 % (0.5 h) 25 % (0.5 h)	Peralta-Zamora <i>et al.</i> (2003)

Table 2.5: Dye decolourization with immobilized lignin-degrading enzymes

Enzyme	Source	Immobilization method	Dyes	Decolourization efficiency	References
Laccase	<i>Trametes villosa</i>	Covalent Al_2O_3	on Reactive black 5	98 % (24 h)	Zille <i>et al.</i> (2003)
Laccase	<i>Sclerotium rolfsii</i>	Covalent Al_2O_3	on Commercial dye mixture		Ryan <i>et al.</i> (2003)
Laccase	<i>Trametes hirsuta</i>	Covalent Al_2O_3	on Reactive blue 221 (heterocycle), Reactive black 5 (azo), Direct blue 71 (triazole), Basic red 9 Base (triphenylmethane), Reactive blue 19 (anthraquinone), Acid blue 225 (anthraquinone), Acid blue 74 (indigoid), Dye effluent (Reactive blue 19, Reactive blue 221)		Abadulla <i>et al.</i> (2000)

Table 2.6: Dye decolourization with immobilized lignin-degrading enzymes

Enzyme	Source	Immobilization method	Dyes	Decolourization efficiency	References
Laccase	<i>Cerrera unicolor</i>	Activated silica with various silanes	Acid blue 74 (indigo carmine)	78 - 85 (5h) %	Rekuć <i>et al.</i> (2009a)
Laccase	Denilite (Novozymes)	IIS Alginate/PEG blend	Reactive red B-3BF	50 - 100 % (Depending on the blend)	Wang <i>et al.</i> (2008a)
Laccase	<i>Rhus vernicifera</i>	Poly(GMA/EDGMA)	Reactive red 120	91 % (10h)	Arica <i>et al.</i> (2009)
Laccase	<i>Pleurotus ostreatus</i>	Eupergit C (epoxy activated acrylic carrier)	Reactive blue 19	56 % (continuous, HRT=9.3 min)	Russo <i>et al.</i> (2008)
Mn-peroxidase	<i>Bjerkandera sp</i>	Membrane retention	Orange II (azo)	92 % (50 min)	López <i>et al.</i> (2004)
Peroxidase	<i>Saccharum spontaneum</i>	Covalent on polyethylene	Procion Blue navy HER, Procion blue H-7G, Procion green HE-4BD, Supranol green	100 % for all dyes (6 - 8h)	Shaffiqu <i>et al.</i> (2002)

Table 2.7: Dye decolourization with immobilized lignin-degrading enzymes

Enzyme	Source	Immobilization method	Dyes	Decolourization efficiency	References
Peroxidase	<i>Mormodica charantia</i>	Affinity to concanavalin A	Reactive blue 4 (anthraquinone), Reactive blue 160 and 121 (azo), Reactive red 11 and 120 (azo), Reactive orange 4 and 86, Reactive yellow 84	91 - 98 % (1h) depending on the dye	Akhtar <i>et al.</i> (2005)
Lignin peroxidase	<i>P. chrysosporium</i>	Covalent epoxy-activated disks	Mahogany (azo)	59 %	Podgornik and Podgornik (2002)

2.6 Objectives of research project

According to the literature, laccase has been the preferred lignin-degrading enzyme for dye decolourization and immobilized laccase reactors have been studied more than immobilized peroxidases (Duran *et al.*, 2002) most likely because the enzyme requires only oxygen as a co-substrate. The relatively high optimum temperatures of the enzyme ranging from 50 to 70°C (Wang and Ng, 2006; Rebrikov *et al.*, 2006; Linke *et al.*, 2005; Han *et al.*, 2005) makes it ideal for industrial applications and it should be more easily integrated into industrial processes. Furthermore, new laccases have been isolated every year since 2004. For these reasons, this research is focusing on laccase for dye decolourization.

The impact of common textile waste effluent components on enzyme activity has not thoroughly been investigated. Most studies have focused on the disappearance of dyes and have not attempted to determine the cause(s) of activity loss. Studying dye degradation kinetics by immobilized laccase can give more insight on how it is affected by the composition of dye effluents and help predict the kinetic behaviour of the enzyme in industrial dye decolourization. Protein immobilization is an economical and effective means of stabilizing and reusing an enzyme but, as mentioned, the nature of the material can influence the enzyme activity retention. Therefore, the ultimate goals of this research project are to characterize the dye decolourization by laccase immobilized on silica beads and to determine the effects of auxiliary chemicals on the degradation kinetics of Reactive blue 19, an anthraquinone dye. To attain these objectives, the research was divided into two main parts:

2.6.1 Characterization of dye decolourization by *Trametes versicolor* laccase immobilized on controlled porosity carrier silica (CPC) beads and immobilization of laccase on PMMA.

In the third chapter, dye decolourization by immobilized laccase on controlled porosity carrier (CPC) silica beads was characterized. The effect of immobilization on the pH activity profile of the enzyme toward ABTS and Reactive blue 19 and the contribution of dye adsorption in decolourization were analyzed. In chapter 3, the decolourization of two anthraquinone, two azo and one indigoid dyes by free and immobilized laccase was compared and the toxicity of decolourized solutions was analyzed. Chapter four focused on the immobilization of laccase on polymethyl methacrylate (PMMA). PMMA was chosen since it is an abundant and relatively economical material and less brittle than CPC-silica beads. Furthermore, this polymer is the least hydrophobic of the elastomers and could be sufficiently hydrophilic for good immobilized laccase activity.

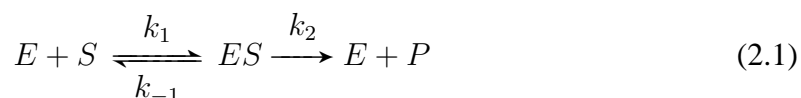
2.6.2 Impact of auxiliary chemicals on dye decolourization by *T.versicolor* laccase

In the second phase, decolourization kinetics of textile dyes and the effects of common auxiliary chemicals like surfactants and salts were investigated. Since surfactant, Surfactants may impact enzyme activity. Therefore, chapter five focuses on the effects of a non-ionic surfactant, Merpol, on dye decolourization and these were quantified by steady-state kinetics. Merpol is a non-ionic ethoxylated based surfactant used as a wetting agent and detergent to clean fabrics during dyeing processes. Finally in chapter six, the effects of sodium chloride and sodium sulfate on dye decolourization were analyzed and a new dye

decolourization chloride inhibition rate equation was proposed.

2.7 Enzyme kinetics fundamentals

This review on enzyme kinetics is based on enzyme kinetic textbooks by Segel (1993) and Leskovic (2003) and is presented so explain the development kinetic models developed in chapter six and seven and how they were derived. All concentrations and equilibrium constants are assumed to be in units of molarity unless stated otherwise. An enzyme (E) accelerates the rate of a chemical reaction by lowering its activation energy. First, it specifically binds the substrate (S) and second, it converts substrate to the product (P) (equation 6.1).



The variable k_2 is the first order rate constant describing the catalytic conversion of S to P, and k_1 and k_{-1} are the rate constants for the substrate binding and complex dissociation respectively.

2.7.1 Derivation of rate equations

Enzyme rate equations can be derived using either the rapid equilibrium or steady-state assumption.

Rapid equilibrium assumption

Consider the previous single substrate reaction (equation 6.1) in which an enzyme catalyzes the conversion of a substrate to a product. The binding of S is reversible and the conversion of S to P, the catalytic step, is irreversible or the conversion of the product back to the substrate is negligible (e.g. at the onset of a reaction). According to the rapid equilibrium assumption, the rate of association of the substrate to the enzyme, and the rate of dissociation of the complex is much greater than the rate of generation of the product P enough that a rapid equilibrium can be established between enzyme-substrate complex, the free enzyme and the substrate. The procedure to derive a rate equation according to the rapid equilibrium assumption is as follows:

1. Write a mass balance for the enzyme species. The total enzyme concentration (in molarity) $[E]_t$ is equal to the sum of concentrations of the free enzyme, $[E]$, and of the enzyme-substrate complex, $[ES]$.

$$[E]_t = [E] + [ES] \quad (2.2)$$

2. Write the rate equation as a function of the enzyme-substrate complex

$$v = k_2[ES] \quad (2.3)$$

The unit of the reaction rate, v , is molar concentration per time (e.g., $\mu\text{M}/\text{min}$) and k_2 is a first order rate constant reciprocal time as a unit.

3. Divide the rate equation 2.3 by the mass balance (equation 2.2)

$$\frac{v}{[E]_t} = \frac{k_2[ES]}{[E] + [ES]} \quad (2.4)$$

4. Express the concentration of each enzyme species in terms of E and S. When the binding step (binding and dissociation) is at equilibrium, the binding rate between the free enzyme and free substrate is equal to the dissociation rate of the enzyme-substrate complex.

$$k_1[E][S] = k_{-1}[ES] \quad (2.5)$$

5. The dissociation constant is defined as the ratio of the dissociation step over the binding step. The dissociation is also the inverse of the true equilibrium constant for the binding step.

$$K_S = \frac{k_{-1}}{k_1} = \frac{[E][S]}{[ES]} = \frac{1}{K_{eq,S}} \quad \therefore [ES] = \frac{[E][S]}{K_S} \quad (2.6)$$

6. Substitute the equilibrium expression (equation 2.6) in equation 2.4

$$\frac{v}{[E]_t} = \frac{k_2 \frac{[E][S]}{K_S}}{[E] + \frac{[E][S]}{K_S}} \quad (2.7)$$

7. Eliminate [E] and multiply the numerator and denominator in the right hand-side of equation 2.7

$$v = \frac{k_2[E]_t[S]}{K_S + [S]} = \frac{V_{max}[S]}{K_S + [S]} \quad (2.8)$$

where $V_{max} = k_2[E]_t$. The dissociation constant K_S in units of molar concentration indicates the affinity of the enzyme for the substrate or the strength of binding. It is also the substrate concentration at half the maximum initial rate. This mathematical definition differs from the Michaelis constant which will be explained in the next section.

Steady-state or Briggs-Haldane assumption

In the steady-state assumption, the enzyme-substrate concentration is assumed to be much less than the substrate concentration and therefore, the rate of change of the complex concentration is so small relative to that of the reactant concentration that it can be approximated to be zero ($\frac{d[ES]}{dt} = 0$). The molar concentrations of ES, E and S do not need to be in equilibrium and no assumption is made about the relative magnitude of the rate of product generation and the rate of complex dissociation. When deriving a steady-state rate equation, the enzyme complex species balances are expressed by a set of differential equations describing the reactions that have to be solved.

1. Write the set of differential species balance describing the reactions and the enzyme conservation equation

$$\frac{d[E]}{dt} = (k_1 + k_2)[ES] - k_1[E][S] \quad (2.9)$$

$$\frac{d[S]}{dt} = k_{-1}[ES] - k_1[E][S] \quad (2.10)$$

$$\frac{d[ES]}{dt} = k_1[E][S] - (k_1 + k_2)[ES] \quad (2.11)$$

$$\frac{d[P]}{dt} = k_2[ES] \quad (2.12)$$

$$[E]_t = [E] + [ES] \quad (2.13)$$

2. [ES] is re-expressed in term of [E] and [S] from its corresponding differential balance, $\frac{d[ES]}{dt}$. From the steady-state assumption, $\frac{d[ES]}{dt} = 0$,

$$0 = k_2[ES] - (k_{-1} + k_2)[ES] \quad (2.14)$$

$$[ES] = \frac{k_1[E][S]}{k_{-1} + k_2} \quad (2.15)$$

3. Divide the velocity equation (2.3) by the enzyme conservation equation (2.13) to obtain equation 2.4
4. Substitute [ES] (equation 2.15) into equation 2.4,

$$\frac{v}{[E]_t} = \frac{k_2 \frac{k_1[E][S]}{k_{-1} + k_2}}{[E] + \frac{k_1[E][S]}{k_{-1} + k_2}} \quad (2.16)$$

5. Divide the numerator and denominator by [E], and multiply by $\frac{k_{-1} + k_2}{k_1}$

$$\frac{v}{[E]_t} = \frac{k_2[S]}{\frac{k_{-1} + k_2}{k_1} + [S]} \quad (2.17)$$

$$v = \frac{k_2[E]_t[S]}{K_M + [S]} = \frac{V_{max}[S]}{K_S + [S]} \quad (2.18)$$

The catalytic constant, k_2 , is also the turnover number which is the number of substrate molecules converted to products per mole of enzyme per second and has units of inversed time (usually sec^{-1}). The Michaelis constant, K_M , is the molar concentration of the substrate that yields half the maximum reaction rate and is equal to $\frac{k_{-1} + k_2}{k_1} = K_S + \frac{k_2}{k_1}$. The constant approximates the affinity of the enzyme for its substrate or the strength of binding between the enzyme and the substrate when the dissociation constant k_{-1} is larger than k_2 . However, the constant has a kinetic component that is directly proportional to the relative magnitude of k_2 to k_{-1} and can be significant in certain cases. The catalytic efficiency of the enzymatic reaction is defined as ratio of k_2 to K_M

$$\frac{k_2}{K_M} = k_1 \frac{k_2}{k_1 + k_2} \quad (2.19)$$

The catalytic efficiency (in $\text{M}^{-1}\text{sec}^{-1}$) represents the number or frequency of collisions between the enzyme and the substrate, (k_1), multiplied by the fraction of productive collisions (equation 2.19) between the enzyme and the substrate, that is the fraction of collisions that leads to the formation of the product.

In many cases, either assumption will give the same rate equation for a given kinetic scheme but the mathematical definitions or meaning of the equation constants will differ (e.g. K_S vs K_M). Otherwise, when the value k_2 approaches that of k_{-1} , steady-state rate equations must be used because the concentration of [ES] is no longer dependent on [E] and [S] only. The rapid equilibrium assumption is used in chapter six and seven to derive the kinetic models and to analyze the initial rate data since it is the simplest and most direct method to derive enzyme rate equations for simple and more complex multi-ligands reaction schemes and should be considered first. If the rapid equilibrium equation

fits the initial rate data, then the simplest kinetic mechanism is tentatively found and has to be validated with independent experiments (Segel, 1993). Otherwise, the steady-state assumption must be used. The algebraic manipulations may become more complicated as the number of enzyme intermediates increases and schematic (graphical) methods for deriving rate equations like that of King and Altman (1956) must be used to minimize the risks of mistakes.

2.7.2 Reaction catalysis with two or more substrates

Laccases catalyze the reactions of two substrates to yield two products. Oxygen, the electron acceptor, can bind to the enzyme to be reduced to water before the electron donor (e.g. phenol or ABTS) binds to the enzyme to convert to the second product. The reaction mechanism is the ping pong type since the enzyme switches from the stable native reduced state (E^{red}) to the stable oxidized state (E^{ox}) and release water. The steady-state rate equation for ping-pong mechanism assuming that the reversed reaction is negligible is

$$v = \frac{V_{max}[A][B]}{K_{M,B}[A] + K_{M,A}[B] + [A][B]} \quad (2.20)$$

During a steady-kinetics experiment with a bisubstrate reaction, one substrate concentration is varied while the other is kept constant. For laccase, the oxygen is concentration is assumed to be constant (at 8.04 mg/l or 259 μ M) for the duration of the enzyme assay if the substrate conversion does not exceed 10 % and if the substrate concentration largely exceeds that of the enzyme. It is then possible to rearrange equation 2.20 to the general Michaelis-Menten form with respect for substrate A,

$$v_A = \frac{\left(\frac{V_{max,A}}{\frac{K_{M,B}}{[B]} + 1} \right) [A]}{\left(\frac{K_{M,A}}{\frac{K_{M,B}}{[B]} + 1} \right) + [A]} = \frac{k_{cat,A,app}[E]_t[A]}{K_{M,A,app} + [A]} \quad (2.21)$$

and for substrate B,

$$v_B = \frac{\left(\frac{V_{max,B}}{\frac{K_{M,A}}{[A]} + 1} \right) [B]}{\left(\frac{K_{M,B}}{\frac{K_{M,A}}{[A]} + 1} \right) + [B]} = \frac{k_{cat,B,app}[E]_t[B]}{K_{M,B,app} + [B]} \quad (2.22)$$

2.7.3 Experimental determination of Michaelis-Menten parameters

Steady-state kinetic experiments are conducted to determine the the Michaelis-Menten catalytic parameters. $K_{M,app}$ and $V_{max,app}$ can be roughly estimated by plotting rate data according to graphical methods that are based on the linearization of the Michaelis-Menten model. These plotting methods are very useful for determining the nature (linear or non-linear) and the type of enzyme inhibition (competitive, non-competitive, and uncompetitive) .

Lineweaver-Burk plot

The reciprocal of initial rates are plotted against the reciprocal substrate concentrations and the result is a straight line described by the linearized form of the Michaelis-Menten equation:

$$\frac{1}{v} = \frac{1}{V_{max}} + \frac{K_M}{V_{max}} \frac{1}{[S]} \quad (2.23)$$

The intercept is $\frac{1}{V_{max}}$, the slope $\frac{K_M}{V_{max}}$ and K_M is determined from the abscissa at $y = 0$ (Figure 2.7A). The turnover number can be calculated from $k_{cat} = \frac{V_{max}}{[E]_t}$. The errors are amplified by the inversion (particularly at lower substrate concentrations) and the data points must be weighted to improve the accuracy of the estimates if this method is to be used primarily for the numerical estimation of k_{cat} and K_M . However, this practice is discouraged as Dowd and Riggs (1965) showed that this method out of all the linearization transformations (Lineweaver-Burk, Eadie-Hoftsee, and Wolfe-Hanes (not covered in this review)) systematically yields the estimates with the largest errors. The weighting method or factors depends on the error trend or structure associated with the parameter estimates (Dowd and Riggs, 1965; Wilkinson, 1961).

Eadie-Hoftsee plot

In this graphical method, rates divided by their corresponding concentration ($\frac{v}{[S]}$) are plotted against the initial rate v and the line has the following equation

$$\frac{v}{[S]} = \frac{V_{max}}{K_M} - \frac{v}{K_M} \quad (2.24)$$

The K_M is determined from the slope $\frac{-1}{K_M}$ and V_{max} is calculated from the intercept $\frac{V_{max}}{K_M}$ (Figure 2.7B). On the hand, the error associated with the initial velocity, v , is not amplified.

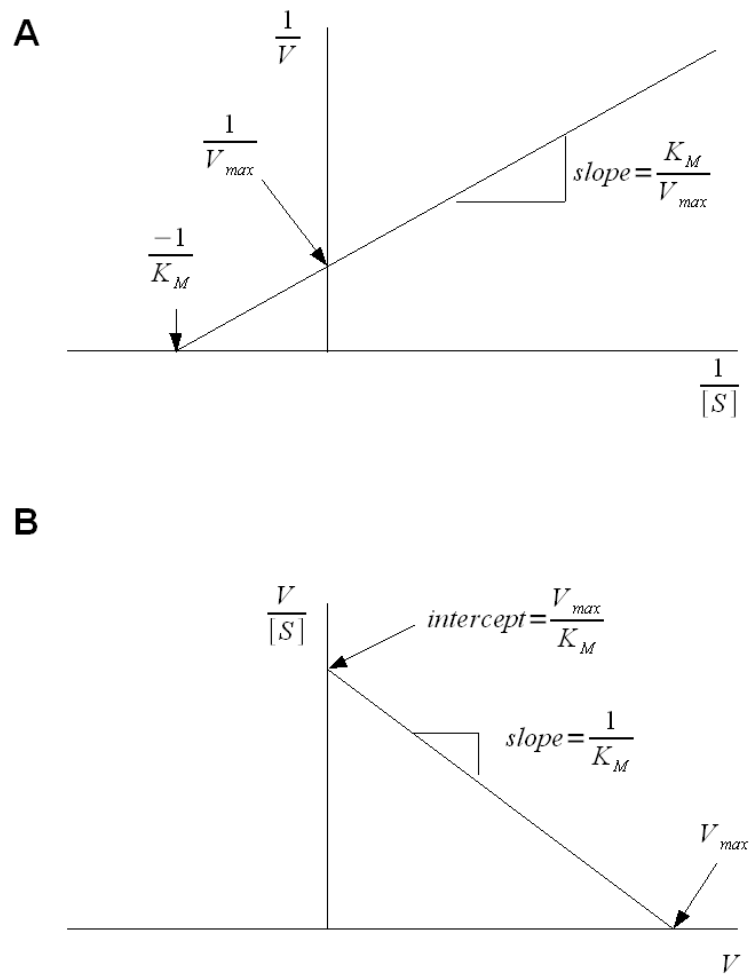


Figure 2.7: Lineweaver-Burk (A) and Eadie Hofstee (B) plots

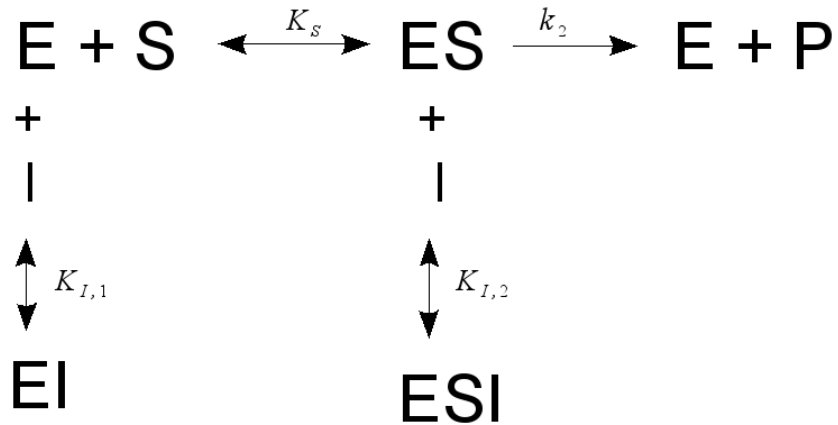


Figure 2.8: Mixed type enzyme inhibition

2.7.4 Linear enzyme inhibition

Most enzyme inhibition occurs through basic mechanisms that can be derived from Figure 2.8. The above kinetic mechanism is mixed-inhibition and is described by the general rate equation,

$$v = \frac{k_2[E]_t[S]}{K_M \left(1 + \frac{[I]}{K_{I,1}}\right) + [S] \left(1 + \frac{[I]}{K_{I,2}}\right)} \quad (2.25)$$

Here in the equation, $K_M = \frac{k_{-1} + k_2}{k_1}$, K_{i1} and K_{i2} are the dissociation constants for the binding of the inhibitor to the free enzyme and the enzyme-substrate complex respectively and are defined as

$$K_{I,1} = \frac{k_{-I,1}}{k_{I,1}} \quad (2.26)$$

$$K_{I,2} = \frac{k_{-I,2}}{k_{I,2}} \quad (2.27)$$

k_{-i} and k_i are the dissociation and association rate constants, respectively.

Competitive inhibition

The inhibitor competes with the substrate to bind to the active site and does not bind the enzyme-substrate complex, i.e. $K_{i2} \rightarrow \infty$. A greater substrate concentration is necessary to achieve half the maximal velocity, i.e., a greater substrate concentrations is needed to displace inhibitor molecules from the active site. V_{max} or k_2 (turnover number) is not affected while the apparent Michaelis constant, $K_{M,app}$, increases as the inhibitor concentration increases. The rate equation is

$$v = \frac{k_{2,app}[E]_t[S]}{K_{M,app} + [S]} = \frac{k_2[E]_t[S]}{K_M \left(1 + \frac{[I]}{K_{I,1}} \right) + [S]} \quad (2.28)$$

The Lineweaver-Burk plot indicates competitive inhibition when the straight lines have the same intercept and their slope increases as the inhibitor concentration increases (Figure 2.9A).

Non-competitive inhibition

In non-competitive inhibition, the inhibitor binds the free enzyme and the enzyme-substrate with equal affinity ($K_{I,1} = K_{I,2}$), i.e. the inhibitor binds a non-catalytic site that affect the conversion of the substrate to the product. In that respect, the apparent turnover number $k_{2,app}$ decreases and the apparent Michaelis constant is equal to the true value.

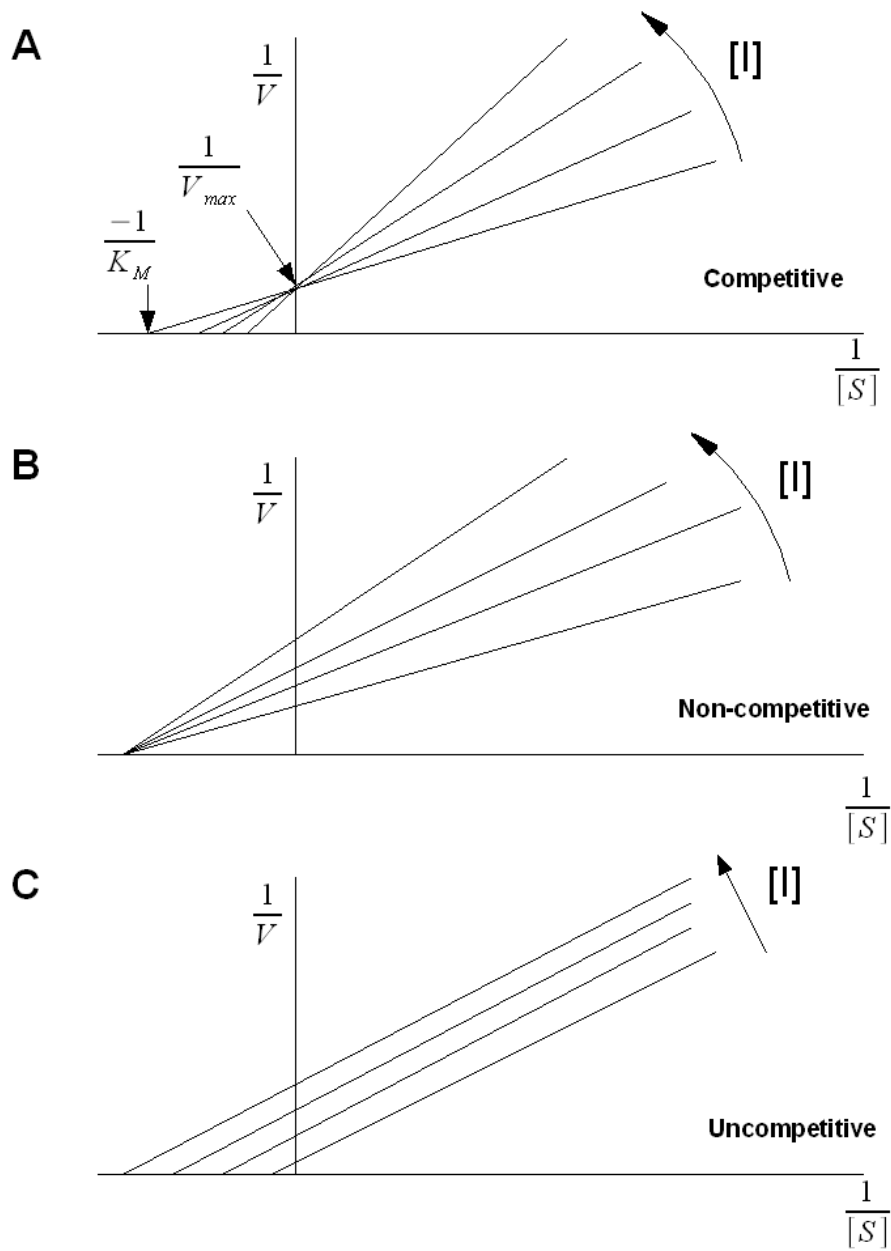


Figure 2.9: Lineweaver-Burk plots of the competitive, non-competitive and uncompetitive inhibitions

$$v = \frac{k_{2,app}[E]_t[S]}{K_{M,app} + [S]} = \frac{\left(\frac{k_2}{1 + \frac{[I]}{K_{I,2}}} \right) [E]_t[S]}{K_M + [S]} \quad (2.29)$$

The Lineweaver-Burk plot shows straight lines that have the same abscissa and different intercepts. The slopes of the line increase as the inhibitor concentration increases (Figure 2.9B).

Uncompetitive inhibition

In uncompetitive inhibition, the inhibitor only binds to the enzyme-substrate complex and not the free enzyme ($K_{I,1} \rightarrow \infty$). The inhibitor binding site appears only when the substrate is bound to the enzyme. The true K_M and k_2 are decreased to the same extent so that the catalytic efficiency is not altered.

$$v = \frac{k_{2,app}[E]_t[S]}{K_{M,app} + [S]} = \frac{\left(\frac{k_2}{1 + \frac{[I]}{K_{I,2}}} \right) [E]_t[S]}{K_M \left(1 + \frac{[I]}{K_{I,2}} \right) + [S]} \quad (2.30)$$

The Lineweaver-Burk yields a set of parallel lines (identical slopes) with different intercepts, which increase with the inhibitor concentration (Figure 2.9C).

Mixed inhibition

In this type of inhibition, the inhibitor binds to both the free enzyme and the enzyme-substrate complex with different affinity so that the alteration in the true $k_{2,app}$ and $K_{M,app}$ varies according to the affinity of the inhibitor to enzyme species:

$$v = \frac{k_{2,app}[E]_t[S]}{K_{M,app} + [S]} = \frac{\left(\frac{k_2}{1 + \frac{[I]}{K_{I,2}}} \right) [E]_t[S]}{K_M \left(\frac{1 + \frac{[I]}{K_{I,1}}}{1 + \frac{[I]}{K_{I,2}}} \right) + [S]} \quad (2.31)$$

2.7.5 Non-linear enzyme inhibition

The theory of the non-linear inhibition is presented in this section and includes the derivation of the rate equations 7.2 and 7.3 in chapter 7. There are two types of non-linear inhibition. Hyperbolic (partial) mixed-type inhibition occurs when the enzyme can generate a product despite being bound to an inhibitor and parabolic inhibition occurs if more than one inhibitor molecule can bind to the enzyme. The enzyme-inhibitor, EI, in Figure 2.10 is

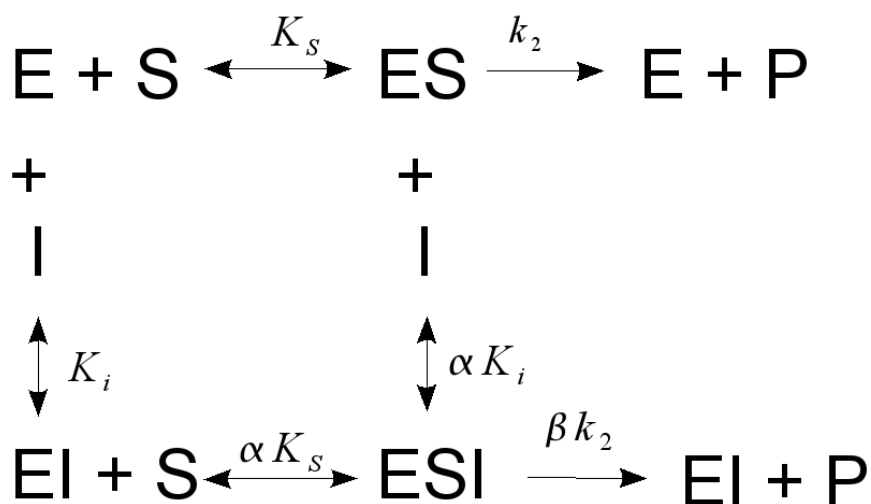


Figure 2.10: General partial mixed inhibition (hyperbolic)

allowed to bind to the substrate and to generate a product. The bound inhibitor can affect

the enzymes affinity for the substrate by factor α . The parameter β is a fraction and is the effectiveness for the complex ESI to generate the product and can take values between 0 and 1. The rate equation describing the kinetic scheme is

$$v = \frac{k_2[E]_t[S] \left(1 + \frac{\beta[I]}{\alpha K_I}\right)}{K_S \left(1 + \frac{[I]}{K_I}\right) + [S] \left(1 + \frac{[I]}{\alpha K_I}\right)} \quad (2.32)$$

Hyperbolic inhibition can be detected by plotting the slopes or the intercepts from the Lineweaver-Burk plots as function of the inhibitor concentration and the curve will be hyperbolic (Figure 2.11A).

Parabolic inhibition occurs when more than one inhibitor binding site exist and is usually complete, i.e. no product can be generated by the enzyme when all inhibitor sites are occupied. Parabolic inhibition is indicated if the replot of the Lineweaver-Burk slopes shows a parabolic curve (Figure 2.11B). Consider the parabolic inhibition kinetic in Figure 2.12. In this scheme, the inhibitor (I) can bind two independent sites with the same affinity, i.e., the inhibition constant, K_I , is identical for both inhibitor binding sites. The α factor indicates that binding of the inhibitor affects the binding of the substrate S. The enzyme-substrate with one inhibitor molecule can generate the product by a fraction β of k_2 but it cannot when two inhibitor molecules are bound. The rate equation for this kinetic scheme is

$$v = \frac{k_2[E]_t[S] \left(1 + \frac{2\beta[I]}{\alpha K_I}\right)}{K_S \left(1 + \frac{2[I]}{K_I} + \frac{[I]^2}{K_I^2}\right) + [S] \left(1 + \frac{2[I]}{\alpha K_I} + \frac{[I]^2}{\alpha^2 K_I^2}\right)} \quad (2.33)$$

(See appendix C for derivation)

To recapitulate, this section on enzyme kinetics has been presented to explain the development of the kinetic models developed in chapter six and seven, the process by which they were derived, and how to interpret them.

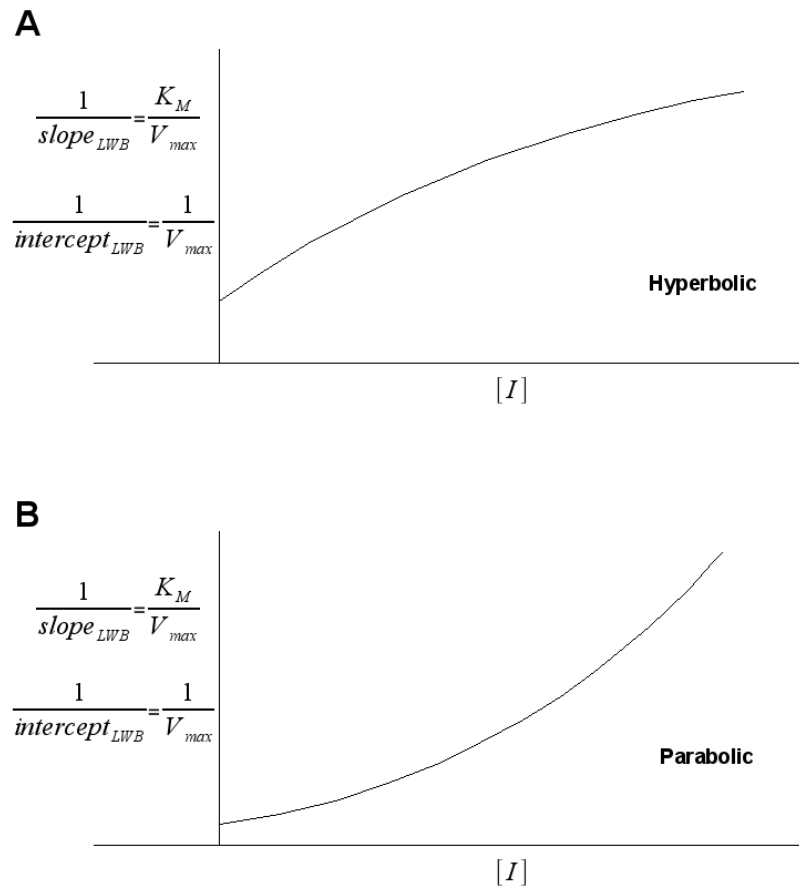


Figure 2.11: Replots of Lineweaver-Burk slopes or intercepts for the detection of non-linear inhibition

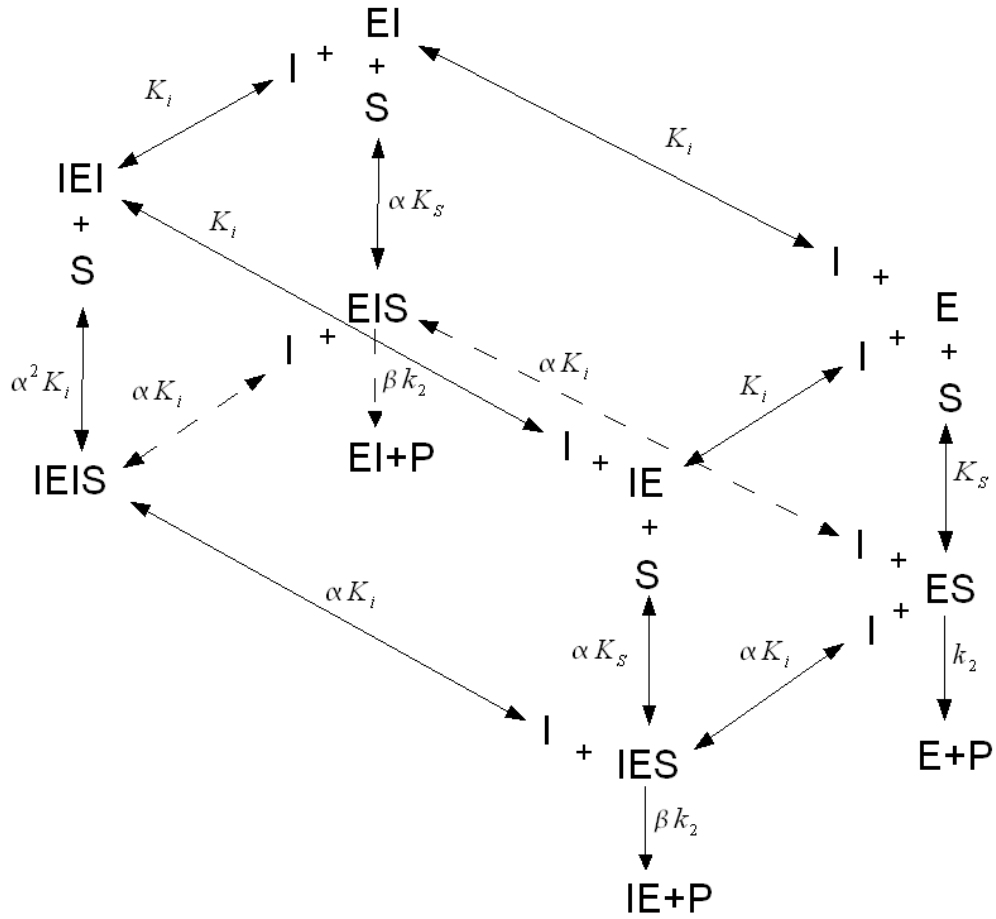


Figure 2.12: Inhibition with 2 inhibitor binding sites affecting the binding of the substrate

Bibliography

- Abadulla E, Tzanov T, Costa S, Robra KH, Cavaco-Paulo A, Gübitz GM. 2000. Decolorization and detoxification of textile dyes with a laccase from *Trametes hirsuta*. *Appl Environ Microbiol* **66**(8): 3357–62.
- Aitken M. 1993. Waste treatment applications of enzymes: opportunities and obstacles. *Chem Eng J* **52**(2): 49–58.
- Akhtar S, Khan AA, Husain Q. 2005. Potential of immobilized bitter melon (*Momordica charantia*) peroxidases in the decolorization and removal of textile dyes from polluted wastewater and dyeing effluent. *Chemosphere* **60**(3): 291–301.
- Alshamsi F, Albadwawi A, Alnuaimi M, Rauf M, Ashraf S. 2007. Comparative efficiencies of the degradation of Crystal Violet using UV/hydrogen peroxide and Fenton's reagent. *Dyes and pigments* **74**(2): 283–287.
- Arica MY, Altintas B, Bayramoğlu G. 2009. Immobilization of laccase onto spacer-arm attached non-porous poly(gma/egdma) beads: application for textile dye degradation. *Bioresour Technol* **100**(2): 665–669.
- Asgher M, Batool S, Bhatti H, Noreen R, Rahman S, Asad MJ. 2008a. Laccase mediated decolorization of vat dyes by *Coriolus versicolor* ibl-04. *Int Biodeterior Biodegrad* **62**(4): 465–470.
- Asgher M, Kausar S, Bhatti H, Shah S, Ali M. 2008b. Optimization of medium for decolorization of solar golden yellow direct textile by *Schizophyllum commune* ibl-06. *Int Biodeterior Biodegrad* **61**(2): 189–193.
- Ay F, Catalkaya EC, Kargi F. 2009. A statistical experiment design approach for advanced oxidation of direct red azo-dye by photo-fenton treatment. *J Hazard Mater* **162**(1): 230–236.
- Bakshi DK, Sharma P. 2003. Genotoxicity of textile dyes evaluated with ames test and textitrec-assay. *J Environ Pathol Toxicol Oncol* **22**(2): 101–9.

- Baldrian P. 2006. Fungal laccases - occurrence and properties. *FEMS Microbiol Rev* **30**(2): 215–42.
- Ball A, Betts W, McCarthy A. 1989. Degradation of lignin-related compounds by actinomycetes. *Appl Environ Microbiol* **55**(6): 1642–1644.
- Banci L. 1997. Structural properties of peroxidases. *J Biotechnol* **53**(2-3): 253–63.
- Barragán B, Costa C, Carmen Márquez M. 2007. Biodegradation of azo dyes by bacteria inoculated on solid media. *Dyes and Pigments* **75**(1): 73–81.
- Bertrand T, Jolivald C, Briozzo P, Caminade E, Joly N, Madzak C, Mougín C. 2002. Crystal structure of a four-copper laccase complexed with an arylamine: insights into substrate recognition and correlation with kinetics. *Biochemistry* **41**(23): 7325–7333.
- Bhatti HN, Akram N, Asgher M. 2008. Optimization of culture conditions for enhanced decolorization of cibacron red fn-2bl by *Schizophyllum commune* ibl-6. *Appl Biochem Biotechnol* **149**(3): 255–264.
- Bohm B. 1994. A test method to determine inhibition of nitrification by industrial wastewaters. *Wat Sci Tech* **26**: 169–172.
- Boominathan K, Reddy CA. 1992. camp-mediated differential regulation of lignin peroxidase and manganese-dependent peroxidase production in the white-rot basidiomycete *Phanerochaete chrysosporium*. *Proc Natl Acad Sci U S A* **89**(12): 5586–5590.
- Bromley-Challenor K, Knapp J, Zhang Z, Gray N, Hetheridge M, Evans M. 2000. Decolorization of an azo dye by unacclimated activated sludge under anaerobic conditions. *Water Research* **34**(18): 4410–4418.
- Bryjak J, Kruczkiewicz P, Rekuć A, Peczyńska-Czoch W. 2007. Laccase immobilization on copolymer of butyl acrylate and ethylene glycol dimethacrylate. *Biochem Eng J* **35**(3): 325–332.
- Bukh C, Lund M, Bjerrum MJ. 2006. Kinetic studies on the reaction between *Trametes villosa* laccase and dioxygen. *J Inorg Biochem* **100**(9): 1547–1557.
- Cameron MD, Timofeevski S, Aust SD. 2000. Enzymology of phanerochaete chrysosporium with respect to the degradation of recalcitrant compounds and xenobiotics. *Appl Microbiol Biotechnol* **54**(6): 751–758.
- Chagas E, Durrant L. 2001. Decolorization of azo dyes by *Phanerochaete chrysosporium* and *Pleurotus sajorcaju*. *Enzyme Microb Technol* **29**: 473–477.
- Champagne PP, Ramsay JA. 2005. Contribution of manganese peroxidase and laccase to dye decoloration by *Trametes versicolor*. *Appl Microbiol Biotechnol* **69**(3): 276–285.

- Chao W, Lee S. 1994. Decolorization of azo dyes by three white-rot fungi: influence of carbon source. *World J Microbiol Biotechnol* **10**: 556–559.
- Christiana V, Shrivastava R, Shukla D, Modib H, Vyas B. 2005. Mediator role of veratryl alcohol in the lignin peroxidase-catalyzed oxidative decolorization of remazol brilliant blue r. *Enzyme Microb Technol* **36**: 426–431.
- Christie R. 2001. *Colour chemistry*. Royal Society of Chemistry: Cambridge (UK), 1st edn, ISBN 0854045732.
- Chu H, Chen K. 2002. Reuse of activated sludge biomass: I. Removal of basic dyes from wastewater by biomass. *Process biochemistry* **37**(6): 595–600.
- Chung N, Aust SD. 1995. Inactivation of lignin peroxidase by hydrogen peroxide during the oxidation of phenols. *Arch Biochem Biophys* **316**(2): 851–855.
- City of Kingston CotCoK. 2000. By-law to control waste discharges to municipal sewers (by-law (2000-263)).
- City of Toronto CotCoT. 2000. Chapter 681 sewers: sewage and land drainage (municipal by-law article 1).
- Claus H. 2003. Laccases and their occurrence in prokaryotes. *Arch Microbiol* **179**(3): 145–50.
- Claus H. 2004. Laccases: structure, reactions, distribution. *Micron* **35**(1-2): 93–6.
- Conesa A, Punt PJ, van den Hondel CAMJJ. 2002. Fungal peroxidases: molecular aspects and applications. *J Biotechnol* **93**(2): 143–58.
- Couto SR, Sanromán MA, Hofer D, Gübitz GM. 2004. Stainless steel sponge: a novel carrier for the immobilisation of the white-rot fungus *Trametes hirsuta* for decolourization of textile dyes. *Bioresour Technol* **95**(1): 67–72.
- Cripps C, Bumpus JA, Aust SD. 1990. Biodegradation of azo and heterocyclic dyes by *Phanerochaete chrysosporium*. *Appl Environ Microbiol* **56**(4): 1114–1118.
- de Jong E, J F, J B. 1994. Aryl alcohols in the physiology of ligninolytic fungi. *FEMS Microbiol Rev* **13**: 153–188.
- dos Santos AZ, Neto JMC, Tavares CRG, da Costa SMG. 2004. Screening of filamentous fungi for the decolorization of a commercial reactive dye. *J Basic Microbiol* **44**(4): 288–295.
- Dosoretz CG, Chen HC, Grethlein HE. 1990. Effect of environmental conditions on extracellular protease activity in lignolytic cultures of *phanerochaete chrysosporium*. *Appl Environ Microbiol* **56**(2): 395–400.

- Dowd J, Riggs D. 1965. A comparison of estimates of Michaelis-Menten kinetic constants from various linear transformations. *J Biol Chem* **240**(2): 863–869.
- Dubrow S, Boardman G, Michelsen D. 1996. *Chemical pretreatment and aerobic-anaerobic degradation of textile dye wastewater*, ch. Chemical pretreatment and aerobic-anaerobic degradation of textile dye wastewater. John Wiley & Sons, pp. 75–102.
- Duran N, Rosa M, DAnnibale A, Gianfreda L. 2002. Applications of laccases and tyrosinases (phenoloxidases) immobilized on different supports: a review. *Enzyme Microb Technol* **31**(7): 907–931.
- Essadki A, Bennajah M, Gourich B, Vial C, Azzi M, Delmas H. 2008. Electrocoagulation/electroflotation in an external-loop air-lift reactor - application to the decolorization of textile dye wastewater: A case study. *Chem Eng Prog* **47**: 1211–1223.
- ETAD. 1996. German ban of use of certain azo compounds in some consumers goods. *Text Chem Color* **28**: 11–13.
- Faraco V, Pezzella C, Miele A, Giardina P, Sannia G. 2009. Bio-remediation of colored industrial wastewaters by the white-rot fungi *Phanerochaete chrysosporium* and *Pleurotus ostreatus* and their enzymes. *Biodegradation* **20**(2): 209–20.
- Ferreira-Leitão V, de Carvalho M, Bon E. 2007. Lignin peroxidase efficiency for methylene blue decolouration: Comparison to reported methods. *Dyes and Pigments* **74**(1): 230–236.
- González S, Petrović M, Radetic M, Jovancic P, Ilic V, Barceló D. 2008. Characterization and quantitative analysis of surfactants in textile wastewater by liquid chromatography/quadrupole-time-of-flight mass spectrometry. *Rapid Commun Mass Spectrom* **22**(10): 1445–1454.
- Goszczynski S, Paszczynski A, Pasti-Grigsby MB, Crawford RL, Crawford DL. 1994. New pathway for degradation of sulfonated azo dyes by microbial peroxidases of *Phanerochaete chrysosporium* and streptomyces chromofuscus. *J Bacteriol* **176**(5): 1339–1347.
- Guimaraes C, Porto P, Oliveira R, Mota M. 2005. Continuous decolourization of a sugar refinery wastewater in a modified rotating biological contactor with *Phanerochaete chrysosporium* immobilized on polyurethane foam disks. *Process Biochem* **40**(2): 535–540.
- Hagen AJ, Hatton TA, Wang DIC. 2006. Protein refolding in reversed micelles. 1990. *Biotechnol Bioeng* **95**(2): 285–294.
- Hai F, Yamamoto K, Fukushi K. 2007. Hybrid treatment systems for dye wastewater. *Critical Reviews in Environmental Science and Technology* **37**(4): 315–377.

- Hameed BH, Tan IAW, Ahmad AL. 2008. Optimization of basic dye removal by oil palm fibre-based activated carbon using response surface methodology. *J Hazard Mater* **158**(2-3): 324–332.
- Han M, Choi H, Song H, *et al.* 2005. Purification and characterization of laccase from the white rot fungus *Trametes versicolor*. *J Microbiol* **43**(2): 555–560.
- Hassan MM, Hawkyard CJ. 2002. Decolourisation of aqueous dyes by sequential oxidation treatment with ozone and fenton's reagent. *J. of Chem. Tech. and Biotech.* **77**: 834–841.
- Heinfling A, Martínez MJ, Martínez AT, Bergbauer M, Szewzyk U. 1998. Transformation of industrial dyes by manganese peroxidases from *Bjerkandera adusta* and *Pleurotus eryngii* in a manganese-independent reaction. *Appl Environ Microbiol* **64**(8): 2788–2793.
- Hofrichter M. 2002. Review: lignin conversion by manganese peroxidase (MnP). *Enzyme and Microb Technol* **30**(4): 454–466.
- Hoigné J. 1998. Chemistry of aqueous ozone and transformation of pollutants by ozonation and advanced oxidation processes. *The handbook of environmental chemistry* **5**: 83–142.
- Hu MR, Chao YP, Zhang GQ, Xue ZQ, Qian S. 2009. Laccase-mediator system in the decolorization of different types of recalcitrant dyes. *J Ind Microbiol Biotechnol* **36**(1): 45–51.
- Johansson T, Nyman PO. 1993. Isozymes of lignin peroxidase and manganese(ii) peroxidase from the white-rot basidiomycete *Trametes versicolor*. i. isolation of enzyme forms and characterization of physical and catalytic properties. *Arch Biochem Biophys* **300**(1): 49–56.
- Kandelbauer A, Maute O, Kessler RW, Erlacher A, Gübitz GM. 2004. Study of dye decolorization in an immobilized laccase enzyme-reactor using online spectroscopy. *Biotechnol Bioeng* **87**(4): 552–563.
- Kang Q. 2007. Residual color profiles of simulated reactive dyes wastewater in flocculation processes by polydiallyldimethylammoniumchloride. *Separation and Purification Technology* **57**(2): 356–365.
- Kapdan I, Kargia F, McMullan G, Marchant R. 2000. Effect of environmental conditions on biological decolorization of textile dyestuff by *Coriolus versicolor* in a rotating biological contactor. *Enzyme Microb Technol* **26**(5-6): 381–387.
- Khadhraoui M, Trabelsi H, Ksibi M, Bouguerra S, Elleuch B. 2009. Discoloration and detoxification of a congo red dye solution by means of ozone treatment for a possible water reuse. *J Hazard Mater* **161**(2-3): 974–981.

- Kim B, Kim Y, Yamamoto T. 2008. Adsorption characteristics of bamboo activated carbon. *Korean J of Chem Eng* **25**(5): 1140–1144.
- Kim GY, Lee KB, Cho SH, Shim J, Moon SH. 2005. Electroenzymatic degradation of azo dye using an immobilized peroxidase enzyme. *J Hazard Mater* **126**(1-3): 183–8.
- King E, Altman C. 1956. A schematic method of deriving the rate laws for enzyme-catalyzed reactions. *J Phys Chem* **60**(10): 1375–1378.
- Kirk TK, Farrell RL. 1987. Enzymatic “combustion”: the microbial degradation of lignin. *Annu Rev Microbiol* **41**: 465–505.
- Knapp J, Newby P. 1995. The microbiological decolorization of an industrial effluent containing a diazo-linked chromophore. *Water Res* **29**(7): 1807–1809.
- Kolekar YM, Pawar SP, Gawai KR, Lokhande PD, Shouche YS, Kodam KM. 2008. Decolorization and degradation of disperse blue 79 and acid orange 10, by *Bacillus fusiformis* kmk5 isolated from the textile dye contaminated soil. *Bioresour Technol* **99**(18): 8999–9003.
- Kunamneni A, Ghazi I, Camarero S, Ballesteros A, Plou F, Alcalde M. 2008. Decolorization of synthetic dyes by laccase immobilized on epoxy-activated carriers. *Process Biochem* **43**(2): 169–173.
- Leonowicz A, Cho NS, Luterek J, Wilkolazka A, Wojtas-Wasilewska M, Matuszewska A, Hofrichter M, Wesenberg D, Rogalski J. 2001. Fungal laccase: properties and activity on lignin. *J Basic Microbiol* **41**(3-4): 185–227.
- Leskovac V. 2003. *Comprehensive enzyme kinetics*. Kluwer Academic Publishers: New York, 1st edn, ISBN 978-0306467127.
- Levin L, Papinutti L, Forchiassin F. 2004. Evaluation of argentinean white rot fungi for their ability to produce lignin-modifying enzymes and decolorize industrial dyes. *Bioresour Technol* **94**(2): 169–176.
- Lewis D. 1999. Coloration in the next century. *Review of Progress in Coloration and Related Topics* **29**(1): 23–28.
- Li X, Jia R. 2008. Decolorization and biosorption for congo red by system rice hull- *Schizophyllum* sp. f17 under solid-state condition in a continuous flow packed-bed bioreactor. *Bioresour Technol* **99**(15): 6885–92.
- Li X, Jia R, Li P, Ang S. 2009. Response surface analysis for enzymatic decolorization of Congo red by manganese peroxidase. *Journal of Molecular Catalysis. B, Enzymatic* **56**(1): 1–6.

- Libra JA, Borchert M, Banit S. 2003. Competition strategies for the decolorization of a textile-reactive dye with the white-rot fungi *Trametes versicolor* under non-sterile conditions. *Biotechnol Bioeng* **82**(6): 736–44.
- Linke D, Bouws H, Peters T, Nimtz M, Berger R, Zorn H. 2005. Laccases of *Pleurotus sapidus*: characterization and cloning. *J Agric Food Chem* **53**(24): 9498–9505.
- Liu G, Zhou J, Qu Y, Ma X. 2007. Decolorization of sulfonated azo dyes with two photosynthetic bacterial strains and a genetically engineered *Escherichia coli* strain. *World J of Microbiol Biotechnol* **23**(7): 931–937.
- López C, Moreira MT, Feijoo G, Lema JM. 2004. Dye decolorization by manganese peroxidase in an enzymatic membrane bioreactor. *Biotechnol Prog* **20**(1): 74–81.
- Lu X, Yang B, Chen J, Sun R. 2009. Treatment of wastewater containing azo dye reactive brilliant red x-3b using sequential ozonation and upflow biological aerated filter process. *J Hazard Mater* **161**(1): 241–5.
- Madaeni S, Rostami E. 2008. Spectroscopic Investigation of the Interaction of BSA with Cationic Surfactants. *Chem Eng Technol* **31**(9).
- Maguire R. 1992. Occurrence and persistence of dyes in a canadian river. *Water Sci Technol* **25**(11): 265–270.
- Mason R, Peterson F, Holtzman J. 1978. Inhibition of Azoreductase by Oxygen The Role of the Azo Anion Free Radical Metabolite in the Reduction of Oxygen to Superoxide. *Molecular Pharmacology* **14**(4): 665–671.
- Matsui M. 1996. *Environmental chemistry of dyes and pigments*, ch. Ozonation. John Wiley & sons Inc.: New York, pp. 43–59.
- Mendonça RT, Jara JF, González V, Elissetche JP, Freer J. 2008. Evaluation of the white-rot fungi *ganoderma australe* and *ceriporiopsis subvermispora* in biotechnological applications. *J Ind Microbiol Biotechnol* **35**(11): 1323–1330.
- Michniewicz A, Ledakowicz S, Ullrich R, Hofrichter M. 2008. Kinetics of the enzymatic decolorization of textile dyes by laccase from *Cerrena unicolor*. *Dyes and Pigments* **77**(2): 295–302.
- Moawad H, El-Rahim W, Khalafallah M. 2003. Evaluation of biotoxicity of textile dyes using two bioassays. *J Basic Microbiol* **43**(3): 218–229.
- Moreira M, Feijoo G, Lema J. 2003. Fungal bioreactors: applications to white-rot fungi. *Rev Environ Sci and Biotechnol* **2**(2): 247–259.

- Mosbach R, Koch-Schmidt AC, Mosbach K. 1976. *Immobilized enzymes, Methods in Enzymology*, vol. 44, ch. Immobilization of enzymes to various acrylic copolymers. Elsevier, ISBN 978-0-12-181944-6, pp. 53–65.
- Murugesan K, Yang IH, Kim YM, Jeon JR, Chang YS. 2009. Enhanced transformation of malachite green by laccase of *Ganoderma lucidum* in the presence of natural phenolic compounds. *Appl Microbiol Biotechnol* **82**(2): 341–50.
- Nilsson I, Möller A, Mattiasson B, Rubindamayugi M, Welander U. 2006. Decolorization of synthetic and real textile wastewater by the use of white-rot fungi. *Enzyme Microb Technol* **38**(1-2): 94–100.
- Nunes AA, Franca AS, Oliveira LS. 2009. Activated carbons from waste biomass: an alternative use for biodiesel production solid residues. *Bioresour Technol* **100**(5): 1786–92.
- Nyanhongo GS, Gomes J, Gübitz GM, Zvauya R, Read J, Steiner W. 2002. Decolorization of textile dyes by laccases from a newly isolated strain of *trametes modesta*. *Water Res* **36**(6): 1449–1456.
- of public works M, government services Canada. 2001. Canadian environmental protection act 1999 - priority substances list assessment report - textile mill effluents. Technical report, Environment Canada - Health Canada.
- Ollikka P, Alhonmaki K, Leppanen V, Glumoff T, Rajjola T, Suominen I. 1993. Decolorization of azo, triphenyl methane, heterocyclic, and polymeric dyes by lignin peroxidase isoenzymes from *Phanerochaete chrysosporium*. *Applied and Environmental Microbiology* **59**(12): 4010–4016.
- O'Neill C, Hawkes F, Hawkes D, Lourenco N, Pinheiro H, Delee W. 1999. Colour in textile effluents-sources, measurement, discharge consents and simulation: a review. *J Chem Technol Biotechnol* **74**(11).
- O'Neill C, Lopez A, Esteves S, Hawkes FR, Hawkes DL, Wilcox S. 2000. Azo-dye degradation in an anaerobic-aerobic treatment system operating on simulated textile effluent. *Appl Microbiol Biotechnol* **53**(2): 249–254.
- Otzen D, Sehgal P, Westh P. 2009. α -Lactalbumin is unfolded by all classes of surfactants but by different mechanisms. *J Colloid Interface Sci* **329**(2): 273–283.
- Palma C, Moreira M, Mielgo I, Feijoo G, Lema J. 1999. Use of a fungal bioreactor as a pretreatment or post-treatment step for continuous decolorisation of dyes. *Water Sci Technol* **40**(8): 131–136.
- Pasti-Grigsby MB, Paszczynski A, Goszczynski S, Crawford DL, Crawford RL. 1992. Influence of aromatic substitution patterns on azo dye degradability by *Streptomyces* spp. and *Phanerochaete chrysosporium*. *Appl Environ Microbiol* **58**(11): 3605–3613.

- Paszczynski A, Pasti-Grigsby MB, Goszczynski S, Crawford RL, Crawford DL. 1992. Mineralization of sulfonated azo dyes and sulfanilic acid by *Phanerochaete chrysosporium* and *Streptomyces chromofuscus*. *Appl Environ Microbiol* **58**(11): 3598–3604.
- Peralta-Zamora P, Pereira C, Tiburtius E, Moraes S, Rosa M, Minussi R, Durán N. 2003. Decolorization of reactive dyes by immobilized laccase. *Appl Catal B* **42**(2): 131–144.
- Pierce J. 1994. Colour in textile effluents-the origins of the problem. *J Soc Dyers Colourists* **110**: 131–133.
- Podgornik H, Grgić I, Perdih A. 1999. Decolorization rate of dyes using lignin peroxidases of *Phanerochaete chrysosporium*. *Chemosphere* **38**(6): 1353–1359.
- Podgornik H, Podgornik A. 2002. Characteristics of LiP immobilized to CIM monolithic supports. *Enzyme Microb Technol* **31**(6): 855–861.
- Pointing SB. 2001. Feasibility of bioremediation by white-rot fungi. *Appl Microbiol Biotechnol* **57**(1-2): 20–33.
- Ramsay JA, Goode C. 2004. Decoloration of a carpet dye effluent using *Trametes versicolor*. *Biotechnol Lett* **26**(3): 197–201.
- Rebrikov D, Stepanova E, Koroleva O, Budarina Z, Zakharova M, Yurkova T, Solonin A, Belova O, Pozhidaeva Z, Leontevsky A. 2006. Laccase of the lignolytic fungus *Trametes hirsuta*: Purification and characterization of the enzyme, and cloning and primary structure of the gene. *Appl Biochem Microbiol* **42**(6): 564–572.
- Reid R. 1996. Go green-a sound business decision (part I). *J Soc Dyers Colour* **112**.
- Reife A, Freeman H. 1996. *Environmental chemistry of dyes and pigments*, ch. Carbon adsorption of dyes and selected intermediates. John Wiley & Sons Inc: New York, ISBN 978-0471589273, pp. 3–29.
- Rekuć A, Bryjak J, Szymańska K, Jarzebski A. 2009a. Laccase immobilization on mesostructured cellular foams affords preparations with ultra high activity. *Process Biochem* **44**(2): 191–198.
- Rekuć A, Jastrzemska B, Liesiene J, Bryjak J. 2009b. Comparative studies on immobilized laccase behaviour in packed-bed and batch reactors. *J Mol Catal B: Enzym* **57**(1-4): 216–223.
- Rekuć A, Kruczkiewicz P, Jastrzemska B, Liesiene J, Peczyńska-Czoch W, Bryjak J. 2008. Laccase immobilization on the tailored cellulose-based granocel carriers. *Int J Biol Macromol* **42**(2): 208–215.

- Reyes P, Pickard M, Vazquez-Duhalt R. 1999. Hydroxybenzotriazole increases the range of textile dyes decolorized by immobilized laccase. *Biotechnol Lett* **21**(10): 875–880.
- Robinson T, McMullan G, Marchant R, Nigam P. 2001. Remediation of dyes in textile effluent: a critical review on current treatment technologies with a proposed alternative. *Bioresour Technol* **77**(3): 247–255.
- Robinson T, Nigam PS. 2008. Remediation of textile dye waste water using a white-rot fungus *Bjerkandera adusta* through solid-state fermentation (ssf). *Appl Biochem Biotechnol* **151**(2-3): 618–628.
- Rodriguez Couto S, Rivela I, Munoz M, Sanromán A. 2000. Ligninolytic enzyme production and the ability of decolourisation of Poly R-478 in packed-bed bioreactors by *Phanerochaete chrysosporium*. *Bioprocess Biosyst Eng* **23**(3): 287–293.
- Russ R, Rau J, Stolz A. 2000. The function of cytoplasmic flavin reductases in the reduction of azo dyes by bacteria. *Appl Environ Microbiol* **66**(4): 1429–1434.
- Russo M, Giardina P, Marzocchella A, Salatino P, Sannia G. 2008. Assessment of anthraquinone-dye conversion by free and immobilized crude laccase mixtures. *Enzyme Microb Technol* **42**(6): 521–530.
- Ryan S, Schnitzhofer W, Tzanov T, Cavaco-Paulo A, Gübitz G. 2003. An acid-stable laccase from *Sclerotium rolfsii* with potential for wool dye decolourization. *Enzyme Microb Technol* **33**(6): 766–774.
- Schliephake K, Lonergan G, Jones C, Mainwaring D. 1993. Decolourisation of a pigment plant effluent by *Pycnoporus cinnabarinus* in a packed-bed bioreactor. *Biotechnology Lett* **15**(11): 1185–1188.
- Segel I. 1993. *Enzyme kinetics: behavior and analysis of rapid equilibrium and steady-state enzyme systems*. Wiley Classics Library, John Wiley & Sons: New York, ISBN 978-0471303091.
- Shaffiqu TS, Roy JJ, Nair RA, Abraham TE. 2002. Degradation of textile dyes mediated by plant peroxidases. *Appl Biochem Biotechnol* **102-103**(1-6): 315–326.
- Shahvali M, Assadi M, Rostami K. 2000. Effect of environmental parameters on decolorization of textile wastewater using *Phanerochaete chrysosporium*. *Bioprocess Biosyst Eng* **23**(6): 721–726.
- Shaul G, Holdsworth T, Dempsey C, Dostal K. 1991. Fate of water soluble azo dyes in the activated sludge process. *Chemosphere* **22**(1): 107–119.
- Shrivastava R, Christian V, Vyas B. 2005. Enzymatic decolorization of sulfonphthalein dyes. *Enzyme and Microbial Technology* **36**(2-3): 333–337.

- Slokar Y, Majcen Le Marechal A. 1998. Methods of decoloration of textile wastewaters. *Dyes and Pigments* **37**(4): 335–356.
- Smith B. 1986. *Identification and reduction of pollution sources in textile wet processing*. Pollution Prevention Pays Program, Dept. of Natural Resources and Community Development.
- Solomon E, Sundaram U, Machonkin T. 1996. Multicopper oxidases and oxygenases. *Chem Rev* **96**(7): 2563–2606.
- Spadaro JT, Renganathan V. 1994. Peroxidase-catalyzed oxidation of azo dyes: mechanism of disperse yellow 3 degradation. *Arch Biochem Biophys* **312**(1): 301–307.
- Staszczak M, Zdunek E, Leonowicz A. 2000. Studies on the role of proteases in the white-rot fungus *Trametes versicolor*: effect of pmsf and chloroquine on ligninolytic enzymes activity. *J Basic Microbiol* **40**(1): 51–63.
- Sun S, Li C, Sun J, Shi S, Fan M, Zhou Q. 2009. Decolorization of an azo dye Orange G in aqueous solution by Fenton oxidation process: Effect of system parameters and kinetic study. *J Hazard Mater* **161**(2-3): 1052–1057.
- Supaka N, Juntongjin K, Damronglerd S, Delia M, Strehaiano P. 2004. Microbial decolorization of reactive azo dyes in a sequential anaerobic–aerobic system. *Chem Eng J* **99**(2): 169–176.
- Swamy J, Ramsay J. 1999a. Effects of glucose and nh_4^+ concentrations on sequential dye decoloration by *Trametes versicolor*. *Enzyme Microb Technol* **25**(3-5): 278–284.
- Swamy J, Ramsay J. 1999b. Effects of Mn^{2+} and NH_4^+ concentrations on laccase and manganese peroxidase production and Amaranth decoloration by *Trametes versicolor*. *Appl Microbiol and Biotechnol* **51**(3): 391–396.
- Swamy J, Ramsay J. 1999c. The evaluation of white rot fungi in the decoloration of textile dyes. *Enzyme Microb Technol* **24**(3-4): 130–137.
- Talarposhti AM, Donnelly T, Anderson GK. 2001. Colour removal from a simulated dye wastewater using a two-phase anaerobic packed bed reactor. *Water Res* **35**(2): 425–432.
- Tien M, Kirk TK. 1983. Lignin-degrading enzyme from the hymenomycete phanerochaete chrysosporium burds. *Science* **221**(4611): 661–663.
- Tien M, Kirk TK, Bull C, Fee JA. 1986. Steady-state and transient-state kinetic studies on the oxidation of 3,4-dimethoxybenzyl alcohol catalyzed by the ligninase of *Phanerochaete chrysosporium* burds. *J Biol Chem* **261**(4): 1687–1693.

- Torres E, Bustos-Jaimes I, Le Borgne S. 2003. Potential use of oxidative enzymes for the detoxification of organic pollutants. *Appl Catal, B* **46**(1): 1–15.
- Vandevivere P, Bianchi R, Verstraete W. 1998. Review: Treatment and reuse of wastewater from the textile wet-processing industry: Review of emerging technologies. *J Chem Technol Biotechnol* **72**(4).
- Verma P, Madamwar D. 2002. Decolorization of synthetic textile dyes by lignin peroxidase of *Phanerochaete chrysosporium*. *Folia microbiol* **47**(3): 283–286.
- von Gunten U. 2007. The basics of oxidants in water treatment. part b: ozone reactions. *Water Sci Technol* **55**(12): 25–29.
- Wang C, Yediler A, Lienert D, Wang Z, Kettrup A. 2002. Toxicity evaluation of reactive dyestuffs, auxiliaries and selected effluents in textile finishing industry to luminescent bacteria *Vibrio fischeri*. *Chemosphere* **46**(2): 339–344.
- Wang H, Ng T. 2006. Purification of a laccase from fruiting bodies of the mushroom *Pleurotus eryngii*. *Appl Microbiol Biotechnol* **69**(5): 521–525.
- Wang P, Fan X, Cui L, Wang Q, Zhou A. 2008a. Decolorization of reactive dyes by laccase immobilized in alginate/gelatin blend with PEG. *J Environ Sci* **20**(12): 1519–1522.
- Wang W, Wang YJ, Wang DQ. 2008b. Dual effects of tween 80 on protein stability. *Int J Pharm* **347**(1-2): 31–8.
- Wariishi H, Gold M. 1989. Lignin peroxidase compound III: formation, inactivation, and conversion to the native enzyme. *FEBS Lett* **243**: 165–168.
- Wariishi H, L A, MH G. 1988. Manganese peroxidation from the basidiomycete phanerochaete chrysosporium. *Biochemistry* **27**: 5365–5370.
- Waring D, Hallas G. 1990. *The chemistry and application of dyes*. Topics in Applied Chemistry, Springer, 1st edn, ISBN 978-0306432781.
- Wesenberg D, Kyriakides I, Agathos SN. 2003. White-rot fungi and their enzymes for the treatment of industrial dye effluents. *Biotechnol Adv* **22**(1-2): 161–187.
- Wilkinson G. 1961. Statistical estimations in enzyme kinetics. *Biochem J* **80**(2): 324–332.
- Willmott N, Guthrie J, Nelson G. 1998. The biotechnology approach to colour removal from textile effluent. *J Soc Dyers Colour* **114**(2): 38–41.
- Wong Y, Yu J. 1999. Laccase-catalyzed decolorization of synthetic dyes. *Water Res* **33**(16): 3512–3520.

- Wu J, Doan H, Upreti S. 2008. Decolorization of aqueous textile reactive dye by ozone. *Chemical Engineering Journal* **142**(2): 156–160.
- Xu F. 1996. Oxidation of phenols, anilines, and benzenethiols by fungal laccases: correlation between activity and redox potentials as well as halide inhibition. *Biochemistry* **35**(23): 7608–14.
- Yang F, Yu J. 1996a. Development of a bioreactor system using an immobilized white rot fungus for decolorization - Part I: Cell immobilization and repeated-batch decolorization tests. *Bioprocess Biosyst Eng* **15**(6): 307–310.
- Yang F, Yu J. 1996b. Development of a bioreactor system using an immobilized white rot fungus for decolorization - Part II: Continuous decolorization tests. *Bioprocess Biosyst Eng* **16**(1): 9–11.
- Yang Z, Robb D. 2005. Tyrosinase activity in reversed micelles. *Biocatal Biotransform* **23**(6): 423–430.
- Young L, Yu J. 1997. Ligninase-catalysed decolorization of synthetic dyes. *Water Res* **31**(5): 1187–1193.
- Zhang F, Knapp J, Tapley K. 1999. Development of bioreactor systems for decolorization of Orange II using white rot fungus. *Enzyme Microb Technol* **24**(1-2): 48–53.
- Zhou W, Zimmermann W. 1993. Decolorization of industrial effluents containing reactive dyes by actinomycetes. *FEMS Microbiol Lett* **107**(2-3): 157–161.
- Zhu Y, Kaskel S, Shi J, Wage T, van Pée K. 2007. Immobilization of *Trametes versicolor* Laccase on Magnetically Separable Mesoporous Silica Spheres. *Chem Mater* **19**(26): 6408–6413.
- Zidane F, Drogui P, Lekhlif B, Bensaid J, Blais JF, Belcadi S, Kacemi KE. 2008. Decolourization of dye-containing effluent using mineral coagulants produced by electrocoagulation. *J Hazard Mater* **155**(1-2): 153–163.
- Zille A, Tzanov T, Gübitz GM, Cavaco-Paulo A. 2003. Immobilized laccase for decolourization of reactive black 5 dyeing effluent. *Biotechnol Lett* **25**(17): 1473–1477.

Chapter 3

Reactive blue 19 decolourization by laccase immobilized on silica beads

The final manuscript of this chapter was accepted the 16th of September 2007 for publication in Applied Microbiology and Biotechnology (77:819-823) / Published online: 5 October 2007, Springer-Verlag ©2007

3.1 Abstract

Laccase (31.5 U of activity/g or 4.39 μg of protein/ m^2) from *Trametes versicolor* was immobilized on controlled-porosity-carrier (CPC) silica beads and evaluated for the decolourization of Reactive blue 19, an anthraquinone dye. Immobilizing laccase changed the pH activity profile of ABTS oxidation from a decaying trend to a bell-shaped curve with an optimum at pH 5 but did not affect dye decolourization. Although there was an initial rapid dye adsorption on the beads, 97.5 % of Reactive blue 19 removal was due to enzymatic degradation. Treating the laccase immobilized beads with ethanolamine reduced dye adsorption by 40 %. While the free enzyme lost 52 % of its activity in 48 h, the activity of

the immobilized laccase was unchanged after four months of storage and three successive decolourizations over 120 h.

3.2 Introduction

Environmental regulations of the discharge of coloured effluents have become more stringent because approximately 50,000 tons of toxic textile dyes are released into the environment every year worldwide (Lewis, 1999). In Canada, the discharge of coloured effluents to municipal sewage is prohibited in the cities of Kingston and Toronto (City of Kingston, 2000; City of Toronto, 2000). A combination of physical, chemical and biological processes can efficiently treat coloured effluents (Robinson *et al.*, 2001) but a single technology may be more cost-effective.

White rot fungi degrade a wide range of persistent organic pollutants like phenols (Ko and Chen, 2008; D'Annibale *et al.*, 2000; Hublik and Schinner, 2000; Zhang *et al.*, 2008), pesticides (Jolivalt *et al.*, 2000) and textile dyes with their lignin-degrading enzymes such as lignin peroxidase, manganese (II)-dependent peroxidase and laccase (phenol oxidase). Laccases degrade dyes with phenolic and quinone moieties efficiently and may need a redox mediator like hydroxybenzotriazole for dyes that do not include these molecular features (Reyes *et al.*, 1999; Nyanhongo *et al.*, 2002; Peralta-Zamora *et al.*, 2003; Couto, 2007).

Using enzymes instead of fungal cultures would eliminate the need for laccase production which depends on the cultures metabolic state which, in turn, is affected by conditions such as pH and variation in effluent composition. The enzyme concentration in an immobilized enzyme reactor is more easily controlled than that in fungal bioreactor. Moreover, immobilization of laccase is potentially more cost-effective than using the free enzyme since

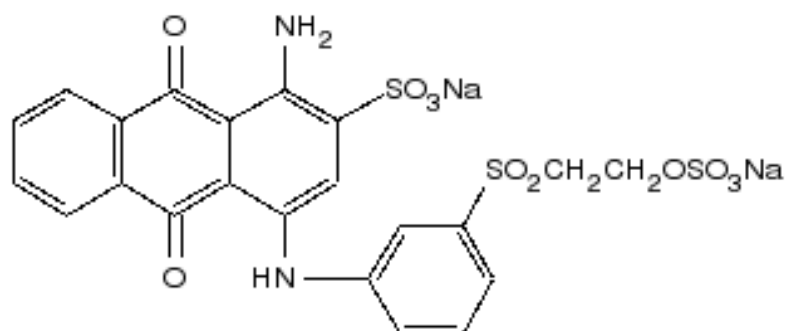


Figure 3.1: Chemical structure of Reactive blue 19

it would greatly reduce enzyme loss and allow re-use. Laccase immobilized on various supports has been evaluated for the treatment of pollutants such as phenols (Shuttleworth and Bollag, 1986; Duran and Esposito, 2000; Duran *et al.*, 2002) but few have investigated dye decolourization. Immobilization of laccase on imidazol-modified silica gel (Peralta-Zamora *et al.*, 2003) and silanized alumina particles (Zille *et al.*, 2003) have shown that while both enzymatic degradation and sorption contributed to dye removal, the contribution of enzymatic decolourization was quite minor.

Although many studies have previously dealt with immobilized laccase on silica (Duran *et al.*, 2002), it has not been used for dye decolourization to our knowledge. In addition, the immobilization can change an enzymes kinetic behaviour and response to environmental conditions and these must also be quantified for design purposes. This study therefore evaluates the decolourization of Reactive blue 19 (Figure 3.1), an anthraquinone dye, by *Trametes versicolor* laccase immobilized on controlled porosity carrier (CPC)-silica beads and the impact of protein immobilization on dye decolourization.

3.3 Materials and Methods

3.3.1 Chemicals

Pre-silanized (with 3-aminopropyltriethoxysilane (APTES)) CPC silica beads, *Trametes versicolor* laccase, Reactive blue 19 and 2,2'-Azino-bis(3-ethylbenzothiazoline-6-sulfonic acid) (diammonium salt) were purchased from Sigma-Aldrich (Oakville, ON, Canada) and glutaraldehyde from Acros (Belgium).

3.3.2 Surface area of beads

The surface area was determined by measuring the amount of N₂ gas adsorbed on the beads at different partial pressures (de Kanel and Morse, 1979) with a Micrometric Tristar 300 (Micrometric Instrument Corp).

3.3.3 Immobilization of laccase on CPC-Silica

Four grams of pre-silanized CPC-silica beads (355 to 600 μm in diameter, an average surface area of 42.1 m²/g and a pore size of 37.5 nm) were immersed in degassed 2.5 % glutaraldehyde in 0.1 M KH₂PO₄ at pH 5.0 for 2 h and thereafter placed in a laccase solution (3 U/ml in 0.1 M KH₂PO₄ pH 5.0) for 36 h at 4°C. The beads were subsequently washed three times with distilled water and twice with phosphate buffer.

3.3.4 Free and immobilized enzyme assay

Laccase activity was measured by monitoring with a spectrophotometer the generation of 2,2'-Azino-bis(3-ethylbenzothiazoline-6-sulfonic acid radicals (ABTS^{•-}) at 420 nm from the oxidation of ABTS (Wolfenden and Willson, 1982) at 23 \pm 1°C using a Spectramax

250 plate reader with the SOFTmax PRO software package (Molecular Devices, CA, USA). The assay mixture contained 0.2 mM ABTS, 100 mM sodium acetate buffer (pH 5.0) and the enzyme sample (Bourbonnais *et al.*, 1995). One unit of laccase activity (U) was defined as the amount of enzyme that formed 1 μmol ABTS \bullet^- per min. Protein concentration was measured as the absorbance at 280 nm and corrected for scattering effects with absorbance readings at 320 nm according to equation 3.1:

$$A_{corr}^{280} = A_{280} - A_{320} * \left(\frac{320}{280} \right)^4 \quad (3.1)$$

For the immobilized laccase system, the CPC silica-laccase packed bed reactor (I.D. = 10 mm, l = 23 mm) was connected to a reservoir containing 100 ml of 50 mM sodium acetate/50 mM KH_2PO_4 (pH 5) via a peristaltic pump. The solution was 100 % re-circulated between the packed bed and the reservoir at a flow rate of 75 ml/min. To determine the immobilized laccase activity, the linear variation of the concentration of ABTS \bullet^- in the reservoir with time was measured for a 6 or 10 minute interval.

3.3.5 Decolourization of Reactive blue 19 by free laccase

Reactive blue 19 (0.036 mM or 22.5 mg/l) was decolorized with 5-7 U laccase in 125-ml Erlenmeyer flasks containing 50 ml 0.1 M KH_2PO_4 at pH 5.0. Controls were identical but did not contained laccase. All experiments were done at 23 ± 1 °C and pH 5. The dye concentration was chosen since it is in the range of the typical dye concentration found in textile wastewaters (O'Neill *et al.*, 1999)

3.3.6 Dye concentration

Reactive blue 19 concentration was measured using a Unicam UV1 spectrophotometer (Spectronic Unicam, Cambridge, UK) at 592 nm, the maximum wavelength of absorbance. The concentration of 0.036 mM (50 ppm) was chosen since it is typical of residual dye concentration found in a textile wastewater (O'Neill *et al.*, 1999).

3.3.7 Decolourization of Reactive blue 19 by immobilized laccase

A solution of Reactive blue 19 (0.036 mM) was continuously re-circulated at 4.15 ml/min (equivalent to a hydraulic retention time of 2.44 min) from a reservoir containing 400 ml of dye solution to a packed bed reactor (I.D. = 1.6 cm, h = 5.0 cm) with 4 g of CPC-silica-laccase beads. Figure 3.2 shows a schematic of the experimental setup. The bed and void volumes were about 10 and 1.6 ml respectively. After decolourization, the beads were stored in 0.1 M KH_2PO_4 buffer at pH 5 and $23 \pm 1^\circ\text{C}$ for 4 months. The rate of decolourization was calculated by dividing the concentration difference between the reactor inlet and outlet by the hydraulic retention time. The average rate was calculated by averaging the decolourization rates in the reactor over the time interval during which the rates were approximately constants. The rate constant was calculated by dividing the rate of decolourization in the reactor by average concentration in the reactor C_{inlet} (see Appendix D.2 for a sample calculation). After storage, Reactive blue 19 decolourization was measured. All experiments were done at $23 \pm 1^\circ\text{C}$ and pH 5.

3.3.8 Effect of enzyme immobilization on the pH profile of laccase

Free and immobilized laccase average reaction rates with 500 μM ABTS or 50 μM Reactive blue 19 were measured in triplicate at pH 3, 4, 5, 6 and 7. For these experiments, the packed

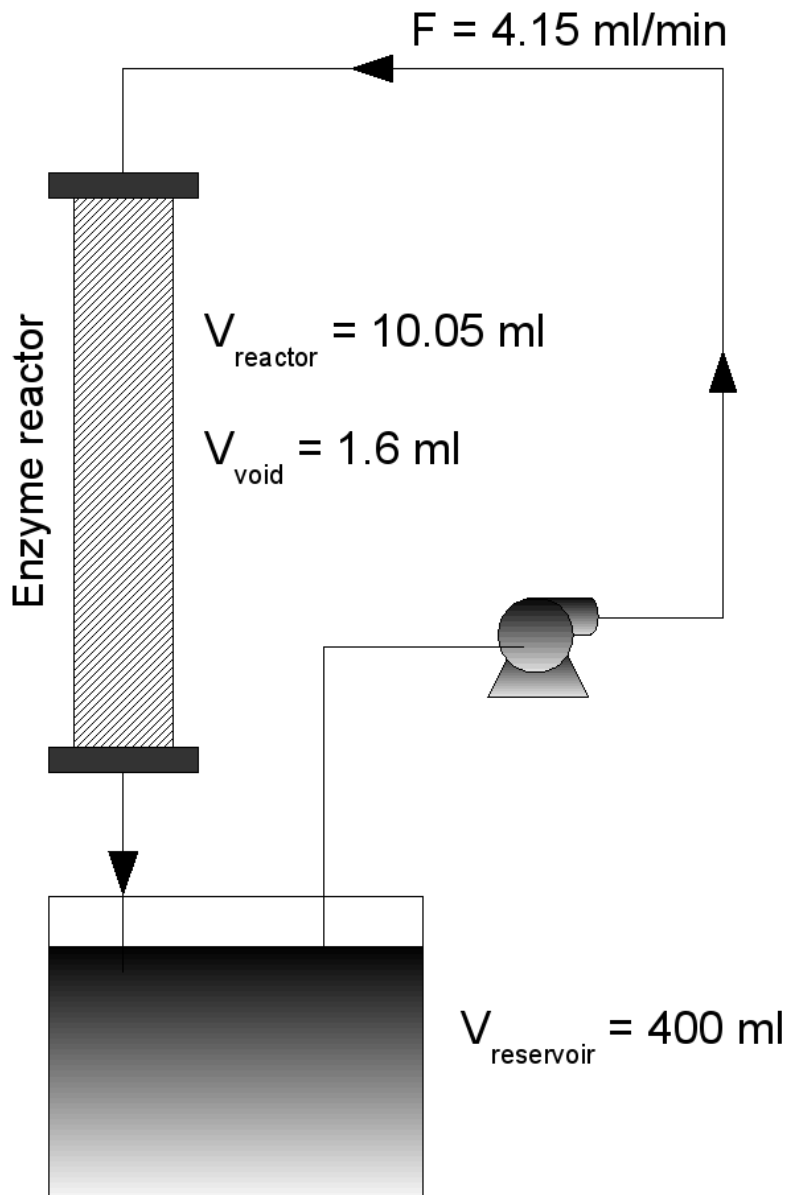


Figure 3.2: Schematic of Immobilized laccase setup

bed reactor of CPC silica-laccase (I.D. = 10 mm, l = 23 mm, 2.5 g CPC-silica-laccase beads) was connected to a reservoir containing 100 ml of 50 mM sodium acetate/50 mM KH_2PO_4 (pH 5) via a peristaltic pump. The solution was 100 % re-circulated between the packed bed and the reservoir at a flow rate of 75 ml/min. The linear variation of the concentration of $\text{ABTS}^{\bullet-}$ or Reactive blue 19 with time in the reservoir was measured over a time interval of 10 minutes to determine the immobilized laccase average rate of reaction.

3.3.9 Reactive blue 19 adsorption and desorption

1.2 l of Reactive blue 19 solution (0.036 mM) was passed through the packed bed of CPC-silica beads (I.D. = 1.6 cm, h = 5.0 cm, 4 g beads) at a flow rate of 32.8 ml/min with active or heat inactivated laccase (autoclaved for 20 min at 121 °C). All other details are as described in the decolourization experiment. The residual aqueous dye concentration in the reservoir was measured and equilibrium was achieved within 3 hours. The dye adsorbed to the beds was extracted with methanol until no further dye could be desorbed.

To determine if ethanolamine treatment after laccase immobilization would reduce dye adsorption, CPC-silica-laccase beads were treated with 1 M ethanolamine and 0.2 M borane-dimethyl amine. Laccase on treated and untreated beads was inactivated by autoclaving for 20 min at 121 °C and thereafter exposed to 50 ml of 0, 39.9, 79.8, 119.7 and 159.6 μM Reactive blue 19 in 50 mM KH_2PO_4 at pH 5 and 23.0 °C for 24 h in 125 ml erlenmeyer flasks. Inactivation was confirmed since no laccase activity was detected after autoclaving. Equilibrium was achieved in approximately 8 h.

3.4 Results

3.4.1 Enzyme immobilization on CPC-silica

Glutaraldehyde was used to crosslink laccase to pre-silanized CPC silica beads. The activity of immobilized laccase calculated from the declined activity in the supernatant from three independent experiments was 31.5 ± 4.3 U/(g beads) with a protein loading of 185 ± 58 $\mu\text{g}/(\text{g beads})$. However, the measured immobilized enzyme activity on the beads was 1.11 ± 0.12 U/g.

3.4.2 Dye decolourization by free or immobilized laccase

Good decolourization rates of Reactive blue 19 were achieved in a re-circulating packed bed reactor with laccase immobilized beads (Figure 3.3). As the recirculation rate increased from 4.15 to 32.8 ml/min, the decolourization rate increased from 11.98 to 47.07 $\mu\text{M}/\text{U}\cdot\text{h}$. These rates are better than those obtained with the free enzyme which decolorized 90 % of Reactive blue 19 at an initial rate of 8.25 $\mu\text{M}/\text{U}\cdot\text{h}$. The free enzyme activity remained constant during the three hours of decolourization.

3.4.3 Stability of decolourizing activity

After 4 months of storage at 23 ± 1 °C and pH 5 in 0.1 M KH_2PO_4 buffer, immobilized laccase decolourized Reactive blue 19 to a similar extent and rate as freshly prepared beads. After storage, 80 to 71 % decolourization was achieved in three successive decolourizations over 120 hours (Figure 3.4) with average pseudo-first order reaction rate constant of 1.28 ± 0.03 , 1.31 ± 0.04 and 1.51 ± 0.03 h^{-1} in the first, second and third decolourizations respectively. The pseudo-first order rate constants were calculated by dividing the

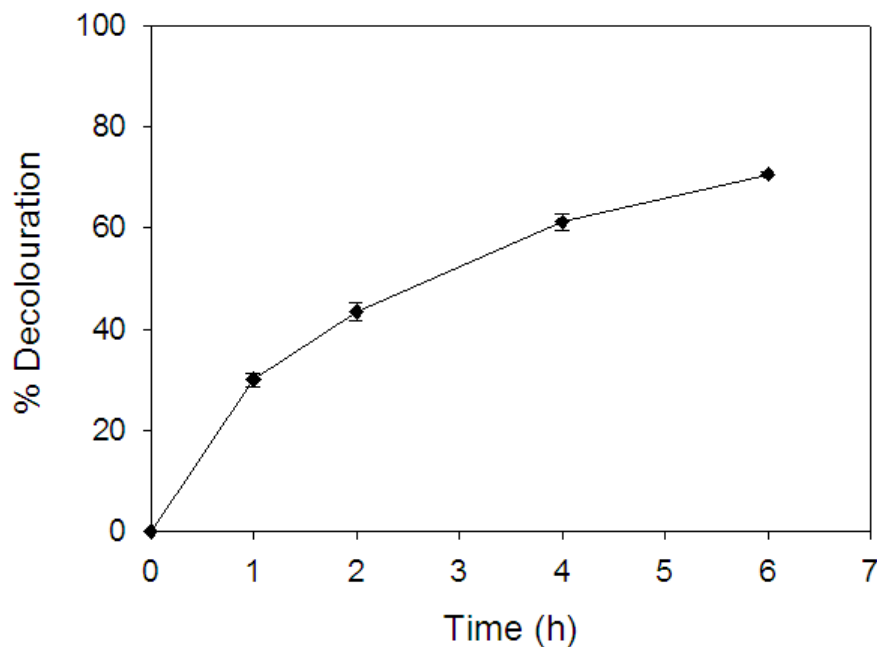


Figure 3.3: Decolourization of Reactive blue 19 by laccase immobilized on CPC-silica beads with 4 g of beads in a packed bed at pH 5.0 and 23 ± 1 °C at a recirculation rate of 4.15 ml/min and an initial dye concentration of 0.036 mM

decolourization rates by the dye concentration at each time point. The enzyme did not leak from the beads as laccase activity was not detected in the aqueous phase.

3.4.4 Effect of enzyme immobilization on the pH profile of laccase

Immobilizing laccase affected the pH profile of ABTS (Figure 3.5A); the pH-activity profile changed from a decaying line to a bell-shaped curve with an optimum pH of 5. However, the pH-activity profile of Reactive blue 19 was not affected by immobilization (Figure 3.5B).

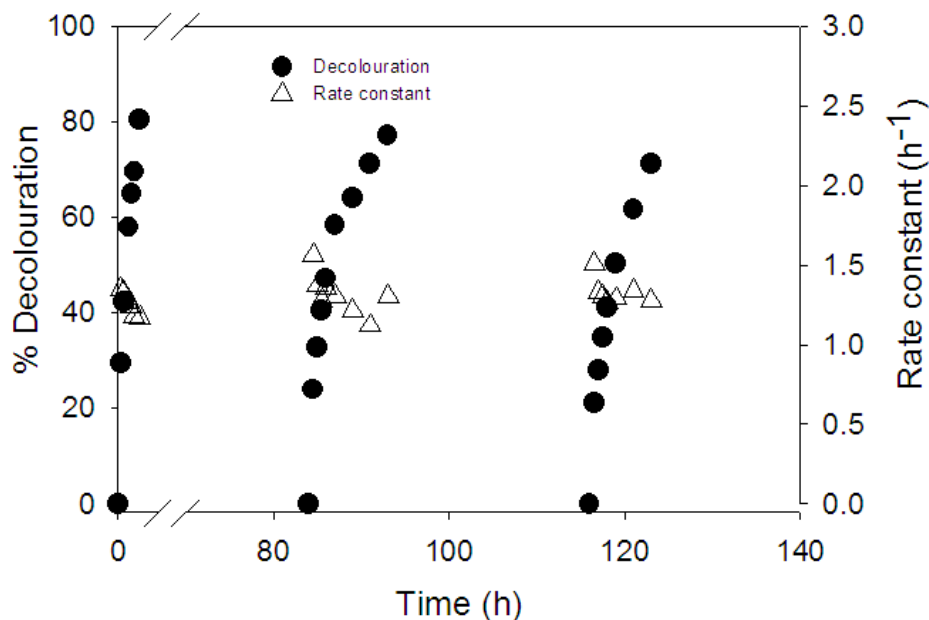
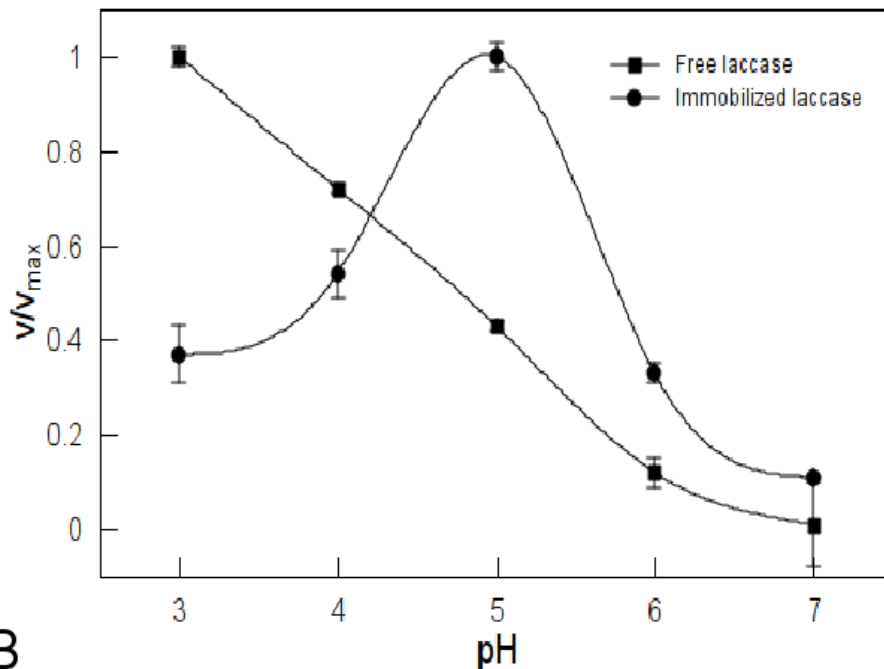


Figure 3.4: Decolourization of Reactive blue 19 in a packed bed by immobilized laccase after 4 months of storage in phosphate buffer at pH 5.0 and 23 ± 1 °C

3.4.5 Contribution of adsorption to dye decolourization

Ethanolamine, commonly used to block remaining aldehyde groups after protein immobilization, was evaluated for its ability to decrease the adsorption of Reactive blue 19. Using different initial dye concentrations in Erlenmeyer flasks, ethanolamine-treated particles adsorbed 40 % less dye than untreated, heat-inactivated particles (Figure 3.6). The partition coefficient, K_p , decreased from 0.214 to 0.131 when the beads were treated. The adsorption equilibrium occurred after 8 h.

Reactive blue 19 adsorbed to ethanolamine-treated beads with an intense blue colour when laccase had been heat inactivated and used in a recirculating packed bed. The color intensity persisted for the duration of the experiment, at least 24 h, with 21.4 % of the initial



B

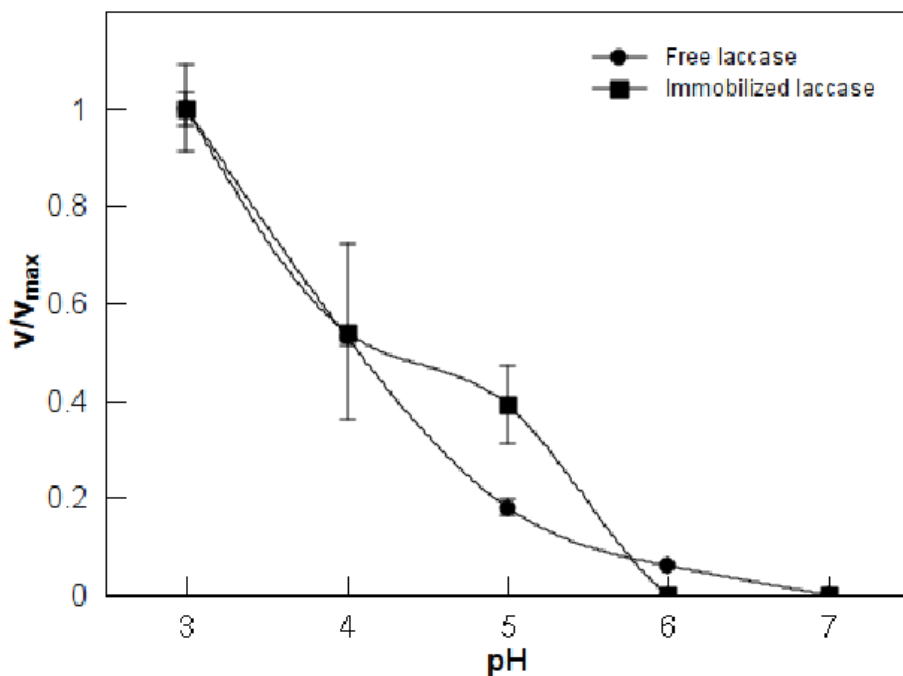


Figure 3.5: Effect of laccase immobilization on the pH profile of ABTS oxidation (A) and the decolourization of Reactive blue 19 (B). The assay mixtures were buffered with 50 mM NaOAc/50 mM NaH₂PO₄. The initial ABTS and Reactive blue 19 concentrations for the free and immobilized laccase were 500 and 50 μ M respectively. Each data point is the average of triplicates and error bars represent the standard error.

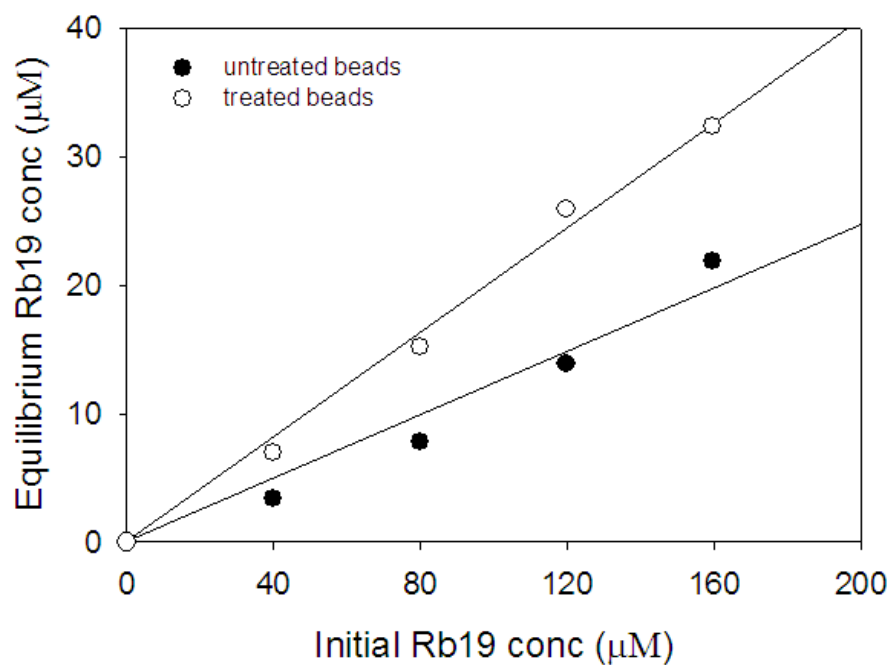


Figure 3.6: Effect of ethanolamine pretreatment on Reactive blue 19 adsorption on laccase immobilized on CPC-silica particles. After immobilization and before the beads were exposed to the dye, the beads were treated with ethanolamine to block reaction sites not occupied by the enzyme, and then laccase was heat inactivated. Experiments were conducted in 50 mM KH_2PO_4 buffer at pH 5.0 and $23 \pm 1^\circ\text{C}$.

Table 3.1: Reactive blue 19 removal in a packed bed reactor with recycle containing laccase CPC-immobilized on silica beads which were pre-treated with ethanolamine before and after heat inactivation. Dye was desorbed by methanol extraction at 22.5 ± 1 °C.

Laccase	Total dye added	After decolourization		
	(mg dye/g beads)	% disappearance	% in solution	% desorbed
Active enzyme	7.47	97.4	2.61	0
Heat-inactivated enzyme	7.38	78.6	21.4	55.3

dye remaining in solution (Table 3.1). The adsorption equilibrium in this case was achieved within 3 hours. However with active laccase, the intensity of the blue colour on the packed bed began to decrease after 4 h when the aqueous dye concentration had decreased to about 50 %. After 8 h, there was no visible color in the aqueous phase, and the bed had a pale pink colour with only 2.61 % of the initial dye measured in solution. While 55.3 % of the dye was recovered by desorption from the heat inactivated bed, no dye was recovered from the active bed.

3.5 Discussion

The retained activity of immobilized laccase based on the declining activity in the supernatant (during the enzyme immobilization) did not reflect the measured activity. The latter was 3.5 % (1.11 U/g) of the calculated activity (31.5 U/g). The ABTS concentration used to measure the immobilized enzyme activity was well above the K_M of the enzyme (50 to 73 μM). Therefore, the lower measured activity may be due to the denaturation of the enzyme

and/or to diffusion limitations. Mass transfer resistance in enzyme reactors is common in packed beds of porous enzyme supports (Barros *et al.*, 1998; Kallenberg *et al.*, 2005).

In the few decolourization studies in which laccase was immobilized on a solid support, the majority of dye removal was due to adsorption. Abadulla *et al.* (2000), Zille *et al.* (2003) and Kandelbauer *et al.* (2004) used the same immobilization method, cross-linking laccase onto silanized alumina with glutaraldehyde. The first two studies both worked with Reactive black 5 but only Zille *et al.* (2003) reported that the majority of dye decoloration (79 %) was due to adsorption and a very minor amount (4 %) to enzymatic activity while Abadulla *et al.* (2000) did not comment on sorption taking place. In another study, Kandelbauer *et al.* (2004) noted that adsorption played a role in decolourization but did not determine the extent of its contribution. Peralta-Zamora *et al.* (2003) showed that the majority of color removal of Reactive blue 19 (also named Remazol Brilliant Blue R in their paper) was due to adsorption with laccase immobilized on imidazol-modified silica gel. In our study, which also used Reactive blue 19, the majority of dye (about 97 %) was enzymatically degraded even though an initial, rapid adsorption occurred. Initially, the rate of adsorption must have been faster than the rate of degradation to obtain the intense blue colour. However, as the aqueous dye concentration decreased, the amount of adsorption must have decreased relative to the rate of dye degradation such that the intense blue colour gradually disappeared leaving a pale pink colour on the active laccase bed.

A key reason why our results differed from those of Peralta-Zamora *et al.* (2003) may be in the immobilization method. They cross-linked laccase to silica gel using propylimidazol. Imidazole groups are known binding sites for metal ions including Cu^{2+} (Kozłowski *et al.*, 2005). Laccase is a metalloprotein with four Cu^{2+} atoms that catalyze the internal electron transfer during oxidation. It is possible that the imidazole groups may have interacted with

copper in laccase leading to enzyme inactivation. In our study, laccase was immobilized on CPC-silica using APTES-glutaraldehyde which linked the amine groups on the enzyme and the bead surface. This method has been shown in the literature to retain a high level of laccase activity (Duran *et al.*, 2002). Furthermore, from our results, laccase activity did not appear to be adversely affected as decolourization rates per unit of enzyme activity for the immobilized enzyme was as good as or better than the free enzyme. In addition, the trend of the pH profile of dye decolourization did not change after immobilization. The low decolourization rates at pH 6 and 7 were difficult to measure probably because of mass transfer resistance.

Immobilizing laccase however drastically altered the pH profile of ABTS oxidation. The two-unit shift of the optimum pH towards more alkaline values indicates that the local immobilized enzyme micro-environment has a net negative charge (Goldstein, 1976). In a negatively charged microenvironment, the local proton concentration is greater than the bulk concentration. The excess pH could have inhibited the enzyme. The pKa of ABTS is 2.2 and it is expected to be in the form of the dianion predominantly (Scott *et al.*, 1993). As it approached the microenvironment however, it may have been neutralized by the excess protons so that its oxidation to a cation was disfavored by the excess of positive charges. As the pH is increased, the concentration of the buffer weak base that transports the protons away from the microenvironments increased. The generation of the cation would be more favorable because of the reduced proton concentration. The large shift differs with the results of Leonowicz *et al.* (1988) who showed a much smaller shift of 0.5 units with *T.versicolor* laccase immobilized on porous glass beads. The difference may be related to the average pore size of the beads used in this study was half of that used by the authors (37.5 Å as opposed to 75 Å). This can greatly restrict the diffusion of the protons thereby

creating a larger pH gradient between micro-environment and the bulk medium.

Although this immobilization technique has been used previously to immobilize laccase on silica for various applications, this is the first report of its use in dye decolourization and the first report of laccase immobilized on a support demonstrating color removal primarily due to the enzymatic activity and not sorption.

Immobilization to a support can minimize the conformational changes that an enzyme may undergo so that over time or when subjected to environmental perturbations, the immobilized enzyme may have better stability. Although in our study, immobilized laccase was more stable than the free enzyme, laccase immobilized on alumina had a lower stability than the free enzyme in dyeing effluents (Zille *et al.*, 2003). The composition of dye effluents and different dye structures will influence enzyme stability (Reyes *et al.*, 1999; Ko and Chen, 2008) as well as decolourization rates. Although this study focused on Reactive blue 19, the decolourization of other dyes and the effect of effluent components need to be investigated before this process can be considered for industrial applications. However, being able to store the immobilized laccase in a simple buffer under ambient conditions would allow their re-use and could have economic and practical advantages.

3.6 Conclusion

In conclusion, we have shown that *T. versicolor* laccase immobilized on CPC-silica beads decolourized Reactive blue 19 in a packed bed reactor and dye removal is primarily enzymatic. Immobilizing laccase considerably changed the pH activity profile of ABTS oxidation but not that of dye decolourization. The activity of the immobilized enzyme was more

stable than the free enzyme and similar decolourization rates were obtained after 4 months of storage in phosphate buffer at room temperature.

Bibliography

- Abadulla E, Tzanov T, Costa S, Robra KH, Cavaco-Paulo A, Gübitz GM. 2000. Decolorization and detoxification of textile dyes with a laccase from *Trametes hirsuta*. *Appl Environ Microbiol* **66**(8): 3357–62.
- Barros RJ, Wehtje E, Adlercreutz P. 1998. Mass transfer studies on immobilized alpha-chymotrypsin biocatalysts prepared by deposition for use in organic medium. *Biotechnol Bioeng* **59**(3): 364–373.
- Bourbonnais R, Paice MG, Reid ID, Lanthier P, Yaguchi M. 1995. Lignin oxidation by laccase isozymes from *Trametes versicolor* and role of the mediator 2,2'-azinobis(3-ethylbenzthiazoline-6-sulfonate) in kraft lignin depolymerization. *Appl Environ Microbiol* **61**(5): 1876–1880.
- City of Kingston CotCoK. 2000. By-law to control waste discharges to municipal sewers (by-law (2000-263)).
- City of Toronto CotCoT. 2000. Chapter 681 sewers: sewage and land drainage (municipal by-law article 1).
- Couto SR. 2007. Decolouration of industrial azo dyes by crude laccase from *Trametes hirsuta*. *J Hazard Mater* **148**(3): 768–770.
- D'Annibale A, Stazi S, Vinciguerra V, Giovannozzi Sermanni G. 2000. Oxirane-immobilized *Lentinula edodes* laccase: stability and phenolics removal efficiency in olive mill wastewater. *J Biotechnol* **77**(2-3): 265–273.
- de Kanel J, Morse J. 1979. A simple technique for surface area determination. *J. Phys. E* **12**: 272–273.
- Duran N, Esposito E. 2000. Potential applications of oxidative enzymes and phenoloxidase-like compounds in wastewater and soil treatment: a review. *Appl Catal B: Environ B* **28**: 83–99.

- Duran N, Rosa M, DAnnibale A, Gianfreda L. 2002. Applications of laccases and tyrosinases (phenoloxidases) immobilized on different supports: a review. *Enzyme Microb Technol* **31**(7): 907–931.
- Goldstein L. 1976. Kinetic behavior of immobilized enzyme systems. *Methods Enzymol* **44**: 397–443.
- Hublik G, Schinner F. 2000. Characterization and immobilization of the laccase from *Pleurotus ostreatus* and its use for the continuous elimination of phenolic pollutants. *Enzyme and microbial technology* **27**(3-5): 330–336.
- Jolivalt C, Brenon S, Caminade E, Mougín C, Pontié M. 2000. Immobilization of laccase from *Trametes versicolor* on a modified PVDF microfiltration membrane: characterization of the grafted support and application in removing a phenylurea pesticide in wastewater. *J Membrane Sci* **180**(1): 103–113.
- Kallenberg A, van Rantwijk F, Sheldon R. 2005. Immobilization of penicillin G acylase: the key to optimum performance. *Adv Synth & Catal* **347**(7-8): 905–926.
- Kandelbauer A, Maute O, Kessler RW, Erlacher A, Gübitz GM. 2004. Study of dye decolorization in an immobilized laccase enzyme-reactor using online spectroscopy. *Biotechnol Bioeng* **87**(4): 552–563.
- Ko C, Chen S. 2008. Enhanced removal of three phenols by laccase polymerization with MF/UF membranes. *Biores Technol* **99**(7): 2293–2298.
- Kozłowski H, Kowalik-Jankowska T, Jezowska-Bojczuk M. 2005. Chemical and biological aspects of Cu²⁺ interactions with peptides and aminoglycosides. *Coordination Chem Rev* **249**(21-22): 2323–2334.
- Leonowicz A, Sarkar J, Bollag J. 1988. Improvement in stability of an immobilized fungal laccase. *Appl Microbiol and Biotechnol* **29**(2): 129–135.
- Lewis D. 1999. Coloration in the next century. *Review of Progress in Coloration and Related Topics* **29**(1): 23–28.
- Nyanhongo GS, Gomes J, Gübitz GM, Zvaunya R, Read J, Steiner W. 2002. Decolorization of textile dyes by laccases from a newly isolated strain of *trametes modesta*. *Water Res* **36**(6): 1449–1456.
- O'Neill C, Hawkes F, Hawkes D, Lourenco N, Pinheiro H, Delee W. 1999. Colour in textile effluents-sources, measurement, discharge consents and simulation: a review. *J Chem Technol Biotechnol* **74**(11).
- Peralta-Zamora P, Pereira C, Tiburtius E, Moraes S, Rosa M, Minussi R, Durán N. 2003. Decolorization of reactive dyes by immobilized laccase. *Appl Catal B* **42**(2): 131–144.

- Reyes P, Pickard M, Vazquez-Duhalt R. 1999. Hydroxybenzotriazole increases the range of textile dyes decolorized by immobilized laccase. *Biotechnol Lett* **21**(10): 875–880.
- Robinson T, McMullan G, Marchant R, Nigam P. 2001. Remediation of dyes in textile effluent: a critical review on current treatment technologies with a proposed alternative. *Bioresour Technol* **77**(3): 247–255.
- Scott S, Chen W, Bakac A, Espenson J. 1993. Spectroscopic parameters, electrode potentials, acid ionization constants, and electron exchange rates of the 2, 2'-azinobis (3-ethylbenzothiazoline-6-sulfonate) radicals and ions. *J Phys Chem* **97**(25): 6710–6714.
- Shuttleworth K, Bollag J. 1986. Soluble and immobilized laccase as catalysts for the transformation of substituted phenols. *Enzyme Microb Technol* **8**(3): 171–177.
- Wolfenden B, Willson R. 1982. Radical-cations as reference chromogens in kinetic studies of one-electron transfer reactions. *J Chem Soc Perkin Trans* **2**(1982): 805–812.
- Zhang J, Liu X, Xu Z, Chen H, Yang Y. 2008. Degradation of chlorophenols catalyzed by laccase. *Inter Biodeter & Biodeg* **61**(4): 351–356.
- Zille A, Tzanov T, Gübitz GM, Cavaco-Paulo A. 2003. Immobilized laccase for decolourization of reactive black 5 dyeing effluent. *Biotechnol Lett* **25**(17): 1473–1477.

Chapter 4

Dye toxicity and decolourization by laccase immobilized on CPC-silica beads

A manuscript of this chapter is preparation and is to be submitted to Applied Microbiology and Biotechnology (Springer-Verlag)

4.1 Abstract

The toxicity and decolourization of textile dyes by laccase immobilized on CPC-silica beads were evaluated. Anthraquinone (Reactive blue 19 and Dispersed blue 3) and indigoid (Acid blue 74) dyes were degraded more rapidly than the azo dyes (Acid red 27 and Reactive black 5). Furthermore, the immobilization procedure did not alter the laccase decolourization efficiency. Visible dye adsorption correlated with the loss of activity of the free enzyme in the presence of individual dyes. Azo and indigoid dyes were more toxic than anthraquinone dyes as determined by the Microtox assay. However, the toxicity of the azo and indigoid dyes decreased after enzymatic treatment while that of anthraquinone dyes increased. This indicates that the decolourization products of anthraquinone dyes are

potentially more toxic than the parent compounds.

4.2 Introduction

Residual dyes in textile wastewaters, when discharged in aquatic ecosystems, may reduce the amount of sunlight to photosynthetic organisms which results in a decrease oxygen levels. Domestic activated sludge processes poorly remove dyes because they and/or their auxiliary chemicals are generally toxic to microorganisms (Rosa *et al.*, 2001; Moawad *et al.*, 2003; Wang *et al.*, 2002). Physical color removal methods (such as activated carbon and coagulation) require subsequent disposal steps since dyes are not degraded, but just transferred to a different phase (Reife and Freeman, 1996; Robinson *et al.*, 2001). Current individual technologies are not effective with all dye classes and a combination of methods may be required, thus increasing treatment costs (Talarposhti *et al.*, 2001). Therefore, a more cost effective and efficient treatment is needed.

Extracellular lignin-degrading enzymes of white rot fungi like peroxidases and laccases can decolourize dyes in liquid cultures (Kirby *et al.*, 2000; Champagne and Ramsay, 2005; Husain, 2006; Wesenberg *et al.*, 2003). Immobilization of these enzymes is potentially more cost-effective as it would allow their re-use and may improve enzyme stability. Although purified fungal laccases have decolourized azo (Salony *et al.*, 2006), acid (Salony *et al.*, 2006; Younes *et al.*, 2007) and anthraquinone (Lu *et al.*, 2007; Younes *et al.*, 2007) dyes, most studies have evaluated immobilized laccase to remove pollutants such as pesticides and phenols from synthetic wastewaters (Yinghui *et al.*, 2002; Jolivalt *et al.*, 2000). Dye decolourization using laccase immobilized on imidazol-modified silica gel (Peralta-Zamora *et al.*, 2003) or silanized alumina particles (Zille *et al.*, 2003) occurred mainly

by adsorption, and to a lesser extent, by enzymatic decolourization. In Chapter 3, it was demonstrated that laccase immobilized on controlled porosity carrier (CPC) beads using APTES-glutaraldehyde decolourized Reactive blue 19, an anthraquinone dye, mainly by enzymatic degradation. However, the decolourization of other textile dyes by the same immobilized laccase preparation and the effect of immobilization on the decolourizing capability of laccase were not evaluated. The latter is important since immobilization should not impair decolourization efficiency. Furthermore, there are few reports on the toxicity of dyes decolourized by fungal cultures (Ramsay and Nguyen, 2002; Shin and Lee, 2000), and even fewer on dyes decolourized by free or immobilized laccase (Abadulla *et al.*, 2000; Ulson de Souza *et al.*, 2007). Fungal cultures produce mixtures of different chemical composition than purified enzymes, and hence possibly different toxicities. This study compared the decolourization of Reactive blue 19 with another anthraquinone dye (Disperse blue 3), an indigoid dye (Acid blue 74) and two azo dyes (Acid red 27 and Reactive black 5) by *Trametes versicolor* laccase immobilized on CPC-silica beads and the impact of decolourization on toxicity.

4.3 Materials and methods

4.3.1 Chemicals

CPC silica beads pre-silanized with 3-aminopropyltriethoxysilane (APTES), *Trametes versicolor* laccase, Acid red 27, Reactive blue 19, Reactive black 5 and 2,2'-azino-bis(3-ethylbenzothiazoline-6-sulfonic acid) (diammonium salt) were purchased from Sigma-Aldrich (Oakville, ON, Canada). Dispersed blue 3, Acid blue 74 and glutaraldehyde were purchased from Acros (Belgium).

4.3.2 Immobilization of laccase on CPC-silica

Four grams of pre-silanized CPC silica beads (355 to 600 m in diameter, an average surface area of 42.1 m²/g and a pore size of 37.5 nm) were immersed in degassed 2.5 % glutaraldehyde in 0.1 M KH₂PO₄ at pH 5.0 for 2 h and thereafter placed in a laccase solution ($\bar{3}$ U/ml in 0.1 M KH₂PO₄ pH 5.0) for 36 h at 4°C. The beads were then washed three times with distilled water and twice with phosphate buffer.

4.3.3 Free and immobilized enzyme assay

Laccase activity was measured by monitoring with a spectrophotometer the generation of 2,2-azino-bis(3-ethylbenzothiazoline-6-sulfonic acid) radicals (ABTS^{•-}) at 420 nm from the oxidation of ABTS (Wolfenden and Willson, 1982) at 23 ± 1 °C using a Spectramax 250 plate reader with the SOFTmax PRO software package (Molecular Devices, CA, USA). Assays were conducted in 96-well plates (300 μl per well). The assay mixture contained 0.2 mM ABTS, 100 mM sodium acetate buffer (pH 5.0) (Bourbonnais *et al.*, 1995) and the enzyme sample for a total assay volume of 180 μl. The corresponding path length of absorbance was 0.5 cm. One unit of laccase activity (U) was defined as the amount of enzyme that formed 1 μmol ABTS^{•-} per min. Protein concentration was measured as the absorbance at 280 nm and corrected for scattering effects with absorbance readings at 320 nm (equation 4.1).

$$A_{corr}^{280} = A_{280} - A_{320} * \left(\frac{320}{280} \right)^4 \quad (4.1)$$

For the immobilized laccase system, the CPC silica-laccase packed bed reactor (I.D. = 10 mm, l = 23 mm) was connected to a reservoir containing 100 ml of 50 mM sodium acetate/50 mM KH₂PO₄ (pH 5) via a peristaltic pump. The solution was 100 % re-circulated between the packed bed and the reservoir at a flow rate of 75 ml/min. To determine the

immobilized laccase activity, the linear variation of the concentration of $\text{ABTS}^{\bullet-}$ in the reservoir with time was measured for a 6 or 10 minute interval.

4.3.4 Decolourization by free laccase

All dyes were decolourized with 100 -150 U/l (i.e. 5-7.5 U) laccase in 125-ml Erlenmeyer flasks containing 50 ml phosphate buffer (0.1 M KH_2PO_4 at pH 5.0) at 23 ± 1 °C and pH 5. The concentration of Dispersed blue 3 (0.072 M) was twice the concentration of other dyes (0.036 M) as the absorbance of its solution at the lower concentration was too low to monitor its degradation. The concentration of 0.036 mM for each dye (except for Disperse blue 3) was chosen since it is typical of residual dye concentration found in a textile wastewater (O'Neill *et al.*, 1999). Controls contained the dye solutions without laccase. The initial rates of degradations were determined by calculating the tangent of the slope of the decolourization progress curve.

4.3.5 Decolourization by immobilized laccase

Four grams of CPC-silica beads with 31.5 ± 4.3 U of laccase/g (i.e. 0.75 ± 0.10 U/m) or 4.39 ± 1.38 μg of protein/ m^2 immobilized were used in a re-circulating packed or fluidized bed reactor. Anthraquinone or indigo dye solutions were continuously re-circulated at 4.15 ml/min (hydraulic residence time (HRT)= 2.44 min) from a reservoir containing 400 ml of the dye solution to a packed bed (I.D. = 1.6 cm, h = 5.0 cm). For the azo dyes, a similar configuration was used except that the beads were fluidized in a 14-ml bed (I.D. = 1.6 cm, h = 7.0 cm) at a flow rate of 45 and 39 ml/min (HRT = 0.31 min) respectively with 100 ml of dye solution in the reservoir. The rate of decolourization was calculated by dividing the concentration difference from the reactor inlet and outlet by the hydraulic retention time.

The average rate was calculated by averaging the decolourization rates in the reactor at over the time interval in which the rates were approximately constants. Experiments were done at $23 \pm 1^\circ\text{C}$ and pH 5.

4.3.6 Dye concentration

Dye concentration was measured using a Unicam UV1 spectrophotometer (Spectronic Unicam, Cambridge, UK) at the maximum wavelength of each dye (Table 4.1).

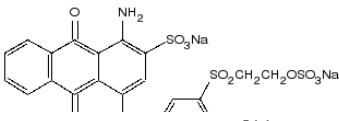
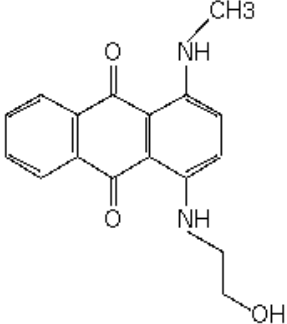
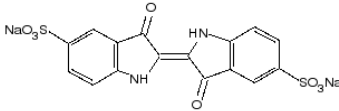
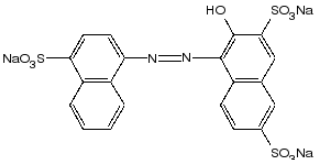
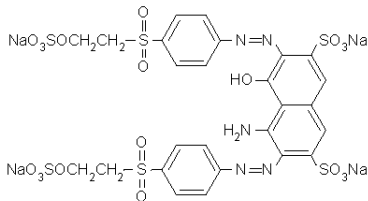
4.3.7 Microtox analysis

The Microtox acute toxicity assay was conducted with a Microtox 500 Analyzer on dye solutions according to the protocols provided by Azur Environmental (Newark, Delaware). The pH of the samples was adjusted where necessary to 6.0 by adding $70 \mu\text{l}$ 1 M NaOH. From eight serial dilutions, the percent dilution which decreased the luminescence of a modified strain of *Vibrio fischeri* after 15 min incubation by 20 % (EC20%) was determined using the Microtox data analysis program (Microtox Omni Software (1999) Azur Environmental, Newark, Delaware, USA). Color correction was not necessary. Solutions of zinc sulfate ($\text{ZnSO}_4 \cdot 7 \text{H}_2\text{O}$) and 1 g glucose/l prepared in distilled water were used as the positive and negative controls respectively. Each EC20% reported was the average of triplicate analyses.

4.4 Results

Immobilized laccase, like the free enzyme, decolourized the indigoid (Acid blue 74) and anthraquinone (Reactive blue 19, Dispersed blue 3) dyes more rapidly than the azo dyes (). The indigoid and anthraquinone dyes did not affect the activity of free laccase in up

Table 4.1: Dye structures and their maximum wavelength of absorption

Dyes	molecular structure	Molecular weight	λ_{max} (nm)
Reactive blue 19		626.5	592
Dispersed blue 3		296.3	719
Acid blue 74		466.3	609
Acid red 27		604.5	523
Reactive black 5		991.8	597

to 3 hours of decolourization, maintaining 100 % of its activity. The free enzyme activity however decreased by 33% and 97 % with azo dyes Acid red 27 and Reactive black 5 respectively after 84 h (Table 4.2). Since a 60 % loss of activity also occurred with no dye after 84 h, Reactive black 5 clearly inhibited laccase activity.

When the dyes were first exposed to the immobilized enzyme, an initial, rapid adsorption to the enzyme bed was observed with all dyes except Acid blue 74. By the end of the decolourization, the adsorbed colour disappeared or persisted to varying degrees depending on how efficiently laccase degraded the dye. At the end of the experiment, the order in which the dyes were visibly adsorbed to the immobilized enzyme bed from the least colour to the most, was Acid blue 74 (no colour) < Reactive blue 19 < Disperse blue 3 < Acid red 27 < Reactive black 5 (most intense colour) (Table 4.2) where laccase was mostly inhibited by Reactive black 5.

Table 4.2: Decolourization of dyes by free and immobilized laccase. The initial concentration of all dyes was 0.036 mM except Dispersed blue 3 which was 0.072 mM. (^a n.a. means not applicable; ^b average of duplicates \pm the difference between the duplicates, all other values in the table are the averages of triplicates with standard deviations; ^c means no color with increasing color intensity to +++)

Dye	Decolourization by free laccase				Decolourization by immobilized laccase			
	(%)	Time to decolourization (h)	% of initial enzyme activity	Initial rate (μ M/U-h)	%	Time to decolourization (h)	Rate (μ M/U-h)	Visible sorption
No dye	n.a. ^a	3	100	n.a.	n.a.	n.a.	n.a.	- ^c
Dispersed blue 3	74 \pm 0.5	1	100	12.5 \pm 0.6 ^b	82 \pm 8.1	17.5	6.06 \pm 2.31	+
Reactive blue 19	73.7 \pm 4.5	0.5	100	8.27 \pm 0.02 ^b	76 \pm 4.7	8	11.98 \pm 2.76	+/-
Acid blue 74	34.6 \pm 1.3	1	100	4.61 \pm 0.18	85.2 \pm 10.1	8	8.66 \pm 1.93	-
Acid red 27	50 \pm 4.3	84	67	0.065 \pm 0.010	27.8 \pm 10.1	22	0.134 \pm 0.056	++
Reactive black 5	16.5 \pm 2.9	84	3	0.017 \pm 0.005	10.3 \pm 5.3	22	0.022 \pm 0.047	+++

4.4.1 Toxicity of decolourized dyes

Microtox analyses were conducted before and after decolourization by free or immobilized laccase. Using the EC20 % and the ranking of Coleman and Qureshi (1985), the toxicity of the dye solutions were categorized as follows: >100 % = non-toxic; 100-75 % = slightly toxic; 75-50 % = moderately toxic; 50-25 % = toxic; < 25 % = very toxic. The negative control (1 g glucose/l) and laccase alone in the same buffer had no effect on the fluorescence of *V. fischeri* (Table 4.3). However, the positive control (1 g ZnSO₄ ·7H₂O/l) was very toxic while the buffer alone was moderately toxic. The azo and indigoid dyes were more toxic than the anthraquinone dyes. Similar results were obtained whether the dyes were decolourized by the free or immobilized enzyme except for Acid red 27 where the toxicity had decreased with the immobilized enzyme but remained unchanged with the free enzyme. Decolourization decreased the toxicity of the indigoid dye but increased the toxicity of the anthraquinone dyes.

Table 4.3: Toxicity of initial and decolourized dye solutions by free and immobilized laccase. The dilutions (%) which decreased the luminescence of *Vibrio fischeri* by 20% (EC20%) after 15 min incubation in the Microtox assay are reported as the averages of triplicate analyses with standard deviations. Dyes were prepared in phosphate buffer while 1 g ZnSO₄ · 7H₂O used as the positive control and 1 g glucose/l as the negative control. (a.n.a. means not applicable)

Dye	Initial dye concentration (mM)	% Decolourization by		EC _{20%} (15 min)		
		free laccase	immobilized laccase		Before decolourization	After decolourization by free laccase
Controls						
Glucose	n.a. ^a	n.a.	n.a.	>100	n.a.	n.a.
Zinc sulfate	n.a.	n.a.	n.a.	1.6 ± 2.1	n.a.	n.a.
buffer alone	n.a.	n.a.	n.a.	69.6 ± 6.4	n.a.	n.a.
buffer + 150 U/l laccase	n.a.	n.a.	n.a.	>100 ± 6.4	n.a.	n.a.
Acid red 27	0.036	80.0	40.6	12 ± 1.3	16.9 ± 6.3	34.7 ± 7.9
Reactive black 5	0.036	18.0	12.0	7.80 ± 1.80	11.3 ± 3.8	15.1 ± 4.9
Acid blue 74	0.036	68.0	74.0	14.1 ± 1.9	42.7 ± 6.9	58.5 ± 10.6
Dispersed blue 3	0.072	87.0	78.0	48.0 ± 3.6	32.1 ± 6.6	28.6 ± 8.7
Reactive blue 19	0.036	90.0	77.0	33.5 ± 5.8	13.4 ± 2.0	11.7 ± 2.1

4.5 Discussion

The present study evaluated the decolourization of a range of dyes by the same immobilized laccase preparation used to decolourize Reactive blue 19 in Chapter 3. Like Reactive blue 19, the immobilized enzyme decolourized Disperse blue 3 (anthraquinone), Acid blue 74 (indigoid), Acid red 27 (azo) and Reactive black 5 (azo) with a similar specificity and rate as the free enzyme (Table 4.2). Protein immobilization can modify or deactivate the enzyme if immobilization conditions are not appropriate. For example, excess glutaraldehyde, a common bifunctional cross-linker, can significantly cross-link enzymes to each other resulting in a loss of functionality. In this study, the specificity of soluble and immobilized laccase toward the dyes was nearly identical (Table 4.2) and there was no systematic variation in the rate of decolourization per unit of enzyme after immobilization. The nearly identical specificity before and after immobilization demonstrates that the enzyme's structure was unaffected during immobilization and/or any change in the enzyme structure did not affect its ability to degrade the dyes after immobilization. Furthermore, the substrate's access to the immobilized enzyme was not restricted by the mass transfer resistance and the recirculation rate in the packed bed reactor was sufficiently high to ensure good mixing. The boundary layer may have been sufficiently thin that forced convection would have been the dominant transport mechanism of the dye to the immobilized laccase rather than free diffusion. In light of these results, the immobilization protocol used in this investigation did not impair enzyme decolourization and may allow advantages in terms of enhanced stability and economy of reusing the immobilized laccase in industrial applications.

Although it was previously shown that decolourization of Reactive blue 19 was mainly enzymatic when laccase was immobilized on CPC-silica, it was observed in the present study that dyes poorly decolorized by the free laccase adsorbed onto the immobilized preparation

(Table 4.3). Dyes, which adsorbed the least or not at all, were decolourized the fastest. Since anthraquinone (Reactive blue 19, Dispersed blue 3) and indigoid (Acid blue 74) dyes were degraded more efficiently than the azo dyes (Acid red 27 and Reactive black 5), they were better substrates for laccase as it is generally reported in the literature (Nyanhongo *et al.*, 2002). Zille *et al.* (2004) has shown that an increased redox potential of the dyes decreased the rate or extent of decolouration with a *T. villosa* laccase. The most poorly decolorized dyes in this study were the azo dyes Acid red 27 and Reactive black 5 and coincidentally, these had the highest redox potentials. The authors found that the addition of a mediator, 1-hydroxybenzotriazole (HBT), enhanced the rate and extent of decolourization of all dyes, including Acid red 27 and Reactive black 5, and attributed this to the higher redox potential of laccase/HBT (+1.084 V vs NHE ie normal hydrogen electrode) compared to laccase alone (+0.780 V vs NHE) (Bourbonnais *et al.*, 1995). The addition of mediators such as hydroxybenzotriazole (HBT) or ABTS has been shown to improve decolourization (Reyes *et al.*, 1999; Zille *et al.*, 2004).

The present study also examined the toxicity of the dyes and their enzymatically decolourized products. Dyes and auxiliary chemicals used in the dyeing process render textile wastewaters toxic for activated sludge processes (Odeigah *et al.*, 1995; Rosa *et al.*, 2001; Wang *et al.*, 2002). Ramsay and Nguyen (2002) have shown that metabolites of *T. versicolor* not associated with decolourization can contribute to toxicity. These metabolites can potentially mask the toxic effects of the parent dye and its daughter products (Ramsay and Nguyen, 2002; Shin *et al.*, 2002; Rosa *et al.*, 2001). Hence, purified enzymes and inorganic buffer were used to eliminate such contributions, and toxicity changes would be due only to decolourized products. Several test organisms such as algae, bacteria, fish and plants have been used to assess effluent toxicity (Rosa *et al.*, 2001). When a variety of assays were

compared, *V. fischeri* (a luminescent bacterium) was the most sensitive, and was considered the most effective and practical for the Microtox assay (Rosa *et al.*, 2001; Wang *et al.*, 2002). Microtox results were shown to correlate to toxicity results in higher organisms.

In our study, the azo and indigoid dyes were more toxic than the anthraquinone dyes (Table 4.3). However, Novotný *et al.* (2006) reported that their anthraquinone dyes (Reactive blue 19 and Dispersed blue 3) were more toxic than their azo dyes (Reactive orange 16 and Congo red) when tested with *V. fischeri* also. Although this appears to be a contradiction, the number of dyes in either study was low and the only dye common to both studies was Dispersed blue 3. In our study, the toxicity analyses were done with the dyes in the enzyme buffer (which had a mild toxic effect) in order to compare them with the decolourized products. Novotný *et al.* (2006) did no decolourization studies and had not specified the exact composition of their dye solutions. Although Abadulla *et al.* (2000) evaluated dye detoxification after decolourization by *T. hirsuta* immobilized laccase, they used a different toxicity assay with *Pseudomonas putida* and did not report the toxicity of the parent dyes.

Abadulla *et al.* (2000) showed that their azo (Reactive black 5 and Direct blue 71) and indigoid (Acid blue 74) dyes as well as their anthraquinone (Reactive blue 19 and Acid blue 225) dyes were detoxified. Our enzymatic decolourization results are different. Likewise to Abadulla *et al.* (2000), the decolourized products of the azo and indigoid dyes were less toxic but those of the anthraquinone dyes were more toxic than the parent dyes. However, the indigoid dye (Acid blue 74) and one azo dye (Reactive black 5) were common to both studies with similar detoxification results even though different toxicity assays were performed. However, there were no anthraquinone dyes common to both studies and it is likely that *V. fischeri* may be more sensitive to anthraquinone dyes and/or their decolourized

products than *P. putida*. This indicates that a much wider range of dyes should be evaluated within the same study as there is no standard assay commonly followed in the literature for dye toxicity or detoxification data to be strictly compared.

In the anaerobic bacterial decolourization of azo dyes, the generation of aromatic amines results in an increase in toxicity (Delee *et al.*, 1998). However, when followed by an aerobic bacterial step, the amines are degraded and the end toxicity is reduced (Gottlieb *et al.*, 2003). On the other hand, it was shown in this study that *T.versicolor* laccase can detoxify azo and indigoid dyes in one step process similarly to Abadulla *et al.* (2000). The decolorization of a greater number of anthraquinone dyes must be conducted to know if the toxicity increase is specific to the dye class or linked to the sensitivity of the micro-organism used in the toxicity assay.

4.6 Conclusion

This present report demonstrated the decolourization of a broader range of dyes by *T.versicolor* laccase immobilized on CPC-silica beads. The immobilization procedure did not affect the enzyme specificity. Decolourization of anthraquinone dyes occurred more rapidly with less tendency for adsorption to occur than azo or indigoid dyes. Although azo and indigoid dyes were more toxic than the anthraquinone dyes, the latter seem to have generated more toxic byproducts while those of azo and indigoid dyes decreased.

Bibliography

- Abadulla E, Tzanov T, Costa S, Robra KH, Cavaco-Paulo A, Gübitz GM. 2000. Decolorization and detoxification of textile dyes with a laccase from *Trametes hirsuta*. *Appl Environ Microbiol* **66**(8): 3357–62.
- Bourbonnais R, Paice MG, Reid ID, Lanthier P, Yaguchi M. 1995. Lignin oxidation by laccase isozymes from *Trametes versicolor* and role of the mediator 2,2'-azinobis(3-ethylbenzthiazoline-6-sulfonate) in kraft lignin depolymerization. *Appl Environ Microbiol* **61**(5): 1876–1880.
- Champagne PP, Ramsay JA. 2005. Contribution of manganese peroxidase and laccase to dye decoloration by *Trametes versicolor*. *Appl Microbiol Biotechnol* **69**(3): 276–285.
- Coleman R, Qureshi A. 1985. Microtox® and *Spirillum volutans* tests for assessing toxicity of environmental samples. *Bull Environ Contam Toxicol* **35**(1): 443–451.
- Delee W, O'Neill C, Hawkes F, Pinheiro H. 1998. Anaerobic treatment of textile effluents: a review. *J Chem Technol & Biotechnol* **73**(4).
- Gottlieb A, Shaw C, Smith A, Wheatley A, Forsythe S. 2003. The toxicity of textile reactive azo dyes after hydrolysis and decolourisation. *J Biotechnol* **101**(1): 49–56.
- Husain Q. 2006. Potential applications of the oxidoreductive enzymes in the decolorization and detoxification of textile and other synthetic dyes from polluted water: a review. *Crit Rev Biotechnol* **26**(4): 201–21.
- Jolivalt C, Brenon S, Caminade E, Mougín C, Pontié M. 2000. Immobilization of laccase from *Trametes versicolor* on a modified PVDF microfiltration membrane: characterization of the grafted support and application in removing a phenylurea pesticide in wastewater. *J Membrane Sci* **180**(1): 103–113.
- Kirby N, Marchant R, McMullan G. 2000. Decolourisation of synthetic textile dyes by *Phlebia tremellosa*. *FEMS Microbiol Lett* **188**(1): 93–96.

- Lu L, Zhao M, Zhang BB, Yu SY, Bian XJ, Wang W, Wang Y. 2007. Purification and characterization of laccase from *Pycnoporus sanguineus* and decolorization of an anthraquinone dye by the enzyme. *Appl Microbiol Biotechnol* **74**(6): 1232–1239.
- Moawad H, El-Rahim W, Khalafallah M. 2003. Evaluation of biotoxicity of textile dyes using two bioassays. *J Basic Microbiol* **43**(3): 218–229.
- Novotný C, Dias N, Kapanen A, Malachová K, Vándrovcová M, Itävaara M, Lima N. 2006. Comparative use of bacterial, algal and protozoan tests to study toxicity of azo- and anthraquinone dyes. *Chemosphere* **63**(9): 1436–1442.
- Nyanhongo GS, Gomes J, Gübitz GM, Zvauya R, Read J, Steiner W. 2002. Decolorization of textile dyes by laccases from a newly isolated strain of *trametes modesta*. *Water Res* **36**(6): 1449–1456.
- Odeigah PG, Osanyinpeju AO, Osanyipeju AO. 1995. Genotoxic effects of two industrial effluents and ethyl methane sulfonate in *Clarias lazera*. *Food Chem Toxicol* **33**(6): 501–505.
- O'Neill C, Hawkes F, Hawkes D, Lourenco N, Pinheiro H, Delee W. 1999. Colour in textile effluents-sources, measurement, discharge consents and simulation: a review. *J Chem Technol Biotechnol* **74**(11).
- Peralta-Zamora P, Pereira C, Tiburtius E, Moraes S, Rosa M, Minussi R, Durán N. 2003. Decolorization of reactive dyes by immobilized laccase. *Appl Catal B* **42**(2): 131–144.
- Ramsay J, Nguyen T. 2002. Decoloration of textile dyes by *Trametes versicolor* and its effect on dye toxicity. *Biotechnology Lett* **24**(21): 1757–1761.
- Reife A, Freeman H. 1996. *Environmental chemistry of dyes and pigments*, ch. Carbon adsorption of dyes and selected intermediates. John Wiley & Sons Inc: New York, ISBN 978-0471589273, pp. 3–29.
- Reyes P, Pickard M, Vazquez-Duhalt R. 1999. Hydroxybenzotriazole increases the range of textile dyes decolorized by immobilized laccase. *Biotechnol Lett* **21**(10): 875–880.
- Robinson T, McMullan G, Marchant R, Nigam P. 2001. Remediation of dyes in textile effluent: a critical review on current treatment technologies with a proposed alternative. *Bioresour Technol* **77**(3): 247–255.
- Rosa EVC, Simionatto EL, de Souza Sierra MM, Bertoli SL, Radetski CM. 2001. Toxicity-based criteria for the evaluation of textile wastewater treatment efficiency. *Environ Toxicol Chem* **20**(4): 839–845.
- Salony, Mishra S, Bisaria VS. 2006. Production and characterization of laccase from *Cyathus bulleri* and its use in decolourization of recalcitrant textile dyes. *Appl Microbiol Biotechnol* **71**(5): 646–653.

- Shin KS, Lee YJ. 2000. Purification and characterization of a new member of the laccase family from the white-rot basidiomycete *Coriolus hirsutus*. *Arch Biochem Biophys* **384**(1): 109–115.
- Shin M, Nguyen T, Ramsay J. 2002. Evaluation of support materials for the surface immobilization and decoloration of amaranth by *trametes versicolor*. *Appl Microbiol Biotechnol* **60**(1-2): 218–223.
- Talarposhti AM, Donnelly T, Anderson GK. 2001. Colour removal from a simulated dye wastewater using a two-phase anaerobic packed bed reactor. *Water Res* **35**(2): 425–432.
- Ulson de Souza S, Forgiarini E, Ulson de Souza A. 2007. Toxicity of textile dyes and their degradation by the enzyme horseradish peroxidase (HRP). *Journal of hazardous materials* **147**(3): 1073–1078.
- Wang C, Yediler A, Lienert D, Wang Z, Kettrup A. 2002. Toxicity evaluation of reactive dyestuffs, auxiliaries and selected effluents in textile finishing industry to luminescent bacteria *Vibrio fischeri*. *Chemosphere* **46**(2): 339–344.
- Wesenberg D, Kyriakides I, Agathos SN. 2003. White-rot fungi and their enzymes for the treatment of industrial dye effluents. *Biotechnol Adv* **22**(1-2): 161–187.
- Wolfenden B, Willson R. 1982. Radical-cations as reference chromogens in kinetic studies of one-electron transfer reactions. *J Chem Soc Perkin Trans* **2**(1982): 805–812.
- Yinghui D, Qiuling W, Shiyu F. 2002. Laccase stabilization by covalent binding immobilization on activated polyvinyl alcohol carrier. *Lett Appl Microbiol* **35**(6): 451–456.
- Younes SB, Mechichi T, Sayadi S. 2007. Purification and characterization of the laccase secreted by the white rot fungus *perenniporia tephropora* and its role in the decolorization of synthetic dyes. *J Appl Microbiol* **102**(4): 1033–1042.
- Zille A, Ramalho P, Tzanov T, Millward R, Aires V, Cardoso MH, Ramalho MT, Gübitz GM, Cavaco-Paulo A. 2004. Predicting dye biodegradation from redox potentials. *Biotechnol Prog* **20**(5): 1588–92.
- Zille A, Tzanov T, Gübitz GM, Cavaco-Paulo A. 2003. Immobilized laccase for decolorization of reactive black 5 dyeing effluent. *Biotechnol Lett* **25**(17): 1473–1477.

Chapter 5

Immobilization of laccase on PMMA

A manuscript of this chapter is in preparation for submission to Biotechnology Progress (Elsevier)

5.1 Abstract

Laccase from *Trametes versicolor* was immobilized on poly(methyl methacrylate) (PMMA). PMMA beads were hydrazinolyzed and the enzyme immobilized on PMMA-hydrazide through its polysaccharide residues yielding a higher specific activity than when glutaraldehyde cross-linking was used. Although the enzyme load was comparable to what has been reported in the literature on commercial acrylic carriers, the specific activity was 50 % lower. However, since the specific activity of immobilized laccase on PMMA was similar to that of CPC-silica-laccase used for dye decolorization, the simple immobilization procedure presented in this investigation offers the possibility of using an inexpensive material for laccase immobilization and dye decolourization.

5.2 Introduction

The use of enzymes in wastewater treatment has recently been the subject of intensive research (Rigo *et al.*, 2008; Leal *et al.*, 2006). Laccases are blue copper oxidases that have attracted great interest for removing residual dyes in textile wastewaters. These enzymes have been shown to efficiently decolourize dye solutions and are most efficient toward anthraquinone dyes (Salony *et al.*, 2006; Nyanhongo *et al.*, 2002; Wong and Yu, 1999). Protein immobilization is an economical and effective means of stabilizing and reusing an enzyme and immobilized laccase reactors have been studied for dye decolourization. The most common inorganic supports to immobilize laccase are alumina (Zille *et al.*, 2003), silica (Peralta-Zamora *et al.*, 2003) and porous glass (Rogalski *et al.*, 1999; Leonowicz *et al.*, 1988). The procedure to immobilize laccase on these supports is to utilize 3-aminopropyltriethoxysilane (APTES) to introduce amines at the surface of the beads and then cross-link the enzyme to the support using glutaraldehyde (Duran *et al.*, 2002). However, these materials are brittle and glutaraldehyde reacts with any primary amine on the enzyme and may lead to its deactivation. More recently, laccase has been immobilized on commercial acrylic co-polymers beads for dye decolorization (Arica *et al.*, 2009; Kunamneni *et al.*, 2008). Poly (methyl methacrylate) (PMMA) is an acrylic, abundant, and relatively inexpensive material that is mechanically more resistant and less brittle than silica or alumina. It is used to fabricate microfluidic devices and chromatography packing material (Brown *et al.*, 2006; Dominick *et al.*, 2003; Fixe *et al.*, 2004).

The polymer at its surface contains ester groups that can be converted to amines which react with an aldehyde to generate an imine ($R_2-C=N-R$) (Schiff base), which is unstable to hydrolysis. Usually, a mild reducing agent like sodium cyanoborohydride or borane dimethyl amine is used to stabilize the imine bond (Hermanson, 1996). Another option is

to convert the ester groups of PMMA to hydrazides which react with aldehydes to form stable hydrazones ($R_2-CH=N-NH_2$) that are resistant to hydrolysis. Furthermore, hydrazides are more reactive than amines towards aldehydes at neutral pH since they are completely deprotonated at pH 5 while amines are deprotonated above pH 9 (Jost *et al.*, 1974). Since laccase is a glycoprotein, it can be immobilized through its polysaccharide residues that can be converted to aldehydes with a mild oxidant like periodate. These glycosyl residues are not involved in catalysis and are located away from the active site. Immobilizing laccase through its glycosidic residues on PMMA has not been reported and could reduce the risk of deactivation. Moreover, the proposed immobilization procedure is an efficient method to orient the enzyme active site toward the bulk liquid (Turková, 1999; Zaborsky, 1976). This study reports the feasibility of immobilizing *Trametes versicolor* laccase by using a mild oxidant to link the glycosyl residue to hydrazide groups on modified PMMA.

5.3 Materials and methods

5.3.1 Chemicals

Altuglas poly(methyl metacrylate) (PMMA) cylindrical pellets (3 mm long with a diameter of 3 mm) were kindly donated by Arkema Canada (Toronto, ON). *Trametes versicolor* laccase, Reactive blue 19, sodium periodate, hydrazine hydrate and dimethyl sulfoxide (DMSO) were purchased from Sigma-Aldrich Canada (Oakville, Ontario). Sodium acetate, sodium sulfate, sodium phosphate and the iodo-beads (Pierce Biotechnologies) were purchased from Fisher Scientific Canada (Ottawa, Ontario). Sodium 125-iodine was purchased from Perkin-Elmer (Waltham, MA, USA) and glutaric acid dialdehyde (glutaraldehyde) was purchased from Acros (Belgium).

5.3.2 Surface area of beads

The specific surface area of the PMMA beads was determined by measuring the amount of N₂ gas adsorbed on the beads at different partial pressures according to the B.E.T. theory (de Kanel and Morse, 1979). The quantity of gas adsorbed was measured with a Micrometric Tristar 300 (Micrometric Instrument Corp) at the Centre for Manufacturing of Advanced Ceramics and Nanomaterials, Queen's University (Ontario, Canada).

5.3.3 Hydrazinolysis of PMMA

Hydrazinolysis of esters on PMMA with hydrazine is based on the procedure of (Holmberg and Hydén, 1985). PMMA pellets were rinsed with 50 % propanol in deionized water and dried under an air stream. The beads were immersed either in a solution of 25 - 30 % hydrazine methanol-deionized water (1:1 v/v) at 50 °C for 24 h.

5.3.4 Enzyme preparation

Four hundred milligrams of lyophilysed *T. versicolor* laccase was dissolved in 60 ml of 20 mM NaH₂PO₄ at pH 7, centrifuged at 10,000 g for 2 hours, and then filtered with a Whatman paper and Millipore filters (0.45 μM). The filtrate containing laccase was dialyzed against 20 mM NaH₂PO₄ pH 7 for 20 hours at a dilution factor of approximately 5,000 and thereafter passed through a Q-sepharose anion exchange column pre-equilibrated with 20 mM NaH₂PO₄ at pH 7. Laccase was eluted in one step using 150 mM NaCl and dialyzed against 50 mM NaOAc/50 mM NaH₂PO₄ pH 5.

5.3.5 Immobilization of laccase through polysaccharide chains (method # 1)

A solution of 1.75 mg/ml laccase was mixed with 12.77 μ l of 0.468 M sodium periodate (10 mM final concentration) and incubated in the dark at 25 °C for 4 hours. The reaction was stopped by adding 75 μ l of ethylene glycol then dialyzed with an Amicon 20 ultrafiltration unit using a polyethersulfone membrane with a molecular cutoff of 3500 MW. For the immobilization, PMMA-hydrazide beads were incubated in a oxidized laccase solution (2070 μ g/ml) buffered with 50 mM sodium acetate pH 5.5, at 22.0 ± 1 °C for 24 h.

5.3.6 Immobilization of laccase by glutaraldehyde activation (method # 2)

Two grams of PMMA-hydrazide were immersed in a solution of 2.5 % aqueous glutaraldehyde for 2 hours at room temperature (22 ± 1 °C). The beads were rinsed with deionized water and immersed in a laccase solution with a protein concentration between 20 to 70 μ g/ml.

5.3.7 Free and immobilized enzyme assay

Laccase activity was measured by monitoring with a spectrophotometer the generation of 2,2-azino-bis(3-ethylbenzothiazoline-6-sulfonic acid) radicals ($ABTS^{\bullet-}$) at 420 nm from the oxidation of ABTS (Wolfenden and Willson, 1982) at 23 ± 1 °C using a Spectramax 250 plate reader with the SOFTmax PRO software package (Molecular Devices, CA, USA). The assay mixture contained 0.2 mM ABTS, 100 mM sodium acetate buffer (pH 5.0) and the enzyme sample (Bourbonnais *et al.*, 1995). One unit of laccase activity (U) was defined as the amount of enzyme that formed 1 mol $ABTS^{\bullet-}$ per min. For the immobilized laccase

system, the PMMA-laccase packed bed reactor (I.D. = 16 mm, l = 55 mm) was connected to a reservoir containing 100 ml of 50 mM sodium acetate/50 mM KH₂PO₄ (pH 5) via a peristaltic pump. The solution was 100 % re-circulated between the packed bed and the reservoir at a flow rate of 75 ml/min. To determine the immobilized laccase activity, the variation of the concentration of ABTS•⁻ in the reservoir with time was measured for a 6 or 10 minute interval during which the variation was linear.

5.3.8 Radio-labeling and quantification of laccase

Laccase was radio-labeled as specified by the supplier's protocol to quantify the amount of enzyme immobilized on the beads. 1 mCi of sodium 125-iodine was oxidized using 2 iodo-beads. The 0.75 ml-solution of the generated 125-iodide was incubated with 0.75 ml of 1.8 mg/ml laccase for 15 min on ice and the reaction stopped with 10 mM sodium metabisulfite. The iodinated laccase solution was separated from the unreacted iodine using a pre-packed Sephadex G-25 column (gel filtration) and one-ml fractions were collected. The fractions were quantified using a 1275 Minigamma gamma counter (LKB-Wallac, Turku, Finland). Laccase was quantified by monitoring the counts per minutes of 125I-laccase on 0.65 g of beads in 15-ml plastic test tubes. The counts were corrected with the count efficiency (96 %) and converted to the mass of laccase using the specific radio-activity. The mass of laccase immobilized was also determined by UV absorbance at 280 nm when laccase was cross-linked with glutaraldehyde. The readings were corrected for Raleigh scattering at 320 nm according to the following formula:

$$A_{corr}^{280} = A_{280} - A_{320} * \left(\frac{320}{280} \right)^4 \quad (5.1)$$

The coefficient of absorption for laccase was $\epsilon_{280}=1.074$ ml/mg and was determined by the ProtoParam program (protein parameter predictor) from the ExPASy website [http](http://) :

[//ca.expasy.org/tools/protparam.html](http://ca.expasy.org/tools/protparam.html).

5.3.9 Dependence of immobilized laccase mass on the initial enzyme concentration

A 1:10 ratio of radio-labeled to non-labeled laccase was modified by periodate oxidation then immobilized on PMMA-hydrazide beads according to the method described previously. A calibration curve with five initial laccase concentrations (25, 50, 100, 200 and 400 $\mu\text{g/ml}$) was used to determine the amount of immobilized laccase by relating laccase concentration with cpm.

5.4 Results

5.4.1 PMMA surface area and quantification of immobilized laccase

Laccase was radio-labeled with 125-iodine to accurately quantify the immobilized enzyme since its concentration was below the detection limit of common protocols (e.g. UV, Lowry and Bradford). The mass of immobilized laccase was determined by measuring the gamma counts generated by immobilized I125-laccase and divided by the total surface area of the beads as determined by the BET method ($194.34 \text{ cm}^2/\text{g}$) to obtain the amount of laccase immobilized per gram of beads. As shown in Figure 5.1, increasing the initial laccase concentration increased the mass of enzyme immobilized. The theoretical maximum amount of laccase that can be immobilized, assuming an effective molecular radius of 4 nm, is $0.218 \mu\text{g/cm}^2$ (for a protein monolayer), or $42.4 \mu\text{g/g}$ PMMA. The maximum experimental mass of enzyme immobilized was $0.0477 \mu\text{g/cm}^2$ or $9.9 \mu\text{g/g}$ and is approximately 4 times lower than the theoretical maximum which could be immobilized.

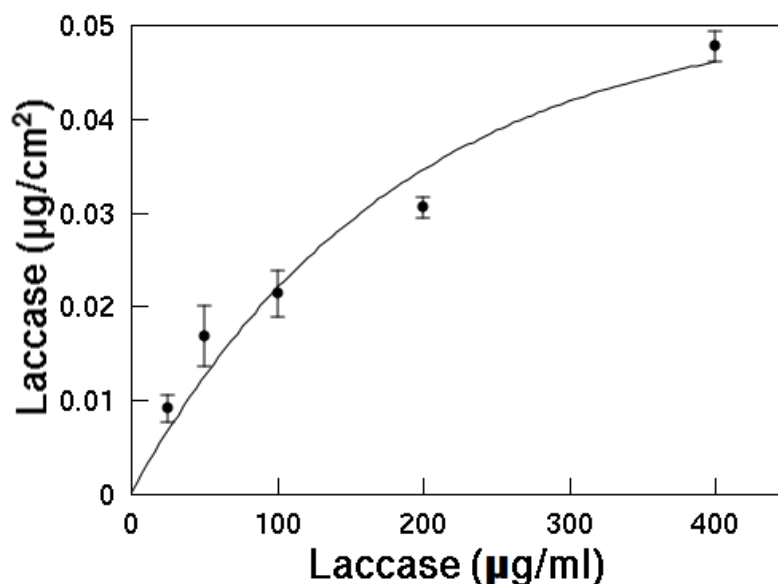


Figure 5.1: Effect of initial laccase concentration on its mass immobilized on PMMA-hydrazide pellets. The error bars represent the standard errors calculated from triplicates.

5.4.2 Effect of initial enzyme concentration, temperature and pH on the specific activity of immobilized laccase

The specific activity was calculated by dividing the measured activity of immobilized laccase by its estimated mass. The initial specific activity of the free enzyme varied between 50 and 80 U/mg (data not shown). The highest immobilized laccase activity on PMMA was achieved at 23 °C and increasing the pH of immobilization from 5 to 7 did not statistically affect the specific activity. The specific activity of immobilized laccase was 110 times higher when the enzyme was immobilized through its polysaccharide chains than when glutaraldehyde cross-linked the enzyme to PMMA (Table 5.1).

Table 5.1: Effect of temperature, pH and initial laccase concentration laccase immobilization on PMMA-hydrazide beads in 50 mM NaOAc buffer with 5 g of PMMA-hydrazide with a (total area of 971.7 cm²)

Immobilization temperature	Immobilization pH	Initial laccase concentration ($\mu\text{g/ml}$)	laccase immobilized (μg)	Specific activity (U/mg)
Periodate oxidation based immobilization				
23	5	35.19	7.56 \pm 0.34	2.82 \pm 0.15
23	5	22.21	4.85 \pm 0.34	2.05 \pm 0.16
5	5	21.39	4.67 \pm 0.34	1.53 \pm 0.12
5	7	29.00	6.28 \pm 0.34	1.30 \pm 0.24
Glutaraldehyde cross-linking				
23	5	63.27	838 \pm 113	0.0204 \pm 0.003

5.5 Discussion

The goal of this study was to assess the feasibility of immobilizing *Trametes versicolor* laccase on PMMA, a relatively inexpensive material, instead of using more expensive commercial protein supports. This was successfully accomplished with both immobilization protocols, i.e., the commonly used glutaraldehyde cross-linking and the milder periodate oxidation. However, using the milder periodate oxidation resulted in higher specific activities suggesting that immobilizing laccase through its sugar residues which are away from the active site is a better strategy for preserving enzyme activity. This may have reduced the risk of deactivating the active site while glutaraldehyde can react with any primary

amine group and lead to enzyme deactivation. The higher quantity of immobilized laccase when cross-linked with glutaraldehyde suggests that multiple layers of laccase were formed. However, due to diffusion limitations, enzymes in the lower layers could be less active.

The mass of protein immobilized on PMMA achieved in this study compares well with those reported with commercial or tailored acrylic carriers (Table 5.2).

Table 5.2: Comparative table of masses immobilized laccase with commercial acrylic-based carriers

Support	Laccase source	Protein concentration ($\mu\text{g}/\text{cm}^2$)	surface	Specific activity (U/mg protein)	References
Sepabead EC-EP3	<i>Myceliophora thermophila</i>	0.0758		6.23	Kunamneni <i>et al.</i> (2008)
Dilbeads NK	<i>Myceliophora thermophila</i>	0.0414		5.11	Kunamneni <i>et al.</i> (2008)
Poly(glycidyl methacrylate)-co-ethylene-dimethacrylate)	<i>Cerrena unicolor</i>	0.241		77.6	Arica <i>et al.</i> (2009)
PMMA	<i>T. versicolor</i>	0.0477		2.82	Present study
CPC-silica beads	<i>T. versicolor</i>	4.39×10^{-3}		1.50	Chapter 3

However, the enzyme was less active by almost 50 % than that reported by Kunamneni *et al.* (2008) and twenty-seven times lower that reported by Arica *et al.* (2009). The large difference may be explained in part by the activity units based on different substrates

(Arica *et al.*, 2009). While the nature of the acrylic monomers of Dilbeads and Sepabeads was not reported, acrylic polymers used for enzyme immobilization generally possess substantial hydrophilicity to favor good enzyme activity retention (Epton *et al.*, 1976; Novick and Dordick, 2000). PMMA may not be as hydrophilic as the Dilbead and Sepabead polymers and this difference may explain the lower laccase specific activity in this investigation. Moreover, (Arica *et al.*, 2009) used spacer arms to retain good enzyme activity. To increase the total immobilized laccase activity, porous beads can be used to increase the protein immobilized and a spacer arm to increase the distance between the enzyme and the carrier to minimize interactions. Nonetheless, the results suggest that PMMA is a suitable support for laccase and can be used for dye decolorization since its specific activity was comparable to that achieved with CPC-silica beads.

There are no reports on the effect of the immobilization temperature on the activity of immobilized laccase. Although Bahar and Celebi (1999) demonstrated that increasing the immobilization temperature of a glucoamylase from 20 to 40 °C did not affect its immobilized activity, in this study, the highest specific activity of immobilized laccase was obtained at room temperature. The results in this study indicate that immobilizing the enzyme at 5 or 23 °C does not affect greatly the activity of the enzyme.

5.6 Conclusion

This investigation has reported for the first time the immobilization of *T.versicolor* laccase through its polysaccharide residues on PMMA beads which were hydrazinolysed in one step. The hydrazinolysis eliminates the need for a polymerization process that can be labor intensive and requires an elaborate setup. The retention of laccase activity on PMMA was lower than some common commercial carriers but may be sufficient for dye decolorization applications. The simple immobilization method may be a viable alternative to using more

expensive commercial beads or the more brittle alumina and silica beads.

Bibliography

- Arica MY, Altintas B, Bayramoğlu G. 2009. Immobilization of laccase onto spacer-arm attached non-porous poly(gma/egdma) beads: application for textile dye degradation. *Bioresour Technol* **100**(2): 665–669.
- Bahar T, Celebi S. 1999. Immobilization of glucoamylase on magnetic poly (styrene) particles. *Journal of Applied Polymer Science* **72**(1): 69–73.
- Bourbonnais R, Paice MG, Reid ID, Lanthier P, Yaguchi M. 1995. Lignin oxidation by laccase isozymes from *Trametes versicolor* and role of the mediator 2,2'-azinobis(3-ethylbenzthiazoline-6-sulfonate) in kraft lignin depolymerization. *Appl Environ Microbiol* **61**(5): 1876–1880.
- Brown L, Koerner T, Horton JH, Oleschuk RD. 2006. Fabrication and characterization of poly(methylmethacrylate) microfluidic devices bonded using surface modifications and solvents. *Lab Chip* **6**(1): 66–73.
- de Kanel J, Morse J. 1979. A simple technique for surface area determination. *J. Phys. E* **12**: 272–273.
- Dominick WD, Berhane BT, Mecomber JS, Limbach PA. 2003. Covalent immobilization of proteases and nucleases to poly(methylmethacrylate). *Anal Bioanal Chem* **376**(3): 349–354.
- Duran N, Rosa M, DAnnibale A, Gianfreda L. 2002. Applications of laccases and tyrosinases (phenoloxidases) immobilized on different supports: a review. *Enzyme Microb Technol* **31**(7): 907–931.
- Epton R, Hibbert B, Thomas T. 1976. Enzymes covalently bound to polyacrylic and polymethacrylic copolymers. *Methods Enzymol* **44**: 84–107.
- Fixe F, Dufva M, Telleman P, Christensen CBV. 2004. One-step immobilization of aminated and thiolated dna onto poly(methylmethacrylate) (pmma) substrates. *Lab Chip* **4**(3): 191–195.

- Hermanson G. 1996. *Bioconjugate techniques*. Academic Press, 1st edn, ISBN # 978-0123423368.
- Holmberg K, Hydén H. 1985. Methods of immobilization of proteins to polymethylmethacrylate. *Prep Biochem* **15**(5): 309–319.
- Jost R, Miron T, Wilchek M. 1974. The mode of adsorption of proteins to aliphatic and aromatic amines coupled to cyanogen bromide-activated agarose. *Biochim biophys acta* **362**(1): 75–82.
- Kunamneni A, Ghazi I, Camarero S, Ballesteros A, Plou F, Alcalde M. 2008. Decolorization of synthetic dyes by laccase immobilized on epoxy-activated carriers. *Process Biochem* **43**(2): 169–173.
- Leal M, Freire D, Cammarota M, SantAnna G. 2006. Effect of enzymatic hydrolysis on anaerobic treatment of dairy wastewater. *Process Biochem* **41**(5): 1173–1178.
- Leonowicz A, Sarkar J, Bollag J. 1988. Improvement in stability of an immobilized fungal laccase. *Appl Microbiol and Biotechnol* **29**(2): 129–135.
- Novick SJ, Dordick JS. 2000. Investigating the effects of polymer chemistry on activity of biocatalytic plastic materials. *Biotechnol Bioeng* **68**(6): 665–71.
- Nyanhongo GS, Gomes J, Gübitz GM, Zvauya R, Read J, Steiner W. 2002. Decolorization of textile dyes by laccases from a newly isolated strain of *trametes modesta*. *Water Res* **36**(6): 1449–1456.
- Peralta-Zamora P, Pereira C, Tiburtius E, Moraes S, Rosa M, Minussi R, Durán N. 2003. Decolorization of reactive dyes by immobilized laccase. *Appl Catal B* **42**(2): 131–144.
- Rigo E, Rigoni R, Lodea P, Oliveira D, Freire D, Luccio M. 2008. Application of Different Lipases as Pretreatment in Anaerobic Treatment of Wastewater. *Environ Eng Sci* **25**(9): 1243–1248.
- Rogalski J, Dawidowicz A, Jóźwik E, Leonowicz A. 1999. Immobilization of laccase from *Cerrena unicolor* on controlled porosity glass. *Journal of Molecular Catalysis. B, Enzymatic* **6**(1-2): 29–39.
- Salony, Mishra S, Bisaria VS. 2006. Production and characterization of laccase from *Cyathus bulleri* and its use in decolourization of recalcitrant textile dyes. *Appl Microbiol Biotechnol* **71**(5): 646–653.
- Turková J. 1999. Oriented immobilization of biologically active proteins as a tool for revealing protein interactions and function. *J Chromatogr B Biomed Sci Appl* **722**(1-2): 11–31.
- Wolfenden B, Willson R. 1982. Radical-cations as reference chromogens in kinetic studies of one-electron transfer reactions. *J Chem Soc Perkin Trans* **2**(1982): 805–812.

- Wong Y, Yu J. 1999. Laccase-catalyzed decolorization of synthetic dyes. *Water Res* **33**(16): 3512–3520.
- Zaborsky O. 1976. Immobilized enzymes-miscellaneous methods and general classification, in immobilized enzymes. *Methods Enzymol* : 317–332.
- Zille A, Tzanov T, Gübitz GM, Cavaco-Paulo A. 2003. Immobilized laccase for decolorization of reactive black 5 dyeing effluent. *Biotechnol Lett* **25**(17): 1473–1477.

Chapter 6

The effects of a non-ionic surfactant, Merpol, on laccase decolourization of Reactive blue 19

6.1 Abstract

Laccase is a multi-copper oxidase that can decolorize textile dyes and there is increasing interest in its use to treat textile wastewaters which also contain auxiliary chemicals such as surfactants and salts. This investigation examines the effect of Merpol, a non-ionic surfactant, on the decolorization of Reactive blue 19, an anthraquinone dye, and on the oxidation of 2,2'-azino-bis(3-ethylbenzothiazoline-6-sulfonic acid) (ABTS) by *Trametes versicolor* laccase. The results show that the surfactant had little effect on the enzyme or on ABTS oxidation which followed Michaelis-Menten kinetics. However, Reactive blue 19 decolorization was inhibited with increasing Merpol concentration. Spectroscopic analysis of

the dye with Merpol and analysis of the kinetic data show that decolorization rates depended on an interaction between the dye and the surfactant. The proposed inhibition by a substrate depletion model in which the dye concentration decreases as a dye molecule binds to a surfactant molecule and/or is sequestered into micelles fits the data suitably and the model was validated by estimating the inhibition constant from independent saturation equilibrium binding assays. This study is the first to investigate the kinetic effect of a surfactant on the enzymatic dye decolorization and to show the depleting effect of Merpol on Reactive blue 19.

6.2 Introduction

Enzymes may be used to effectively remove low concentration pollutants in wastewaters (Karam and Nicell, 1997). The lignin-degrading enzyme laccase has attracted significant interest for treating textile waste effluents and its ability to decolorize dyes (reviewed in Husain (2006)). It is copper oxidase that efficiently degrades anthraquinone dyes and dyes with phenolic moieties (Young and Yu, 1997; Nyanhongo *et al.*, 2002; Champagne and Ramsay, 2005). Unlike lignin or manganese peroxidase, laccase requires only molecular oxygen as a co-substrate and may be more suitable biocatalysts for industrial and bioremediation applications. Laccase can degrade phenolic compounds in wine distillery wastewater (Strong and Burgess, 2008), estrogens in municipal wastewater (Auriol *et al.*, 2007) and textile dyes in textile wastewaters (Reyes *et al.*, 1999). In the latter investigation, immobilized *Coriolopsis gallica* laccase decolorized 10 batches of an industrial waste effluent containing Direct Blue 200, Direct Red 80 and Direct Black 22. The removal efficiency decreased with increasing decolorization batches and the authors could not identify the cause of the enzyme deactivation. Although a few studies have used laccase to decolorize industrial textile waste effluents, there is no kinetic investigation of the effects of the effluent

components on enzyme activity.

Textile wastewaters contain not only residual dyes, but also auxiliary chemicals such as surfactants, salts, oils and greases. Surfactants are amphiphilic molecules with a polar head and hydrophobic carbon chains. Although a growing number of studies focus on laccase activity in reverse micelles (Khmelnitsky *et al.*, 1992; Michizoe *et al.*, 2005; Liu *et al.*, 2006), few investigations have analyzed the effect of surfactants on enzymatic dye decolorization. Harazono and Nakamura (2005) showed that MnP from *Phanerochaete sordida* required Tween 80, a non-ionic surfactant, to decolorize a mixture of reactive dyes (Reactive black 5, Reactive red 120, Reactive green 5 and Reactive orange 14) but was inhibited by another surfactant, polyvinyl alcohol (PVA). The authors thought that inhibition occurred because PVA interrupted the lipid peroxidation which generates reactive radicals. Abadulla *et al.* (2000) reported that Univadine PA (anionic surfactant), Tinegal MR (cationic surfactant) and Albegal FFA (wetting agent) inhibited 2,6-dimethoxyphenol oxidation by *Trametes hirsuta* laccase by 17.9 %, 5.2 % and 2.3 % respectively but the effects on dye decolorization were not examined. Moreover, there are no studies which have examined the effect of surfactants on decolorization kinetics by laccase.

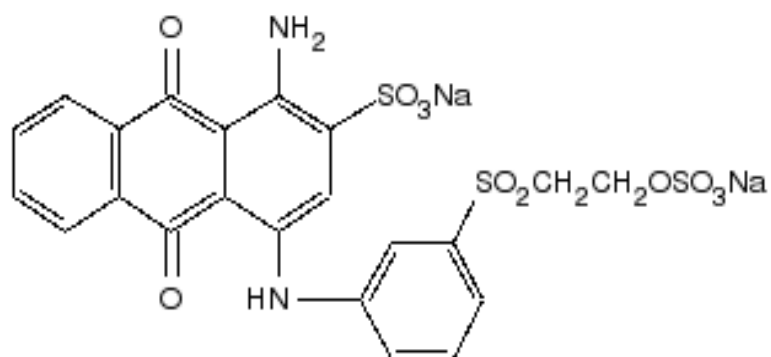
Merpol is a non-ionic, polyethylene oxide surfactant used as a wetting and emulsifying agent to achieve better fabric permeation that allows an even dyeing of textile fabrics. There is no report on the effects of a non-ionic surfactant like Merpol on dye decolorization or decolorization kinetics. Since such a surfactant could be in the dye effluent, it is useful to know whether it affects the enzymatic decolorization. This investigation therefore analyzes the impact of Merpol on the decolorization of an anthraquinone dye, Reactive blue 19 (6.1A), by laccase from *Trametes versicolor* and compares the decolorization kinetics with laccase oxidation of 2,2'-Azino-bis(3-ethylbenzothiazoline-6-sulfonic acid) (6.1B) (ABTS)

6.3 Materials and methods

6.3.1 Chemicals

2,2'-Azino-bis(3-ethylbenzothiazoline-6-sulfonic acid) diammonium salt (ABTS), Reactive blue 19, Merspol HCS, Q-sepharose, sodium dihydrogenophosphate, sodium acetate and *Trametes versicolor* laccase were purchased from Sigma-Aldrich Canada (Oakville ON, Canada).

A



B

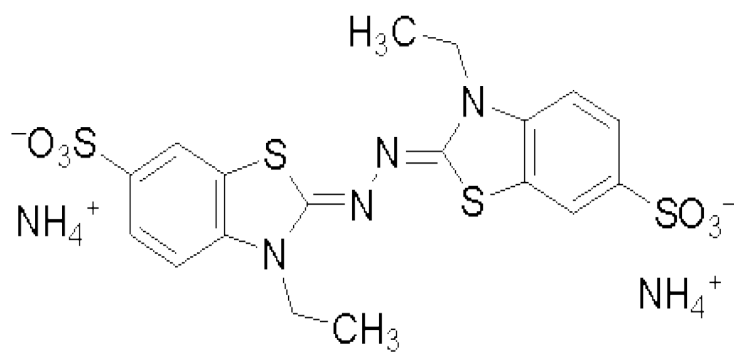


Figure 6.1: Structure of (A) Reactive blue 19 and (B) ABTS

6.3.2 Enzyme preparation

Four hundred milligrams of lyophilized *Trametes versicolor* laccase was dissolved in 60 ml of 20 mM NaH_2PO_4 at pH 7, centrifuged at 10,000 x g for 2 hours, and then filtered with a Whatman paper and Millipore filters (0.45 μM). The filtrate was dialyzed against 20 mM NaH_2PO_4 pH 7 for 20 hours at a dilution factor of approximately 5,000 then passed through a Q-Sepharose anion exchange column pre-equilibrated with 20 mM NaH_2PO_4 at pH 7. Laccase was eluted in one step using 150 mM NaCl. The eluate was dialyzed against 50 mM NaOAc/50 mM NaH_2PO_4 pH 5.

6.3.3 Enzyme assay and quantification

Laccase activity was determined by monitoring with a spectrophotometer the generation of 2,2-azino-bis(3-ethylbenzothiazoline-6-sulfonic acid) radicals (ABTS^\bullet) at 420 nm from the oxidation of ABTS (Wolfenden and Willson, 1982) at $23 \pm 1^\circ \text{C}$ using a Spectramax 250 plate reader with the SOFTmax PRO software package (Molecular Devices, Sunnyvale CA, USA). The assay mixture contained 0.5 mM ABTS, 100 mM sodium acetate buffer (pH 5.0) and the enzyme aliquot for total reaction mixture of 180 μl . The path length of absorbance in the well for this volume was 0.5 cm. One unit of laccase activity (U) was defined as the amount of enzyme that formed 1 μmol ABTS^\bullet per minute. Protein concentration was measured by the absorbance at 280 nm and corrected for scattering effects with absorbance readings at 320 nm.

6.3.4 Dye concentration and spectroscopic analysis

The concentration of Reactive blue 19 was measured with a Unicam UV1 spectrophotometer (Spectronic Unicam, Cambridge, UK) or Spectramax 250 plate reader at the dyes maximum absorption wavelength (592 nm). The absorbance coefficient was determined to

be $10,044 \text{ M}^{-1}\text{cm}^{-1}$ (in 50 mM NaOAc/50 mM NaH_2PO_4 pH 5) with a calibration curve from 0 to $45.3 \mu\text{M}$. Spectral scans of the dye or ABTS with (3.09 g/l) or without Merspol were conducted.

6.3.5 Saturation equilibrium binding

Equilibrium binding assays were conducted by incubating dye concentrations of 16, 32, 48, 64, 80, 96, 112 and $128 \mu\text{M}$ at a fixed Merspol concentration of 0.386, 0.773, or 1.03 g/l. The assay mixture was buffered with 50 mM NaOAc/50 mM NaH_2PO_4 pH 5. Assays were conducted in 96-well plates that were pre-saturated with the surfactant for 4 hours. The dye-Merspol binding was allowed to reach equilibrium for 45 minutes, time after which the absorbance readings did not fluctuate with time. The dye-Merspol complex was monitored with the Spectramax 250 at 630 nm.

6.3.6 Effect of Merspol on Reactive blue 19 decolorization and on ABTS oxidation and kinetic studies

Initial dye decolorization rates were measured in the presence of 0, 0.773, 1.55, 2.58 or 3.09 g/l Merspol. The rate of ABTS oxidation was measured in the presence of 0, 1.55 or 3.09 g/l Merspol. All assays were conducted at pH 5 in 50 mM NaOAc/50 mM NaH_2PO_4 and in 96-well plates (300 μl per well). Each well contained 108 μl of buffer, 36 μl of substrate (in the same buffer), and 36 μl of laccase solution for total reaction mixture of 180 μl . The path length of absorbance in the well for this volume was 0.5 cm. The assay mixture had a final concentration of 0.274 nM laccase with ABTS and 120 nM with Reactive blue 19. For steady-state kinetic analysis, initial rates were similarly determined for 0 to 400 μM Reactive blue 19 and for 0 to 1000 μM ABTS. The reaction was initiated by adding the enzyme aliquot to the assay mixture. Time course curves of 61 absorbance points were

generated over 30 minutes and the initial rate was determined by the software package SOFTmax Pro (Molecular Devices) by calculating the tangent slope to the first five to ten points so that the decrease did not exceed 10 % conversion (see Appendix D.2 for a sample calculation). The initial rates were measured in triplicate at $22 \pm 1^\circ\text{C}$ as described. All experiments were done in triplicate and the results shown are averages with the error bars representing the standard error.

6.3.7 Estimation of kinetic constants

The estimation of kinetic parameters and the inhibition constants were determined by non-linear least square regression (The sums of squares was minimized with the Gauss-Newton algorithm with equal weighting for each parameters) using the R statistical package (R project for statistical computing, CRAN) and Systat (Systat Software, Inc., San Jose, CA, USA). Although in the data analysis each data point was fitted to the model, the triplicates were averaged and the model fitted through the average values for graphical presentation.

6.4 Results

6.4.1 Effect of Merpol on the rate of ABTS oxidation and dye decolorization by laccase

Increasing the Merpol concentration from 0 to 3.09 g/l had little effect on ABTS oxidation while the rate of Reactive blue 19 decolorization decreased significantly from 1.79 to 0.37 $\mu\text{M}/\text{min}$ (Figure 6.2).

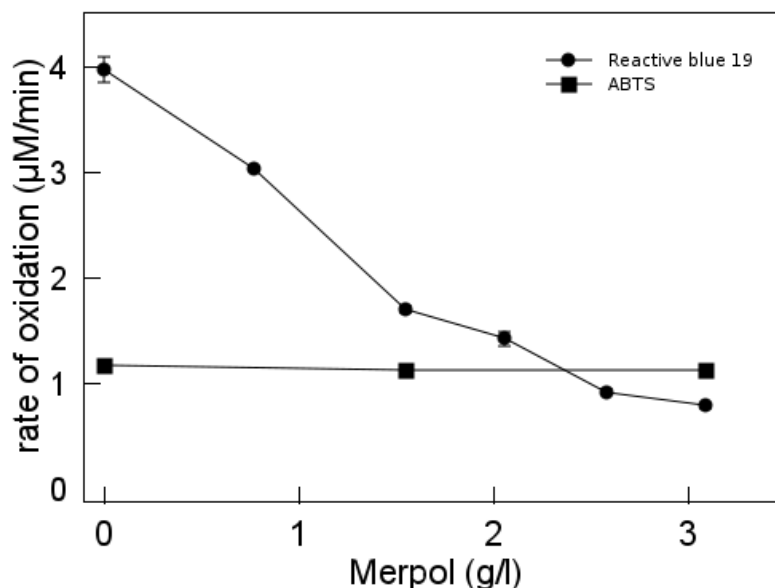
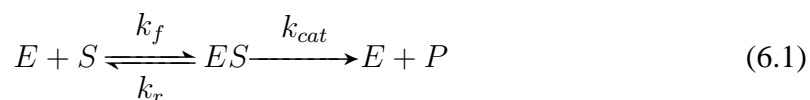


Figure 6.2: Effect of Merspol on the rate of ABTS oxidation and Reactive blue 19 decolourization by laccase. The decolourization assay mixture contained 120 nM laccase in a 50 mM NaOAc/50 mM NaH₂PO₄ pH 5 and the temperature was 22 ± 1 C. Each data point is the average of triplicates and error bars represent the standard deviation.

6.4.2 Effect of Merspol on the kinetics of ABTS oxidation and Reactive blue 19 decolorization

The Michaelis-Menten rate equation (equation 6.2) for an enzyme-catalyzed reaction (equation 6.1) describes the dependence of the reaction rate (v) on the molar concentration of the free substrate $[S]$ and the total enzyme $[E]_{tot}$.



The k_{cat} is the turnover number and is usually expressed in unit of s⁻¹ and K_M is the affinity constant as well as the molar concentration of the free substrate that yields a reaction rate equal to half the maximum rate, V_{max} ($= k_{cat}[E]_{tot}$).

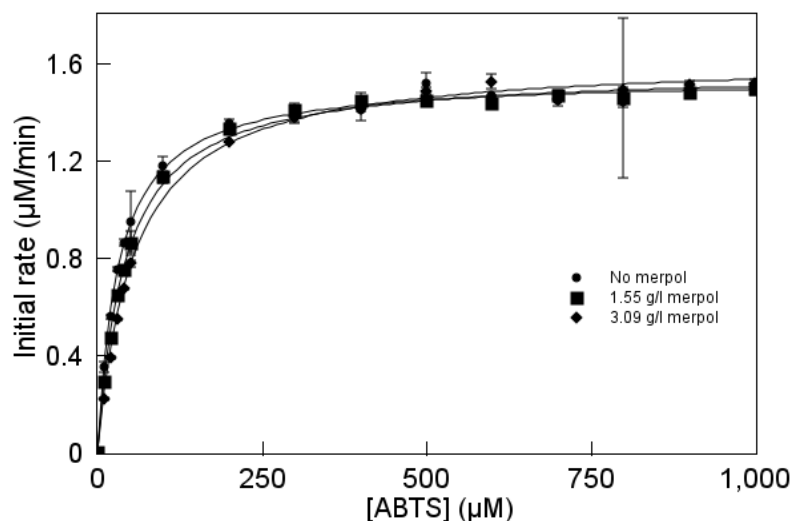


Figure 6.3: Effect of Merspol on ABTS oxidation by 0.274 nM laccase in 50 mM NaOAc/50 mM NaH_2PO_4 at pH 5 ($T = 22 \pm 1^\circ\text{C}$). Comparison of experimental data (each symbol is the average of triplicates and the error bars represent the standard deviation) and the Michaelis-Menten model (equation 1, solid lines).

$$v = \frac{k_{cat}[E]_{tot}[S]}{K_M + [S]} = \frac{V_{max}[S]}{K_M + [S]} \quad (6.2)$$

ABTS oxidation by laccase followed Michaelis-Menten kinetics at all Merspol concentrations tested (0 to 3.09 g/l) (Figure 6.3). Although Figure 3 shows little effect on ABTS oxidation, the k_{cat} increased slightly from 93.6 to 98.3 s^{-1} and the K_M from 32.1 to 54.9 μM (Table 6.1) indicating that the surfactant reduced the affinity of the enzyme for ABTS while slightly enhancing the enzyme activity.

6.4.3 Spectroscopic analysis of Reactive blue 19 with Merspol

Spectroscopic analysis of Reactive blue 19 without Merspol or laccase showed a maximum absorbance at 592 nm. With the addition of 3.09 g/l Merspol, a second peak appeared at

630 nm. There was a slight but not significant shift in the spectral behavior of ABTS after Merspol addition (Figure 6.4A and B) and Merspol alone did not absorb in the visible range (Figure 6.4C).

6.4.4 Saturation equilibrium binding

The dye-Merspol complex was monitored spectrophotometrically at 630 nm. The absorbance at 630 nm shown in Figure 6.5 corresponding to the complex was calculated by subtracting the absorbance of the dye at that wavelength from the absorbance of the dye-surfactant mixture. As shown in the figure, the dye-Merspol complex increased with increasing dye concentration and tended to plateau at high concentrations. The derivation of the model fitted through the points is presented in the next section.

6.4.5 Estimation of K_d from the saturation equilibrium experiment

The equilibrium binding of Reactive blue 19 (S, the ligand) to Merspol (M) to form a complex (SM) is described by



where k_f and k_r are the rate constants for the ligand binding and complex dissociation respectively. At equilibrium, the rate of binding is equal to the rate of dissociation

$$r_{binding} = r_{dissociation} \quad (6.4)$$

$$k_f[M][S] = k_r[SM] \quad (6.5)$$

$$\frac{k_r}{k_f} = \frac{[S][M]}{[SM]} = K_d \quad (6.6)$$

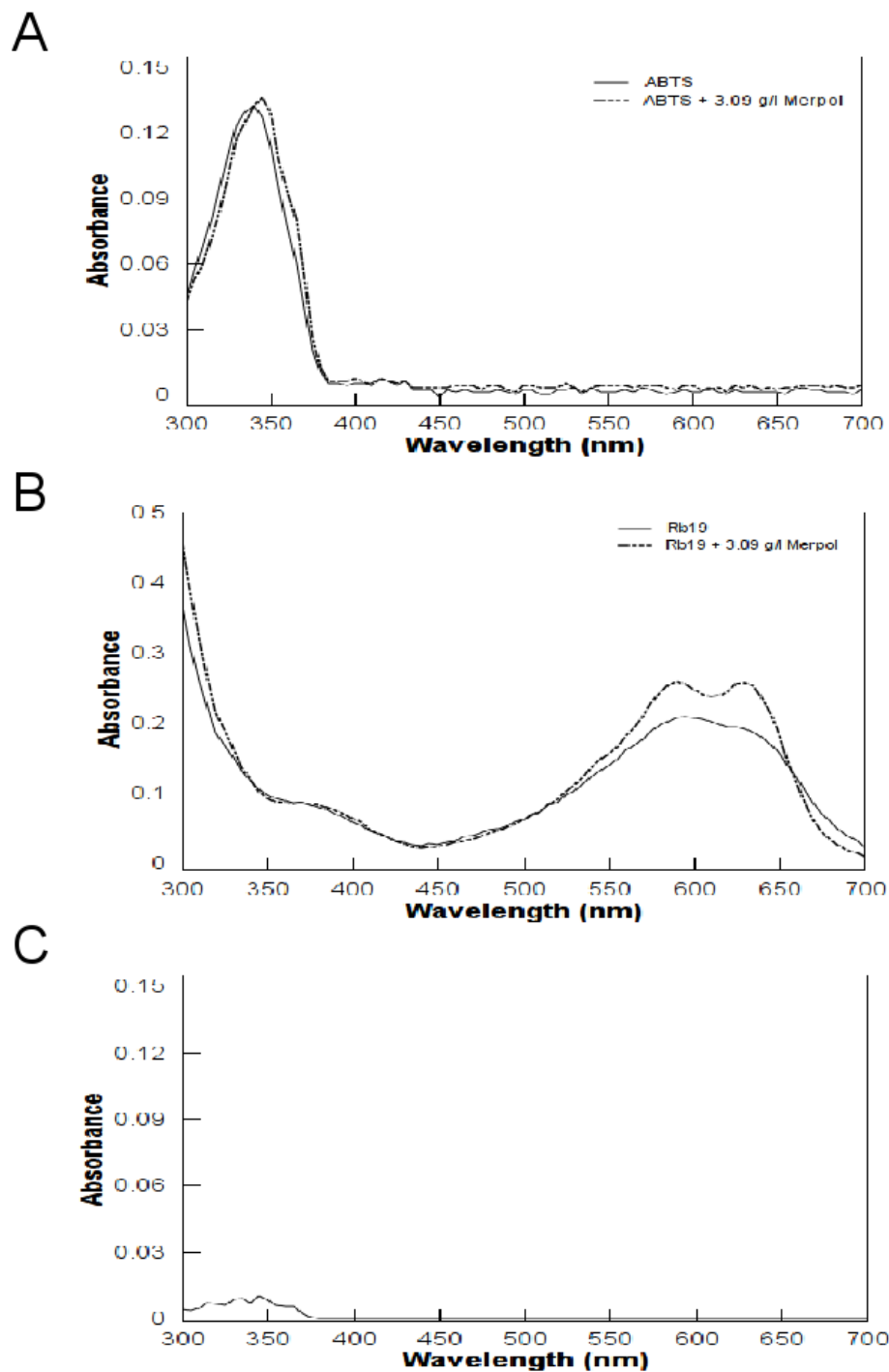


Figure 6.4: Spectrophotometric analysis of (A) ABTS, (B) Reactive blue 19, with and without Merspol and (C) 3.09 g/l Merspol alone. The mixture contained $50 \mu\text{M}$ Reactive blue 19 or $0.5 \mu\text{M}$ ABTS and 3.09 g/l Merspol in 50 mM NaOAc/50 mM NaH_2PO_4 buffer at pH 5 ($T = 22 \pm 1^\circ\text{C}$).

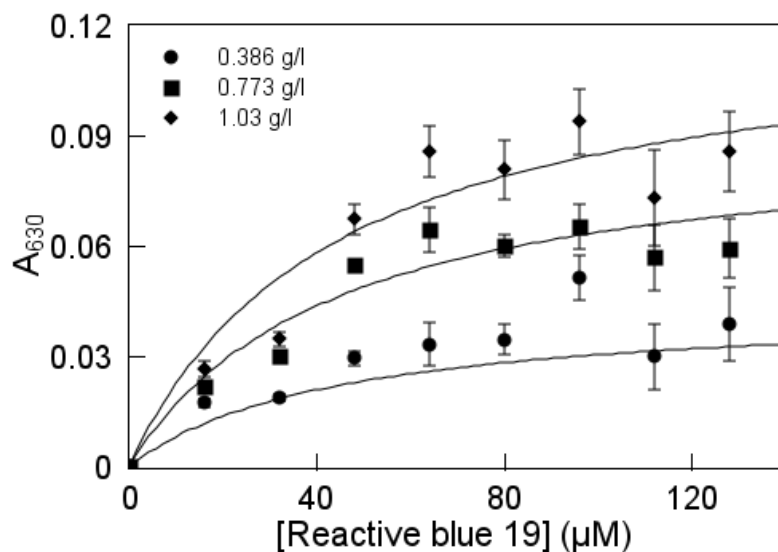


Figure 6.5: Saturation equilibrium of Reactive blue 19 and Merspol binding. The absorbances were calculated by subtracting The assay mixture was buffered with 50 mM NaOAc/50 mM NaH₂PO₄ pH 5 (T = 22 ± 1°C).

K_d is the equilibrium dissociation constant and is in units of concentration. The total concentration of Merspol is

$$[M]_{total} = [M] + [SM] \quad (6.7)$$

Solving equation 6.6 for $[M]$ and substituting into equation 6.7 yields

$$[M]_{total} = \frac{[SM]K_d}{[S]} + [SM] = [SM] \left(\frac{K_d}{[S]} + 1 \right) \quad (6.8)$$

After rearranging equation 6.8, we get

$$[SM] = \frac{[M]_{total}[S]}{K_d + [S]} \quad (6.9)$$

Since the formation of the complex was monitored at 630 nm,

$$[SM] = \frac{A_{630}}{\epsilon_{630} \times l} = \frac{A_{630}}{\epsilon_{630} \times 0.5cm} \quad (6.10)$$

where A_{630} is the absorbance at 630 nm, l is the path length of the medium, and ϵ_{630} is the absorption coefficient (in $M^{-1} cm^{-1}$) at 630 nm. Substituting equation 6.10 into equation 6.9, we obtain

$$A_{630} = \frac{2\epsilon_{630}[M]_{total}[S]}{K_d + [S]} = \frac{\gamma_{630}[M]_{total}[S]}{K_d + [S]} \quad (6.11)$$

where γ_{630} is a lumped absorption coefficient and is equal to $2\epsilon_{630}$. With equation 6.11, K_d was estimated to be $44.1 \pm 10.1 \mu M$ and γ_{630} to be $0.119 \pm 0.010 l g^{-1} cm^{-1}$ (Table I).

6.4.6 Kinetic modeling of the effect of Merspol on the decolorization of Reactive blue 19 by laccase

Without Merspol, the Reactive blue 19 decolorization also followed Michaelis-Menten kinetics (Figure 6.6) but as the Merspol concentration increased, the initial rates decreased and decolorization kinetics became increasingly sigmodal. The dependence of initial rates on initial dye concentrations in the presence of Merspol did not follow Michaelis-Menten kinetics. Hence, a modified rate equation is hypothesized where the inhibitor (M, i.e. Merspol) binds to the free substrate (S, i.e. Reactive blue 19) but not the enzyme (E, laccase) (Figure 6.7).

Furthermore, the enzyme can convert the free dye only to decolorized products (P) as the dye bound by Merspol is unavailable for decolorization. Since the total dye concentration added to the reaction mixture, $[S]_T$, is the sum of the free dye $[S]$, the enzyme-dye complex $[ES]$ and the dye-Merspol complex $[SM]$ concentrations, $[S]$ can be expressed as

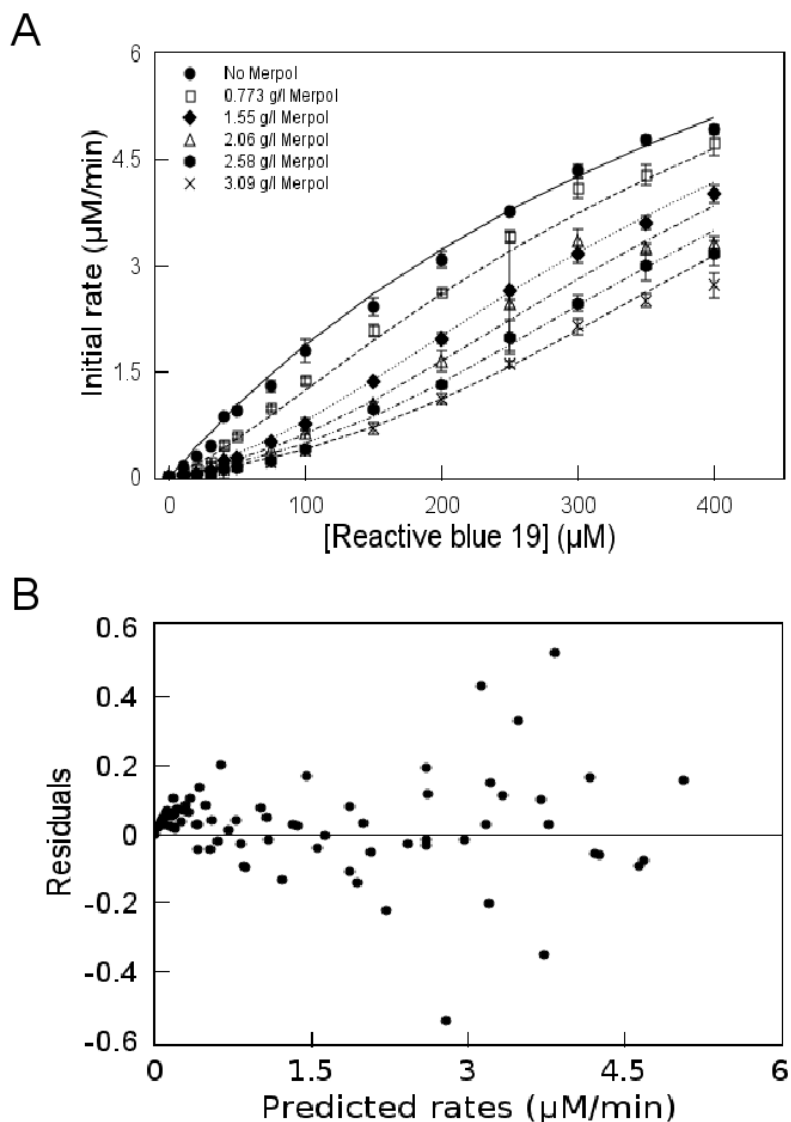


Figure 6.6: Inhibition of laccase decolourization of Reactive blue 19 by Mersol (A) and the residual plot (B). The laccase concentration was 120 nM in 50 mM NaOAc/50 mM NaH_2PO_4 buffered at pH 5. Comparison of experimental data (each symbol is the average of triplicates and the error bars represent the standard deviation) and the substrate depletion model (equation 5, solid lines).

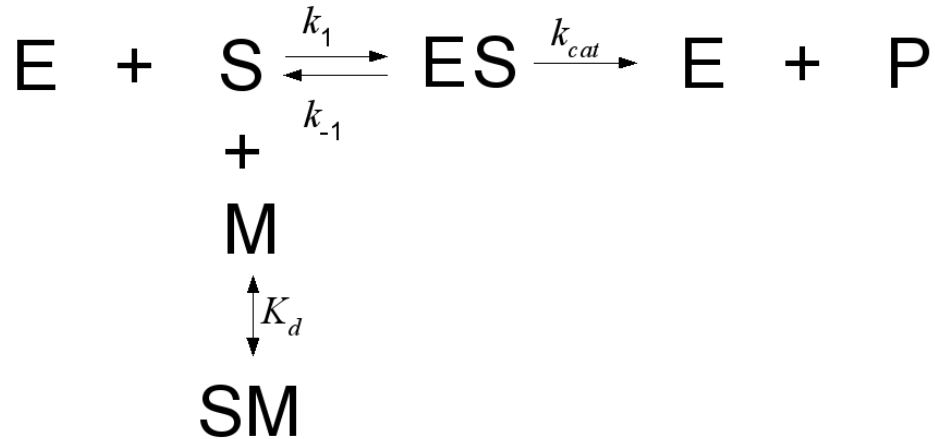


Figure 6.7: Kinetic scheme for the inhibition of dye decolourization by substrate depletion

$$[S] = [S]_T - ([ES] + [SM]) \quad (6.12)$$

Given that $[S] \gg [E]$, then $[S] \gg [ES]$ so that $[ES]$ can be omitted and equation 6.12 simplified to

$$[S] = [S]_T - [SM] \quad (6.13)$$

Similarly, the free Merspol concentration, $[M]$, can be estimated as

$$[M] = [M]_T - [SM] \quad (6.14)$$

where $[M]_T$ is the total Merspol concentration. Substituting equation 6.13 in equation 6.2, we obtain

$$v = \frac{k_{cat}[E]_{tot} ([S]_T - [SM])}{K_M + ([S]_T - [SM])} \quad (6.15)$$

The dissociation constant, K_d , for M binding to S is

$$K_d = \frac{[S][M]}{[SM]} \quad (6.16)$$

Substituting equations 6.13 and 6.14 in equation 6.16 yields

$$K_d = \frac{([S]_T - [SM]) ([M]_T - [SM])}{[SM]} \quad (6.17)$$

Solving equation 6.17 for [SM],

$$[SM] = \frac{1}{2} \left(K_d + [S]_T + [M]_T - \sqrt{(K_d + [S]_T + [M]_T)^2 - 4 \times [S]_T [M]_T} \right) \quad (6.18)$$

The number of inhibitor (Merpol) binding sites, n (μmol per g of Merpol), is proportional to the total inhibitor concentration $[M]_T$ such that

$$[M]_T = n[M]_0 \quad (6.19)$$

where n is the μmoles of dye bound to 1 gram of Merpol and $[M]_0$ is the total surfactant concentration added (in g/l). The correlation between the decolorization rate, the dye and surfactant concentrations was reasonably described by the modified rate equation (equation 6.15) (solid lines) with no bias (Figure 6.6B) which also predicted the sigmoidal kinetic behavior (Figure 6.6A). Kinetic parameters were determined (Table 6.1) and the number of μmoles of dye bound to 1 gram of Merpol, n , was found to be $80.3 \mu\text{mol/g}$.

Table 6.1: Effect of Merspol on ABTS oxidation and the decolourization of Reactive blue 19 by 120 nM laccase in 50 mM NaOAc/50 mM NaH₂PO₄, pH=5. The kinetic parameters for ABTS were determined using the Michaelis-Menten model and for Reactive blue 19 using the derived inhibition model

Steady-state kinetics					
Merspol (g/l)	k_{cat} (s ⁻¹)	K_M (μM)	k_{cat} / K_M (×10 ⁵ M ⁻¹ s ⁻¹)	n (μmol/g)	K_d (μM)
ABTS					
0	93.6 ± 0.7	32.1 ± 1.2	29.2	-	-
1.55	95.2 ± 0.7	42.0 ± 1.4	22.7		
3.09	98.3 ± 1.0	54.9 ± 2.7	18.0		
Reactive blue 19					
0 - 3.09	1.65 ± 0.07	537 ± 36		80.5 ± 2.2	38.3 ± 3.4
Saturation equilibrium binding					
Merspol (g/l)	γ_{630} (l g ⁻¹ cm ⁻¹)	K_d (μM)			
0 - 1.03	0.119 ± 0.010	44.1 ± 10.1			

6.5 Discussion

The results in this study show that Merspol had little effect on laccase but affected the decolorization of Reactive blue 19. Since Merspol slightly increased the ABTS oxidation rate (Table 6.1), the surfactant may have a stabilizing and/or inducing effect on laccase for ABTS. Basto *et al.* (2007) also showed improved laccase stability in the presence of polyvinyl alcohol in the ultrasonic decolorization of Indigo carmine. However, when Reactive blue 19 was the substrate, Merspol clearly inhibited its decolorization. Although Abadulla *et al.* (2000) did not examine the effect of surfactants on enzymatic dye decolorization, they found that Univadine PA (anionic surfactant), Tinegal MR (cationic surfactant) and Albe-gal FFA (wetting agent) inhibited the oxidation of 2,6-dimethoxyphenol by laccase. The inhibition was less severe than that obtained with Reactive blue 19 in the present study. Their highest inhibition of 17.9 % was obtained with 2 g/l Univadine PA while with 2 g/l Merspol, Reactive blue 19 decolorization was inhibited by approximately 50 %.

Merspol may have had a slight enhancing effect on the ABTS oxidation but it did change the kinetics of the reaction. Since Merspol had little effect on the enzymatic oxidation of ABTS but significantly inhibited the enzymatic decolorization of Reactive blue 19, the surfactant must have interacted with the dye. This interaction was detected in the absorbance spectral scan by the appearance of a second peak of at 630 nm (Figure 6.5B) that correspond to the absorption of the dye-Merspol complex. This wavelength shift was not observed for ABTS. It is also clear that Merspol is not responsible for the second peak since it did not absorb in the visible range.

A model of inhibition by substrate depletion where the dye molecules bind to Merspol molecules to reduce the amount of free dye available to react with laccase describes the decolorization kinetics. This model is in good agreement with the experimental data as seen

in Figure 6.6A and the residual plot also shows no bias (Figure 6.6B). In addition, the kinetic mechanism is supported by saturation equilibrium binding data that clearly shows that Mergol binds Reactive blue 19. The difference between the K_d estimated from the equilibrium binding experiment and the from the kinetic model are not statistically significant ($\alpha = 0.05$).

The dye may have interacted with the surfactant molecules or with the micelles as all Mergol concentrations were above the critical micelle concentration of 0.5 g/l. It is not clear why the surfactant interacted with the dye but not with ABTS. Although Reactive blue 19 most likely bears a net negative charge at pH 5, the hydrophobic interactions with Mergol may be dominant. This may partially explain our results as Tokuda *et al.* (1999) has shown that both electrostatic and hydrophobic interactions affected decolorization rates by peroxide bleaching agents in the presence of surfactant molecules.

The proposed inhibition model may also explain the results of Hu *et al.* (2007) where Tween 80 significantly inhibited the oxidation of benzo[*k*]fluoranthene (BaP) by laccase immobilized on kaolinite. Tween 80 was used to increase the solubility of BaP in order to increase its availability to the enzyme. However, as the apparent solubility increased, BaP molecules were probably entrapped inside the micelles which then presented a barrier between BaP and the immobilized laccase and resulted in an apparent inhibition.

This is the first study to show that enzymatic decolorization can be affected by the interaction between a dye and a surfactant. This is significant since surfactants are common in dye effluents and can affect not only biological decolorization (whether enzymatic or with a fungal culture) but also physical or chemical decolorization processes (Tokuda *et al.*, 1999). The efficiency of the process will most likely diminish with the degree of interaction between the dye and the surfactant and the quantity of the surfactant. This impact would be even greater at low dye concentrations which are typical of most dye effluents. Thus it is important to better understand the nature of these interactions, not only to predict

decolorization but also to determine how these interactions can be minimized.

Conclusions

We have examined the effect of a non-ionic surfactant, Mergol, on the enzymatic oxidation of ABTS and decolorization of Reactive blue 19 using laccase. The surfactant has no significant effects on the enzyme itself as it has no effect on ABTS oxidation. Although Mergol had little effect on ABTS oxidation, Reactive blue 19 decolorization was inhibited with increasing surfactant concentration. Spectral scans of the dye with and without Mergol and analysis of kinetic data show that decolorization rates depend on the interaction between the dye and the surfactant. The inhibition model fits the data suitably since the dye concentration decreases as the dye is removed from the reaction as it binds to the surfactant molecule and/or is sequestered into micelles. This is the first study to show this effect in enzymatic dye decolorization.

Bibliography

- Abadulla E, Tzanov T, Costa S, Robra KH, Cavaco-Paulo A, Gübitz GM. 2000. Decolorization and detoxification of textile dyes with a laccase from *Trametes hirsuta*. *Appl Environ Microbiol* **66**(8): 3357–62.
- Auriol M, Filali-Meknassi Y, Rajeshwar D, Adams C. 2007. Laccase-catalyzed conversion of natural and synthetic hormones from a municipal wastewater. *Water Res* **41**: 3281–3288.
- Basto C, Silva C, Gubitz G, Cavaco-Paulo A. 2007. Stability and decolourization ability of *Trametes villosa* laccase in liquid ultrasonic fields. *Ultrason Sonochem* **14**: 355–362.
- Champagne PP, Ramsay JA. 2005. Contribution of manganese peroxidase and laccase to dye decoloration by *Trametes versicolor*. *Appl Microbiol Biotechnol* **69**(3): 276–285.
- Harazono K, Nakamura J. 2005. Decolorization of mixtures of different reactive textile dyes by the white rot basidiomycete *Phanerochaete sordida* and inhibitory effect of polyvinyl alcohol. *Chemosphere* **59**: 63–68.
- Hu X, Zhao X, Hwang H. 2007. Comparative study of immobilized *Trametes versicolor* laccase on nanoparticles and kaolinite. *Chemosphere* **66**: 1618–1626.
- Husain Q. 2006. Potential applications of the oxidoreductive enzymes in the decolorization and detoxification of textile and other synthetic dyes from polluted water: a review. *Crit Rev Biotechnol* **26**(4): 201–21.
- Karam J, Nicell J. 1997. Potential applications of enzymes in waste treatment. *J Chem Technol Biotechnol* **69**(2).
- Khmelnitsky Y, Gladilin A, Roubailo V, Martinek K, Levashov A. 1992. Reversed micelles of polymeric surfactants in nonpolar organic solvents: A new microheterogeneous medium for enzymatic reactions. *Eur J Biochem* **206**: 737–745.
- Liu Z, Shao M, Cai R, Shen P. 2006. Online studies on intermediates of laccase-catalyzed reaction in reversed micelles. *J Colloid Interface Sci* **294**: 122–128.

- Michizoe J, Ichinose H, Kamiya N, Maruyama T, Masahiro G. 2005. Biodegradation of phenolic environmental pollutants by a surfactant-laccase complex in organic media. *J Biosci Bioeng* **99**(6): 642–647.
- Nyanhongo GS, Gomes J, Gübitz GM, Zvaunya R, Read J, Steiner W. 2002. Decolorization of textile dyes by laccases from a newly isolated strain of *trametes modesta*. *Water Res* **36**(6): 1449–1456.
- Reyes P, Pickard M, Vazquez-Duhalt R. 1999. Hydroxybenzotriazole increases the range of textile dyes decolorized by immobilized laccase. *Biotechnol Lett* **21**(10): 875–880.
- Strong P, Burgess J. 2008. Fungal and enzymatic remediation of a wine less and five wine-related distillery wastewaters. *Biores Technol* **99**: 6134–6142.
- Tokuda J, Ohura R, Iwasaki T, Takeuchi Y, Kashiwada, Nango M. 1999. Decolorization of azo dyes by hydrogen peroxide catalyzed by water-soluble manganese porphyrins. *Text Res J* **69**: 956–960.
- Wolfenden B, Willson R. 1982. Radical-cations as reference chromogens in kinetic studies of one-electron transfer reactions. *J Chem Soc Perkin Trans* **2**(1982): 805–812.
- Young L, Yu J. 1997. Ligninase-catalysed decolorization of synthetic dyes. *Water Res* **31**(5): 1187–1193.

Chapter 7

Effects of pH chloride and sodium sulfate on the decolourization of Reactive blue 19

7.1 Abstract

Laccases are phenol-oxidases produced by white rot fungi and their potential application for the decolourization of textile wastewaters has been the object of intensive research. Textile wastewaters contain salts like sodium chloride and sodium sulphate, and their pH may vary between 3 and 12. As these factors may affect enzyme activity, the effects of pH, sodium chloride and ionic strength on *Trametes versicolor* laccase during the decolourization of Reactive blue 19, a model anthraquinone dye, and the oxidation of 2,2-Azino-bis(3-ethylbenzothiazoline-6-sulfonic acid) (ABTS), the reference substrate, were evaluated by steady-state kinetic analysis. The results showed that increasing the pH decreased the rate of ABTS oxidation whereas the decolourization of Reactive blue 19 was optimal at pH

4. While sodium sulphate did not affect laccase activity, sodium chloride inhibited both ABTS oxidation and dye decolourization. However, the type of inhibition was substrate dependent. With ABTS, the inhibition was hyperbolic non-competitive and was parabolic mixed with Reactive blue 19. Furthermore, the results suggested that two chlorides may bind to laccase in the presence of the dye. This investigation is the first to propose a model of laccase inhibition in which the type of inhibition by chloride depends on the substrate.

7.2 Introduction

Laccases are copper oxidases produced by white rot fungi that can degrade a wide range of organic pollutants including textile dyes, and have attracted great interest for their potential application in bioremediation and textile wastewater treatment (Torres *et al.*, 2003; Baldrian, 2006). These enzymes decolourize anthraquinone dyes efficiently and their specificity can be broadened to other classes of dyes by using small molecular weight mediators such as hydroxybenzotriazole (Reyes *et al.*, 1999; Peralta-Zamora *et al.*, 2003; Trovaslet *et al.*, 2007; Murugesan *et al.*, 2007). Fungal laccases contain four coppers organized into two copper clusters. The type 1 copper is located near the active site and receives the electrons extracted from the substrate(s). The electrons are then transferred to the two type 3 coppers, which relay the electrons to type 2 copper where oxygen is reduced to water. The type 2 and type 3 coppers are arranged in a triangle and form the tri-nuclear cluster located at the core of the enzyme. Oxygen must access the tri-nuclear cluster through a channel for its reduction.

Textile wastewaters contain sulphate and chloride salts that vary from 930 to 3460 mg/l and 400 to 16,000 mg/l respectively (Orhon *et al.*, 2001; Vishnu *et al.*, 2008). Their pH may vary from 3 to 12 depending on the dyeing process used (Rutherford *et al.*, 2003; EPA, 1996). Halides salts are known to affect laccase but the effect depends on the enzyme

species. In general, fluoride has been shown to be the strongest inhibitor of laccases relative to chloride and bromide (Farnet *et al.*, 2008; Xu, 1996). More particularly, Koudelka and Ettinger (1988) demonstrated that fluoride partially inhibits *Rhus vernucifora* laccase by binding to type 2 copper. On the other hand, Vaz-Dominguez *et al.* (2008) showed that *Trametes hirsuta* laccase activity was completely suppressed by fluoride and partially by chloride. Hydroxide anions also bind to type 2 copper and prevent the binding of oxygen at alkaline pHs (Koudelka *et al.*, 1985). Furthermore, the redox potential of the substrate may depend on the pH and also influence the shape of the pH activity profile of the enzyme (Xu, 1997). Neither study analyzing the kinetics of laccase inhibition by chloride during dye decolourization nor the effects of sulphate on laccase has been reported. The quantification of these effects would be useful for the design of an enzymatic treatment. Therefore, this investigation will analyse the effects of pH, sodium chloride, and sodium sulphate on the kinetic behaviour of *Trametes versicolor* laccase during the oxidation of ABTS and the decolourization of Reactive blue 19 a model anthraquinone dye.

7.3 Material and methods

7.3.1 Chemicals

Controlled porosity carrier (CPC) silica beads pre-silanized with 3-aminopropyltriethoxysilane (APTES), *Trametes versicolor* laccase, 2,2-Azino-bis(3-ethylbenzothiazoline-6-sulfonic acid) (ABTS) diammonium salt and borane dimethylamine were purchased from Sigma-Aldrich Canada (Oakville, On). Glutaraldehyde (glutaric acid dialdehyde) was purchased from Acros (Belgium).

7.3.2 Enzyme preparation

Four hundred milligrams of lyophilised *T.versicolor* laccase was dissolved in 60 ml of 20 mM NaH₂PO₄ at pH 7, centrifuged at 10,000 x g for 2 hours and thereafter filtered with a Whatman paper and Millipore filters (0.45 μM). The filtrate was dialyzed against 20 mM NaH₂PO₄ pH 7 for 20 hours at a dilution factor of approximately 5,000 then passed through a Q-sepharose anion exchange column pre-equilibrated with 20 mM NaH₂PO₄ at pH 7. Laccase was eluted in one step using 150 mM NaCl. The eluate was dialyzed against 50 mM NaOAc/50 mM NaH₂PO₄ pH 5.

7.3.3 Laccase assay

The activity of laccase was determined by monitoring spectrophotometrically the generation of 2,2-Azino-bis(3-ethylbenzothiazoline-6-sulfonic acid) radicals (ABTS•) at 420 nm from the oxidation of ABTS (Wolfenden and Wilson, 1982) at 23±1°C using a Spectramax 250 plate reader (with the SOFTmax PRO software package (Molecular Devices, Sunnyvale CA, USA)). The assay mixture contained 500 μM ABTS, and 100 mM sodium acetate buffer (pH 5.0) for total reaction mixture of 180 μl. The path length of absorbance in the well for this volume was 0.5 cm. The rate of reaction was expressed in μM/min or in units of laccase.

7.3.4 Protein assay

The protein concentration was determined by UV absorbance at 280 nm and corrected for Raleigh scattering with readings at 320 nm according to the following formula

$$A_{280}^{corr} = A_{280} - A_{320} \times \left(\frac{320}{280}\right)^4 \quad (7.1)$$

The coefficient of absorption for laccase ($\epsilon_{280}=1.074$ ml/mg) was determined by the ProtoParam program (protein parameter predictor) from the ExPASy website (<http://ca.expasy.org/tools/protparam.html>).

7.3.5 Dye concentration and decolorization assay

The Reactive blue 19 concentration was determined spectrophotometrically by monitoring the absorbance at 592 nm. The decolorization activity was calculated by dividing the rate of absorbance change by the coefficient of absorption of $10,044 \text{ M}^{-1}\text{cm}^{-1}$ (determined from a calibration curve from 0 to $45.7 \mu\text{M}$). The rate of decolorization was expressed in $\mu\text{M}/\text{min}$.

7.3.6 Initial rate analysis (steady-state kinetics)

The effects of pH, sodium chloride and sodium sulphate on the free laccase were quantified by initial rate analysis with ABTS, as the reference substrate, and Reactive blue 19. The assay mixture was buffered with 50 mM NaOAc/50 mM KH_2PO_4 and included 0.274 nM laccase with ABTS or 120 nM laccase with Reactive blue 19. All assays were conducted in 96-well plates (300 μl per well). Each well contained 108 μl of buffer, 36 μl of substrate (in the same buffer), and 36 μl of laccase solution for total reaction mixture of 180 μl . The path length of absorbance in the well for this volume was 0.5 cm. The initial ABTS concentrations (unless stated otherwise) were 10, 20, 30, 40, 50, 100, 200, 300, 400, 500, 600, 700, 800, 900 and 1000 μM and the initial dye concentrations were 10, 20, 30, 40, 50, 75, 100, 150, 200, 250, 300, 350 and 400 μM . Time course curves of 61 absorbance points were generated over 30 minutes and the initial rate was determined by the software package of the plate reader, SOFTmax Pro (Molecular Devices) by calculating the tangent slope to the first five points (see Appendix D.2 for a sample calculation). The initial rates

were measured in triplicate at $22 \pm 1^\circ\text{C}$ and the results shown are averages with the error bars representing the standard error.

7.3.7 Effect of pH and salts

Laccase steady-state kinetics with ABTS and Reactive blue 19 were performed at pH 3, 4, 5, 6 and 7 in a 50 mM NaOAc/50 mM KH_2PO_4 buffer and the pH was adjusted with a 6 M H_2SO_4 . For the impact of salts on laccase kinetics, analyses with both substrates were conducted in the presence of 50, 100, 150 or 200 mM sodium chloride and 7, 28, 49 or 70 mM sodium sulphate. The initial ABTS concentrations in the sodium chloride experiment were 0, 10, 20, 30, 40, 50, 60, 70, 80, 90, 100, 200, 300, 400, 500 or 600 μM . All assays were buffered with 50 mM NaOAc/50 mM KH_2PO_4 at pH 5.

7.3.8 Data analysis

The Michaelis-Menten model was used to fit the experimental pH and sodium sulfate data whereas modified rate equations were derived to analyze the effects of sodium chloride. Kinetic parameters and inhibition constants were determined by nonlinear least square regression (The sums of squares was minimized with the Gauss-Newton algorithm with equal weighting for each parameters) using the R statistical package (R project for statistical computing, CRAN) and Systat (Systat Software, Inc., San Jose, CA, USA).

7.4 Results

7.4.1 Effect of pH on the oxidation of ABTS and decolorization of Reactive blue 19

The apparent turnover number, $k_{cat,app}$, and the apparent Michaelis constant, $K_{S,app}$, for ABTS oxidation by laccase decreased from pH 3 to 7 (Figure 7.1A and Table 7.1) whereas the optimum $k_{cat,app}$ for Reactive blue 19 decolourization was at pH 4 (Figure 7.1B and Table 7.2) and the $K_{S,app}$ profile showed a maximum at pH 5. The kinetic parameters from Tables 7.1 and 7.2 were estimated from the initial rates from Figures 7.1A-B.

Table 7.1: Estimation of $k_{cat,app}$ and $K_{S,app}$ for the oxidation of Reactive blue 19 by 120 nM free laccase in 50 mM NaOAc/50 mM NaH_2PO_4 at different pHs. Each data point is the average of triplicates and error bars represent the standard error.

pH	$k_{cat,app}$ (s^{-1})	$K_{S,app}$ (μM)	$(k_{cat}/K_S)_{app}$ ($\times 10^5 \text{ M}^{-1} \text{ s}^{-1}$)
3	252 ± 2	35.3 ± 1.2	71.4
4	179 ± 1	33.9 ± 1.1	52.8
5	110.2 ± 0.4	32.1 ± 0.7	34.3
6	28.7 ± 0.2	13.6 ± 0.6	21.1
7	2.58 ± 0.26	4.5 ± 5.2	5.73

Table 7.2: Estimation of $k_{cat,app}$ and $K_{S,app}$ for the oxidation of Reactive blue 19 by 120 nM free laccase in 50 mM NaOAc/50 mM NaH₂PO₄ at different pHs. Each data point is the average of triplicates and error bars represent the standard error.

pH	$k_{cat,app}$ (s ⁻¹)	$K_{S,app}$ (μM)	$(k_{cat}/K_S)_{app}$ (× 10 ⁵ M ⁻¹ s ⁻¹)
3	4.11 ± 0.24	137 ± 19	27.5
4	4.63 ± 0.38	313 ± 30	15.0
5	2.64 ± 0.23	373 ± 66	0.0592
6	0.567 ± 0.096	248 ± 14	0.0131
7	0.120 ± 0.0114	115 ± 85	0.00349

7.4.2 Effect of ionic strength on the oxidation of ABTS and Reactive blue 19

Both $k_{cat,app}$ and $K_{S,app}$ did not vary significantly, as the ionic strength, i.e. the sodium sulphate concentration, increased from 7 to 49 mM (ionic strength = 0.100 to 0.310 mM) for the ABTS oxidation, or for the Reactive blue 19 decolorization (Figure 7.2A-B)

7.4.3 Effect of sodium chloride on the oxidation of ABTS and decolorization of Reactive blue 19

Exposure of laccase to an increasing chloride concentration non-linearly decreased the apparent turnover number for ABTS oxidation and Reactive blue 19 (Figure 7.3A-B). On the other hand, $K_{S,app}$ for ABTS oxidation increased with salt concentration but decreased for dye decolorization.

The Lineweaver-Burk plot show that laccase inhibition by chloride is partial non-competitive with ABTS (the lines do not intercept at the abscissa) and is mixed with Reactive blue 19 (Figure 7.4A-B). The replot of the Lineweaver-Burk slopes against the salt concentration

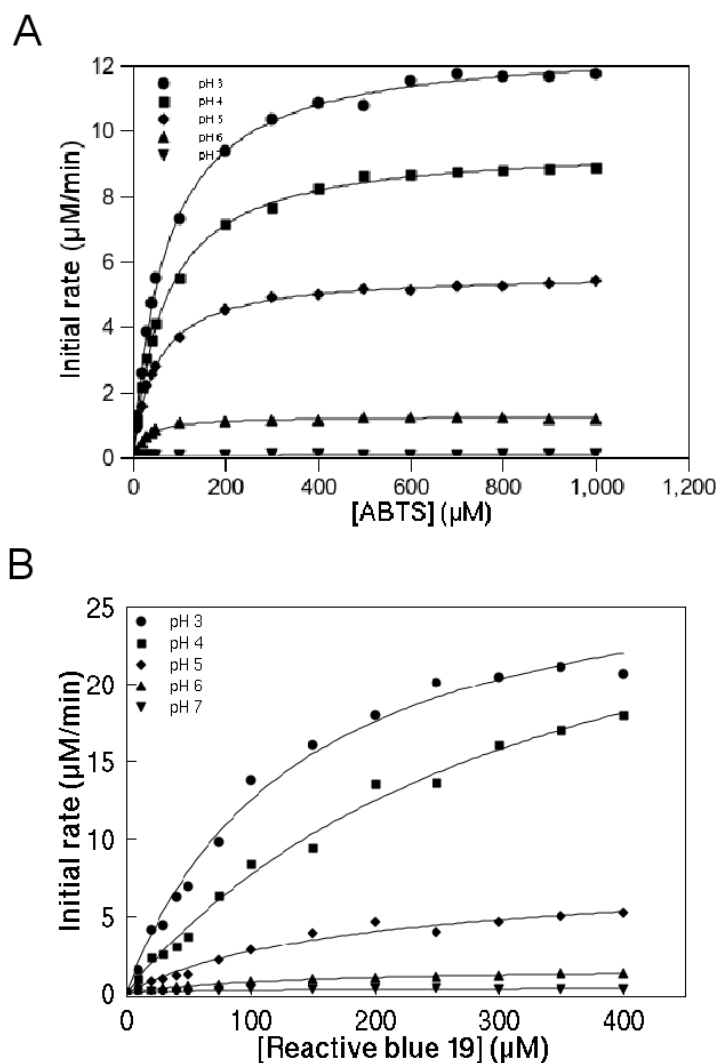
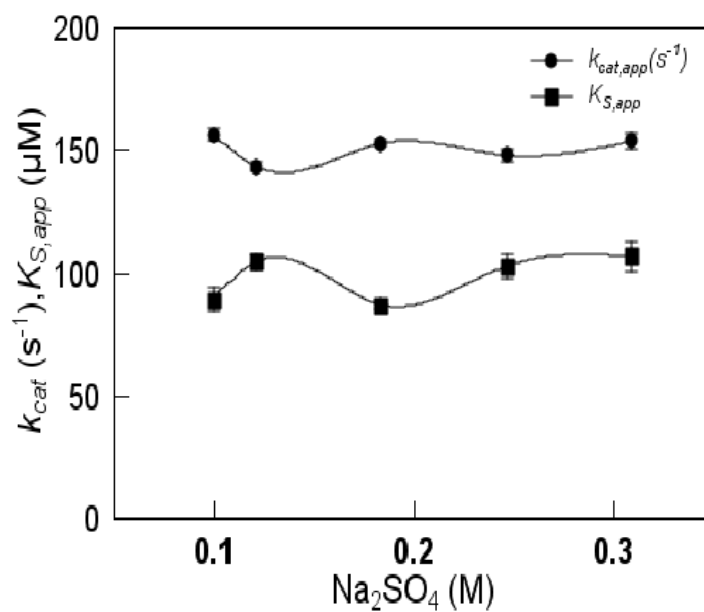


Figure 7.1: The effect of pH on the oxidation kinetics of ABTS and on the decolourization of Reactive blue 19 by free laccase. The laccase concentration for the oxidation of ABTS and the decolourization of Reactive blue 19 were 0.274 nM and 120 nM respectively. The assays were buffered at the selected pHs with 50 mM NaOAc/50 mM NaH₂PO₄. Each data point is the average of triplicates and error bars represent the standard error.

A



B

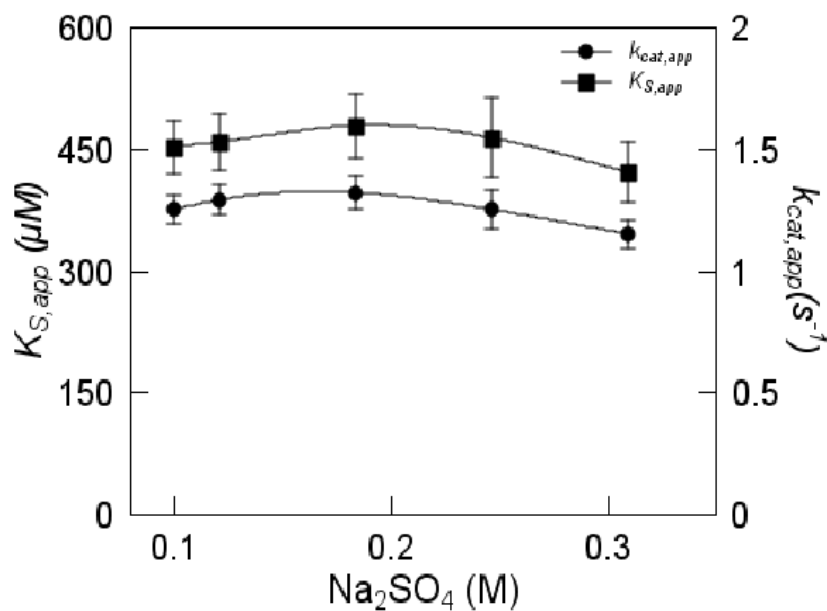


Figure 7.2: Effect of ionic strength on the oxidation of ABTS (A) and Reactive blue 19 (B). The assay mixtures were buffered with 50 mM NaOAc/50 mM NaH_2PO_4 at pH 5 with 0.274 and 120 nM laccase for the oxidation of ABTS and the decolorization of Reactive blue 19 respectively. Each data point is the average of triplicates and error bars represent the standard error.

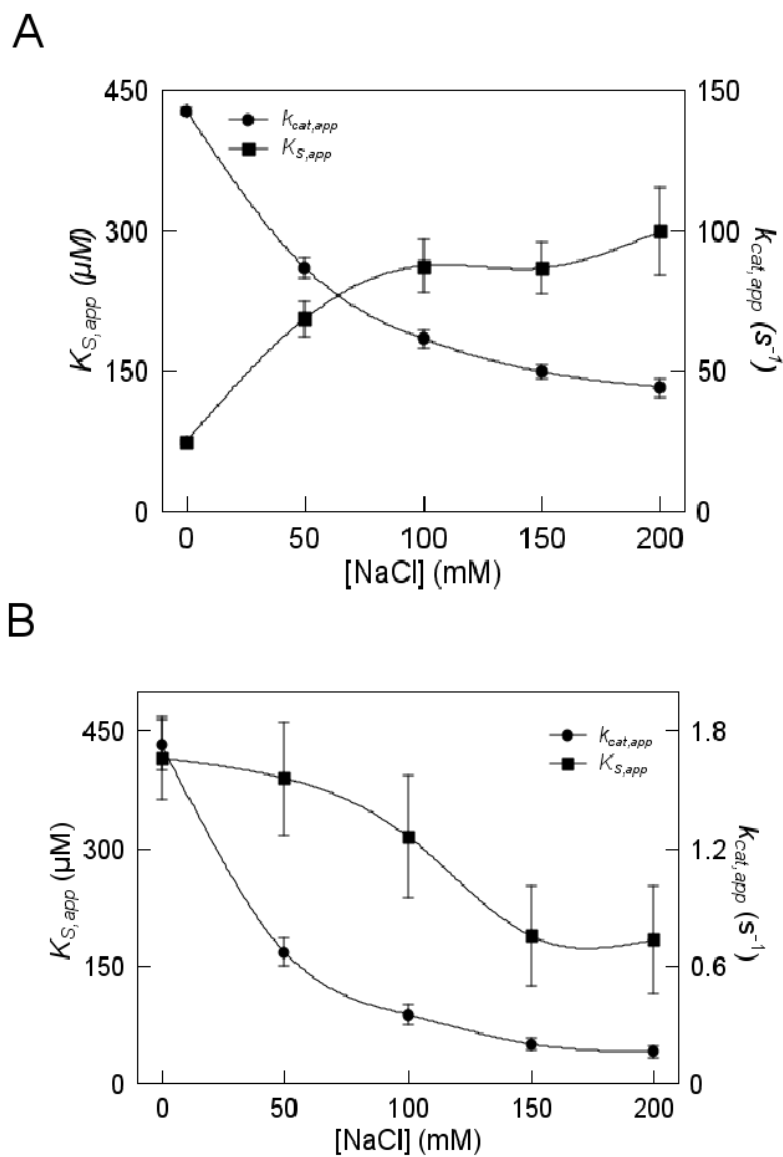


Figure 7.3: Effect of sodium chloride on the oxidation of (A) ABTS and (B) Reactive blue 19 by laccase. The assay mixtures were buffered with 50 mM NaOAc/50 mM NaH₂PO₄ at pH 5 with 0.274 and 120 nM for the oxidation of ABTS and the decolourization of Reactive blue 19 respectively. Each data point is the average of triplicates and error bars represent the standard error.

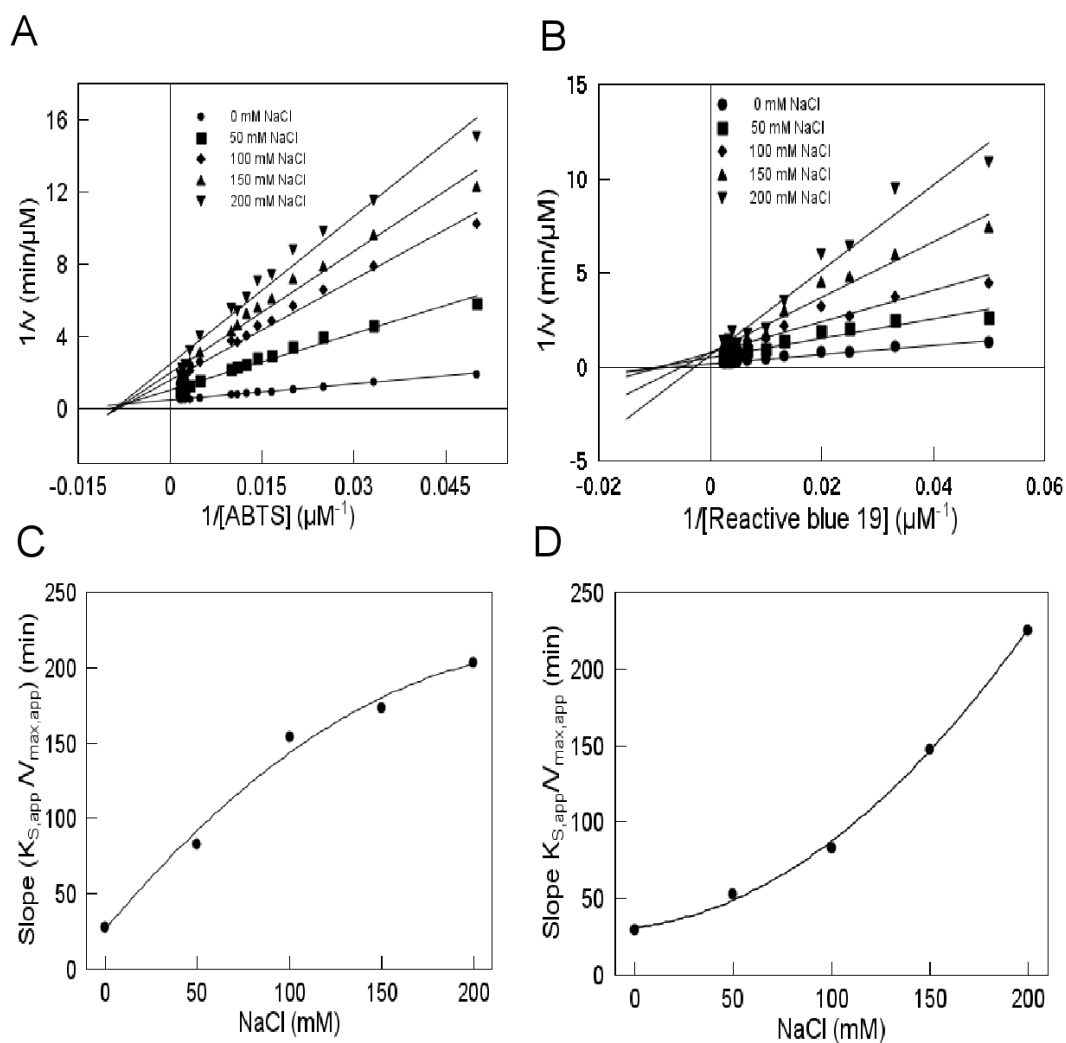


Figure 7.4: Non-linear dependence of slopes from the Lineweaver-Burk plots (K_s/V_{max}) for ABTS (A-C) and Reactive blue 19 (B-D)

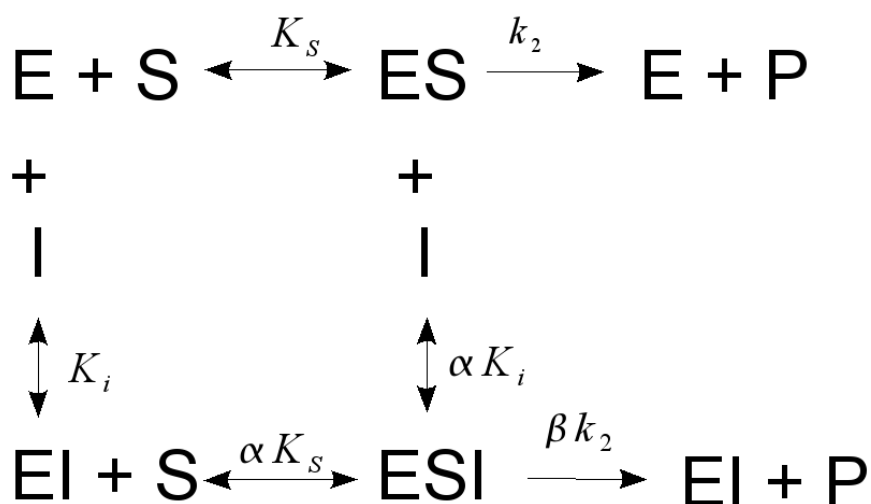


Figure 7.5: Proposed scheme hyperbolic inhibition of laccase for the oxidation of ABTS

for the ABTS oxidation was hyperbolic indicating a partial inhibition (Figure 7.4C) while that for the decolourization of Reactive blue 19 was parabolic (Figure 7.4D) indicating that two inhibitor binding sites exist on the enzyme. Partial inhibition signifies that the enzyme-inhibitor-substrate complex can generate the product. A general hyperbolic mixed-type inhibition was assumed (Figure 7.5) for the ABTS reaction where chloride can bind to the free enzyme and enzyme-substrate complex. The enzyme-substrate-inhibitor complex is able to generate the product (equation 7.2) (Segel, 1993).

$$v = \frac{k_{cat}[E]_t[S] \left(1 + \frac{\beta[I]}{\alpha K_I}\right)}{K_S \left(1 + \frac{[I]}{K_I}\right) + [S] \left(1 + \frac{[I]}{\alpha K_I}\right)} \quad (7.2)$$

where K_i is the inhibition constant describing the dissociation of the enzyme-inhibitor complex into the free enzyme and the inhibitor. The parameter α is the factor by which the enzyme substrate affinity is affected by the bound inhibitor and β is the effectiveness of the enzyme-substrate-inhibitor for generating the product.

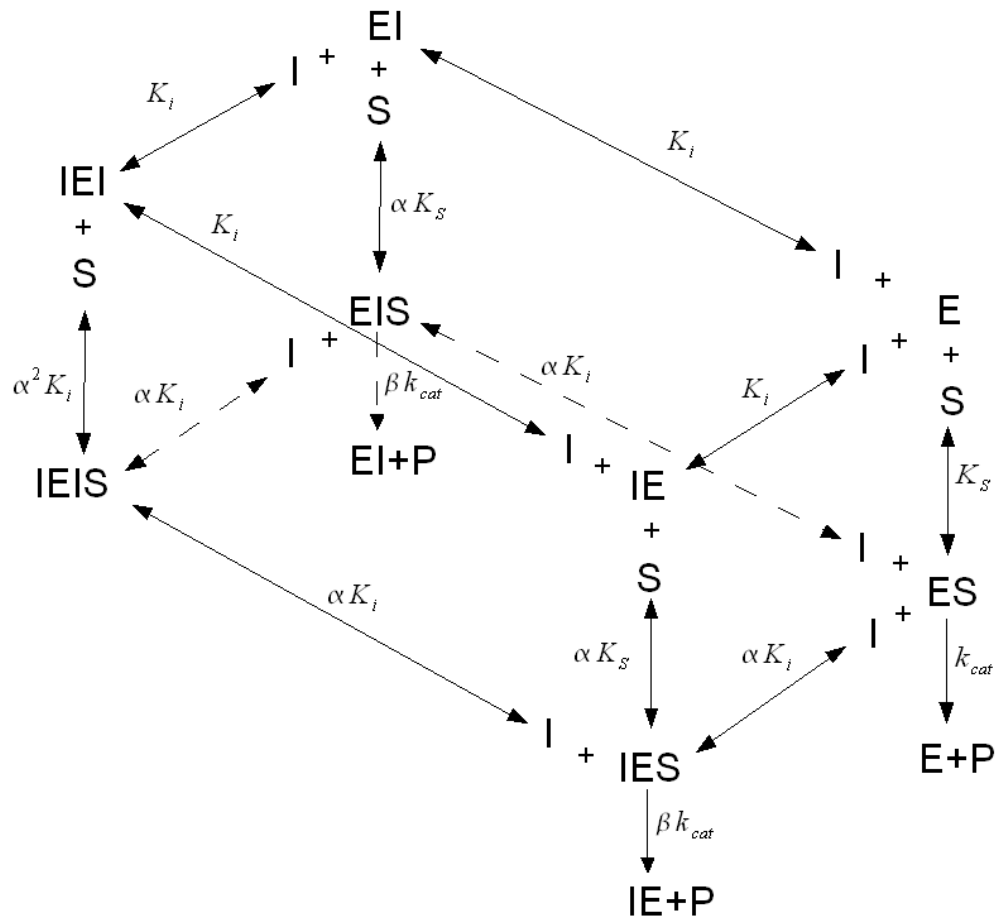


Figure 7.6: Proposed scheme for parabolic inhibition of laccase for the decolourization of Reactive blue 19

A parabolic replot of the Lineweaver-Burk slopes (K_S/V_{max}) against the inhibitor concentration (Figure 7.4D) indicates that two inhibitor binding sites on an enzyme exist (Leskovac, 2003; Segel, 1993). A scheme was elaborated to describe the enzyme inhibition during dye decolorization where two chlorides can bind to the free enzyme and the enzyme substrate complex at two sites that have identical affinity for the inhibitor (Figure 7.6). The enzyme-substrate complex bound by one inhibitor molecule can generate the product by a fraction β of k_{cat} whereas the inhibition is complete when two inhibitor molecules are bound to the enzyme, i.e., it cannot generate the product. Similarly to the ABTS case, the inhibitor can affect the enzymes affinity for the dye by a factor α . The corresponding rate equation for the two-site model is

$$v = \frac{k_{cat}[E]_t[S] \left(1 + \frac{2\beta[I]}{\alpha K_i} \right)}{K_S \left(1 + \frac{2[I]}{K_i} + \frac{[I]^2}{K_i^2} \right) + [S] \left(1 + \frac{2[I]}{\alpha K_i} + \frac{[I]^2}{\alpha^2 K_i^2} \right)} \quad (7.3)$$

Equations 7.2 and 7.3 were fitted to rate data for ABTS oxidation and decolourization of Reactive blue 19 respectively (Figure 7.7A, Figure 7.8A) and the good fit was assessed with the residuals plots showing no biases. The kinetic parameters (Table 7.3) were estimated by nonlinear regression.

7.5 Discussion

A small number of investigations have reported on the effects of pH on dye decolorization by laccase. Nyanhongo *et al.* (2002) showed that the optimum pH of the Reactive blue 19 decolourization by *Trametes modesta* laccase was 4.5 whereas Murugesan *et al.* (2007) reported an optimal pH of 4 for the decolourization of the same dye by *Ganoderma lucidum* laccase. In this study, the decolorization of dye by *Trametes versicolor* laccase was optimal

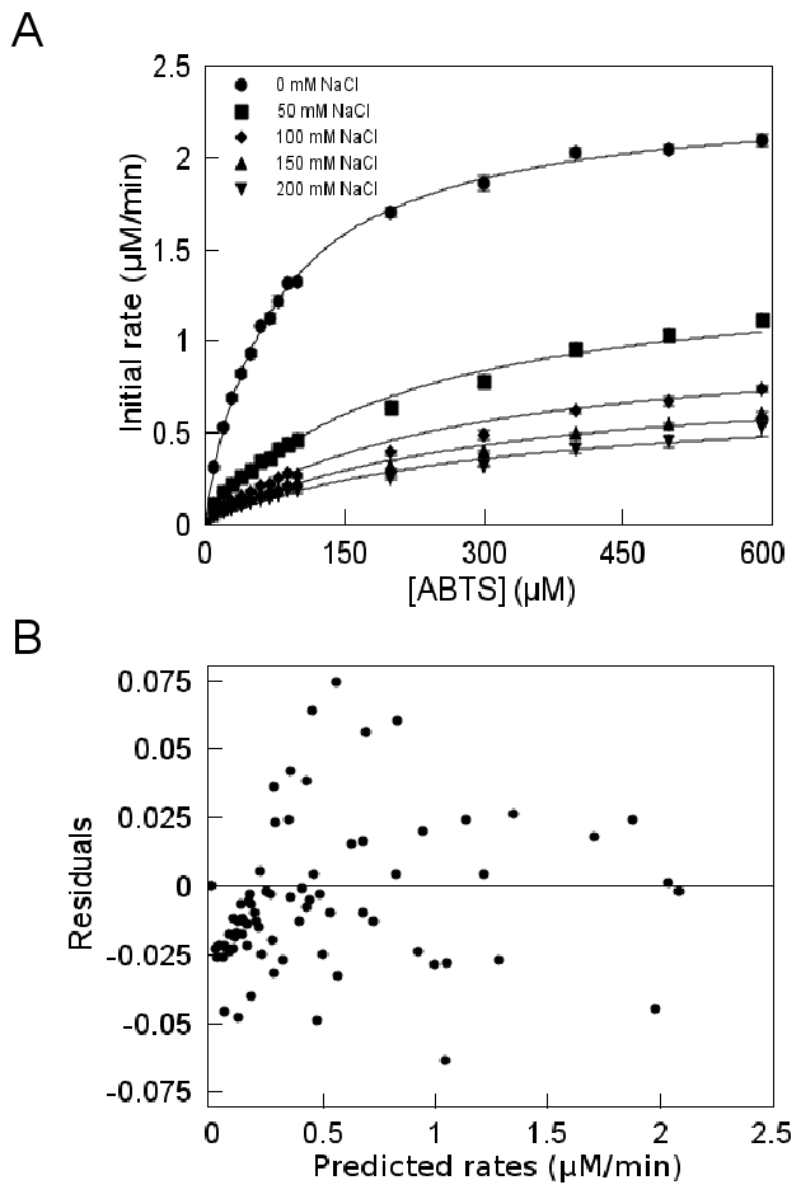


Figure 7.7: Effect of NaCl inhibition on (A) ABTS oxidation and with residuals (B) by free laccase. Comparison of experimental data (each symbol is the average of triplicates and the error bars represent the standard deviation) and the inhibition model for ABTS oxidation (equations 7.2), solid lines.

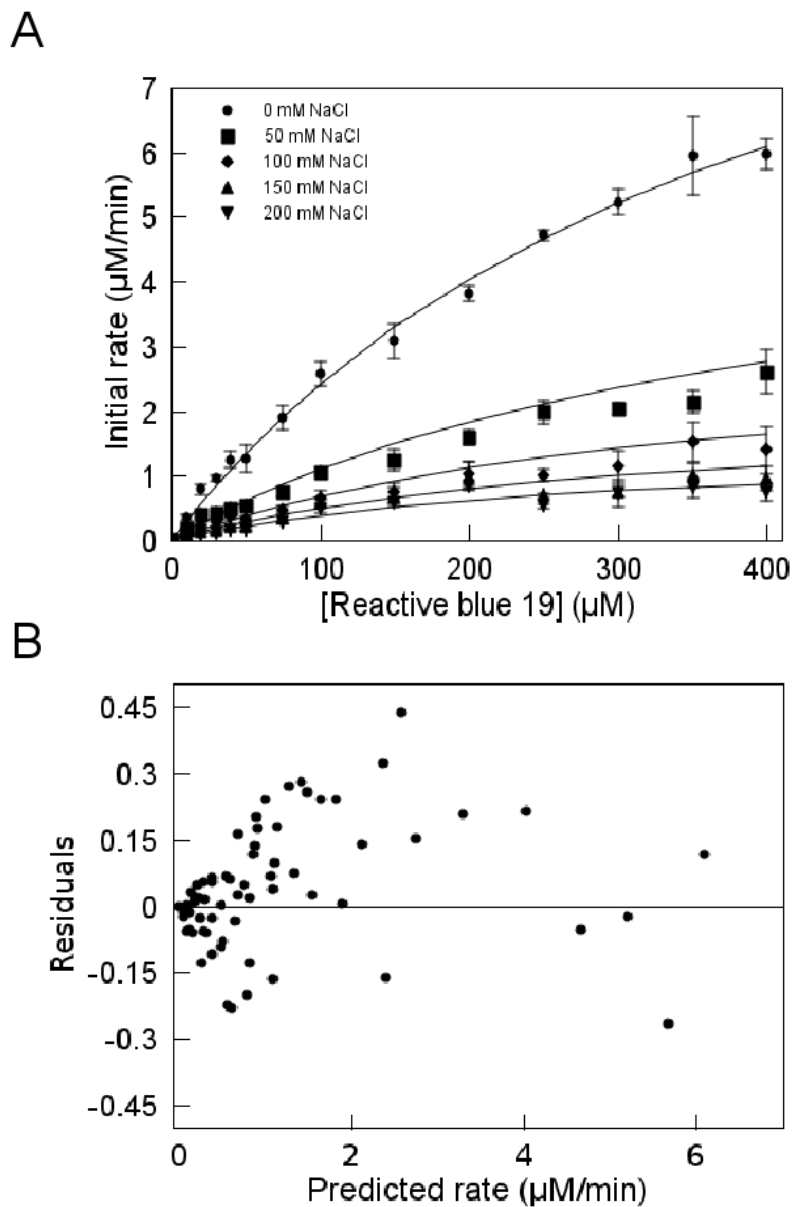


Figure 7.8: Effect of NaCl inhibition on (A) Reactive blue 19 with residuals (B) by laccase. Comparison of experimental data (each symbol is the average of triplicates and the error bars represent the standard deviation) and the inhibition model for ABTS oxidation and Reactive blue 19 (equations 1 and 2 respectively, solid lines).

Table 7.3: Estimation of the kinetic parameters from the proposed models for the oxidation of ABTS (0.274 nM laccase) and for the decolourization of Reactive blue 19 (120 nM laccase) in 50 mM NaOAc/50 mM NaH₂PO₄ pH 5 in presence of 0 - 200 mM sodium chloride. Each data point is the average of triplicates and error bars represent the standard error.

Hyperbolic mixed-type inhibition					
Substrate	$k_{cat,app}$ (s ⁻¹)	$K_{S,app}$ (μM)	K_I (mM)	α	β
ABTS	142 ± 1	73.6 ± 1.8	12.8 ± 0.4	5.06 ± 0.28	0.0777 ± 0.0111
Parabolic inhibition					
Reactive blue 19	1.71 ± 0.09	419 ± 31	54.7 ± 12.0	0.743 ± 0.060	0.274 ± 0.089

at pH 4.

The redox potential of laccase is independent of pH and that of a substrate will decrease with increasing pH if a proton is generated from the reaction (Xu, 1997). The rate of a laccase-catalyzed reaction is proportional to the difference between type 1 copper and the substrate redox potentials (Xu, 1997). Therefore, any variation in the rate is due to a change in the substrate potential. Koudelka *et al.* (1985) showed that enzyme inhibition at alkaline pH was caused by hydroxide anions that bind to type 2 copper where oxygen is reduced to water. Madzak *et al.* (2006) confirmed that the only charged residue, aspartate 206 (negative carboxyl), in the active site of laccase weakly contributed to the pH profile. The redox potential of ABTS is independent of pH since its oxidation does not involve the release of a proton (Xu, 1997). Hence, the gradual inhibition of the enzyme with increasing pH was mainly due to an increasing hydroxide concentration, which caused a strictly declining activity as a function of pH. On the other hand, the decolourization profile of Reactive blue 19 showed an optimum pH of 4 and therefore suggests that the dye decolourization involves the release of a proton; a decrease in the dyes redox potential may have generated the ascending part of the curve and as the pH was further increased, the hydroxide inhibition became dominant and caused the curve to decline.

Few studies have examined the effect of reaction conditions on the kinetics of laccase dye decolourization. Trovaslet *et al.* (2007) showed that sodium chloride and sodium sulfate inhibited the decolourization of Acid blue 62 by *Pycnoporus sanguineus* laccase but no kinetic analysis was conducted. In this present study, sodium sulphate affected neither ABTS oxidation nor the decolourization of Reactive blue 19 (Figure 7.2A B). The rate of a reaction will not be affected if one of the reactants is neutral (Upadhyay, 2006). Since oxygen is neutral, any observed effects on the rate would be due to alterations to the enzyme. Therefore, sodium sulphate or the ionic strength does not affect *T.versicolor* laccase.

Since the ionic strength did not affect laccase, it was clearly inhibited by chloride. Naki and Vorfolomeev (1981) demonstrated that chloride is a competitive inhibitor with various electron donors as substrates whereas in this study, the inhibition of ABTS oxidation by *T. versicolor* laccase was hyperbolic non-competitive in the presence of chloride. The increasing $K_{S,app}$ indicates that chloride decreased the enzyme affinity for ABTS and the inhibition can be considered partial competitive also (Figure A). The apparent turnover $k_{cat,app}$ decreases because chloride decrease the concentration of fully free active enzyme. Since the enzyme-substrate-inhibitor complex is not as efficient as the enzyme-substrate complex to generate the product, the maximum rate of reaction decreases. Vaz-Dominguez *et al.* (2008) showed that chloride is not likely to penetrate the channel leading to type 2 copper because of its size and is not likely to inhibit the reduction of oxygen. Therefore, the decreased $k_{cat,app}$ may also reflect the ability of chloride to suppress the electron transfer from the substrate to type 1 copper, or from type 1 copper to type 3 copper. On the other hand, the inhibition was parabolic mixed when Reactive blue 19 was the substrate (Figure 7.4B-D). Parabolic inhibition occurs when two inhibitor binding sites exist on an enzyme. A kinetic mechanism in which chloride can bind to two sites with equal affinity (i.e., equal K_I) was derived. It was also assumed that the product can be generated when one chloride is bound to laccase, as it is the case in ABTS oxidation, while no product is generated when 2 chlorides are bound to the enzyme (Figure 7.6). It is not clear why parabolic inhibition occurs in dye decolourization but not in ABTS oxidation. As previously mentioned, chloride inhibits laccase by binding to the active site. The α value of 0.743 signifies that chloride increases the affinity of laccase for Reactive blue 19 and vice-versa. Upon binding of the dye, it is possible that the active site may widen or be distorted allowing the binding of a second chloride. The higher value of $K_I = 54.8$ mM relative to 12.8 mM with ABTS, suggest that the inhibitor binding sites resulting from a widening of the active site have lower affinity for chloride. The halide, less tightly bound, would then be less efficient at

suppressing the electron transfer from the substrate to the coppers in the tri-nuclear cluster. This could in turn explain the larger value of Reactive blue 19 decolorization (0.274) than that of ABTS (0.0778). As mentioned, the parameter β is the effectiveness of enzyme to generate a product when bound by one chloride. The binding of two chlorides however, would completely inhibit the enzyme, i.e., completely interrupt the electron transfer from the substrate to the tri-nuclear cluster. To summarize, a halide like fluoride completely inhibits *Trametes hirsuta* laccase (Vaz-Dominguez *et al.*, 2008) by blocking electron transfer at the active site near T1 copper and at the T2 copper through a channel. Since it is not likely that chloride can penetrate the channel leading to type 2 copper because of its larger size, it is proposed that the binding of two chlorides to laccase favoured by Reactive blue 19 completely inhibits the enzyme. This is the first report to the best of our knowledge which proposes a mechanism for the complete inhibition of laccase by chloride.

7.6 Conclusions

This investigation has analyzed the impact of pH, sodium chloride and sodium sulphate on dye decolorization. Alkaline pHs inhibited both the oxidation of ABTS and the Reactive blue 19 decolorization. The Reactive blue 19 decolorization is optimal at 4 and the pH profile suggests that a proton is released from dye decolorization. Ionic strength did not affect ABTS oxidation or dye decolorization. The effects of sodium chloride on laccase kinetics of oxidation of ABTS and on the decolorization of Reactive blue 19 were quantified and the type of laccase inhibition by chloride depended on the substrate. For both reactions, the exposure of laccase to the halide showed non-linear inhibitions. A hyperbolic partial non-competitive inhibition was observed when ABTS was the substrate while a parabolic mixed-type inhibition was occurred with Reactive blue 19. To the best of our knowledge, this is the first study to demonstrate that proposes a mechanism by which chloride can

completely inhibit laccase. The proposed models can be used to estimated the size of an eventual enzyme reactor for design of an enzyme treatment.

Bibliography

- Baldrian P. 2006. Fungal laccases - occurrence and properties. *FEMS Microbiol Rev* **30**(2): 215–42.
- EPA U. 1996. Best management practices for pollution prevention in the textile industry.
- Farnet AM, Gil G, Ferre E. 2008. Effects of pollutants on laccase activities of *Marasmius quercophilus*, a white-rot fungus isolated from a mediterranean schlerophyllous litter. *Chemosphere* **70**(5): 895–900.
- Koudelka G, Ettinger M. 1988. Fluoride effects on the activity of *Rhus* laccase and the catalytic mechanism under steady-state conditions. *J Biol Chem* **263**(8): 3698–3705.
- Koudelka G, Hansen F, Ettinger M. 1985. Solvent isotope effects and the pH dependence of laccase activity under steady-state conditions. *J Biol Chem* **260**(29): 15 561–15 565.
- Leskovac V. 2003. *Comprehensive enzyme kinetics*. Kluwer Academic Publishers: New York, 1st edn, ISBN 978-0306467127.
- Madzak C, Mimmi MC, Caminade E, Brault A, Baumberger S, Briozzo P, Mougin C, Jolivalt C. 2006. Shifting the optimal ph of activity for a laccase from the fungus *Trametes versicolor* by structure-based mutagenesis. *Protein Eng Des Sel* **19**(2): 77–84.
- Murugesan K, Nam I, Kim Y, Chang Y. 2007. Decolorization of reactive dyes by a thermostable laccase produced by *Ganoderma lucidum* in solid state culture. *Enzyme Microb Technol* **40**(7): 1662–1672.
- Nyanhongo GS, Gomes J, Gübitz GM, Zvaunya R, Read J, Steiner W. 2002. Decolorization of textile dyes by laccases from a newly isolated strain of *trametes modesta*. *Water Res* **36**(6): 1449–1456.
- Orhon D, Babuna FG, Kabdaslı I, Insel FG, Karahan O, Dulkadiroğlu H, Doğruel S, Sevimil F, Yediler A. 2001. A scientific approach to wastewater recovery and reuse in the textile industry. *Water Sci Technol* **43**(11): 223–231.
- Peralta-Zamora P, Pereira C, Tiburtius E, Moraes S, Rosa M, Minussi R, Durán N. 2003. Decolorization of reactive dyes by immobilized laccase. *Appl Catal B* **42**(2): 131–144.

- Reyes P, Pickard M, Vazquez-Duhalt R. 1999. Hydroxybenzotriazole increases the range of textile dyes decolorized by immobilized laccase. *Biotechnol Lett* **21**(10): 875–880.
- Rutherford L, Garron C, Ernst W, Kennedy K. 2003. The Aquatic Environment and Textile Mill Effluents An Ecological Risk Assessment. *Human Ecological Risk Assess* **9**(2): 589–606.
- Segel I. 1993. *Enzyme kinetics: behavior and analysis of rapid equilibrium and steady-state enzyme systems*. Wiley Classics Library, John Wiley & Sons: New York, ISBN 978-0471303091.
- Torres E, Bustos-Jaimes I, Le Borgne S. 2003. Potential use of oxidative enzymes for the detoxification of organic pollutants. *Appl Catal, B* **46**(1): 1–15.
- Trovaslet M, Enaud E, Guiavarch Y, Corbisier A, Vanhulle S. 2007. Potential of a *Pycnoporus sanguineus* laccase in bioremediation of wastewater and kinetic activation in the presence of an anthraquinonic acid dye. *Enzyme Microb Technol* **41**(3): 368–376.
- Upadhyay S. 2006. *Chemical kinetics and reaction dynamics*. Kluwer Academic Pub.
- Vaz-Dominguez C, Campuzano S, Rüdiger O, Pita M, Gorbacheva M, Shleev S, Fernandez VM, Lacey ALD. 2008. Laccase electrode for direct electrocatalytic reduction of O_2 to H_2O with high-operational stability and resistance to chloride inhibition. *Biosens Bioelectron* **24**(4): 531–7.
- Vishnu G, Palanisamy S, Kurian J. 2008. Assessment of fieldscale zero liquid discharge treatment systems for recovery of waste and salt from textile effluents. *J Clean Prod* **16**: 1081–1089.
- Xu F. 1996. Oxidation of phenols, anilines, and benzenethiols by fungal laccases: correlation between activity and redox potentials as well as halide inhibition. *Biochemistry* **35**(23): 7608–14.
- Xu F. 1997. Effects of redox potential and hydroxide inhibition on the pH activity profile of fungal laccases. *J Biol Chem* **272**(2): 924–928.

Chapter 8

Conclusions

1. The decolourization of Reactive blue 19 by laccase immobilized on CPC-silica beads was mainly enzymatic although dye adsorption occurred. Dye adsorption was reduced by treating CPC- silica-laccase beads with ethanolamine which blocks the unreacted aldehyde groups after laccase immobilization
2. Immobilizing laccase on silica beads change its pH activity profile for oxidizing ABTS oxidation but did not affect that for decolourizing Reactive blue 19. Furthermore, the dye specificity of the enzyme was not affected by immobilization since it was similar for immobilized and free laccase. Azo dyes were the least efficiently decolourized most likely because of their high redox potentials.
3. The toxicity of the parent dyes and their degradation product(s) varied with the dye. After a laccase treatment, Indigoid and azo dye were detoxified whereas the decolourization of the anthraquinone dyes led to an increased toxicity.
4. Merspol inhibited the decolourization of Reactive blue 19 by *T.versicolor* laccase by substrate depletion. A Michaelis-Menten like model in which Merspol binds the dye

was derived. The proposed kinetic mechanism of inhibition is supported by statistically similar Mersol-dye dissociation constants estimated by steady-state kinetics and by saturation equilibrium binding.

5. Increasing pH inhibited the laccase ABTS oxidation while the optimum pH of Reactive blue 19 decolourization was 4. While sodium sulfate did not affect laccase, sodium chloride inhibited laccase ABTS oxidation and dye decolourization. When ABTS was the substrate, the inhibition was hyperbolic non-competitive and from the rate model, it was suggested that one chloride anion was bound to the enzyme. With Reactive blue 19, the parabolic mixed inhibition suggested that two chlorides bind to laccase for its complete inhibition. A proposed model in which the dye increases the affinity of the enzyme for chloride enough to favour the binding of a second anion was derived.
6. *T. versicolor* laccase was immobilized through its polysaccharide residues on PMMA and the enzyme load compared well with commercial protein supports. Immobilizing laccase through its sugar residues favoured higher specific immobilized enzyme activity than using glutaraldehyde cross-linking. The specific activity of laccase on PMMA was higher than that achieved on the CPC-silica beads and suggests that PMMA is suitable support for dye decolourization.

Chapter 9

Contributions

9.1 Decolourization of Reactive blue 19 by laccase immobilized on CPC-silica beads

In the analysis of the decolourization of Reactive blue 19 by immobilized laccase, dye removal was mainly enzymatic. It was possible to reduce dye adsorption by treating the beads with ethanolamine to block the aldehyde groups not occupied by laccase. With other dyes, it was also discovered that significant dye adsorption occurred when the enzyme was inefficient at decolorizing the dyes. These findings contributed to understanding some of the possible reasons why dye adsorption occurred during decolourization by an immobilized enzyme.

9.2 Immobilization of laccase on PMMA

Laccase was successfully immobilized on PMMA. This investigation was the first to report the immobilization of laccase on a relatively inexpensive material. Moreover, this is a

convenient method that can be used without an elaborate experimental setup or the use of more expensive commercial protein supports.

9.3 Effect of Mergol on the decolourization of Reactive blue 19 by laccase

Since Mergol is a surfactant used as a wetting agent and detergent in the dyeing process, it was relevant to analyze its impact on dye decolourization by laccase. Mergol, a non-ionic surfactant, inhibited the decolourization of Reactive blue 19 by substrate depletion; by spectroscopic analysis, it was demonstrated that the dye interacted with the surfactant and the binding quantified. A rate model was developed to describe the kinetic mechanism. The main contribution of this investigation is that it is the first to report on Mergol inhibition of laccase decolourization of Reactive blue 19 and to elucidate the kinetic mechanism of inhibition. Moreover, the kinetic model was supported by a qualitative (spectroscopy) and quantitative (equilibrium binding) analyses of the interaction between Reactive blue 19 and Mergol. The model developed can be used to estimate the size of a laccase reactor for the treatment of textile wastewaters.

9.4 Effect of Sodium chloride and ionic strength on the decolourization of Reactive blue 19 by laccase

It was shown that laccase was not affected by ionic strength and that chloride inhibited its decolourization of Reactive blue 19. As previously shown, when ABTS was the substrate, the inhibition was hyperbolic non-competitive whereas when Reactive blue 19 was the substrate, the inhibition was parabolic mixed. The main contribution of this section is

that this is the first investigation to demonstrate that the mechanism of chloride inhibition depended on the substrate and an appropriate kinetic model was proposed. The kinetics models developed can be used to estimate the size of a laccase reactor for the treatment of textile wastewaters.

Chapter 10

Recommendations

10.1 To investigate the influence of the nature of the enzyme support on enzymatic dye decolourization

Since the specific activities of immobilized laccase on silica and PMMA beads differed and the enzyme pH profile was modified, it is clear that the support materials analyzed in this research influenced the activity of immobilized laccase. More materials should be evaluated to understand their effect on laccase activity. The importance of material hydrophilicity for laccase immobilization should be investigated to determine if the activity retention can be improved without the use of commercial supports. The activity of laccase immobilized on support with increasing hydrophilicity should be analyzed. (e.g. poly(ethylene-co-butyl metha acrylate), PMMA, polyhydroxyethyl methacrylate).

10.2 Immobilization of laccase on porous PMMA beads

Laccase was successfully immobilized on PMMA beads and the retained laccase activity was higher than on silica beads. To increase the mass of enzyme immobilized, laccase should be immobilized on porous PMMA beads and the preparation tested for dye decolourization.

10.3 Characterize laccase kinetic in real textile wastewaters

The effects of individual auxiliary chemicals on dye decolourization were analyzed in a synthetic buffer to understand their impact on the decolourization mechanism. However, the combined effect(s) of these components in a textile wastewater may be different. It is recommended that the kinetic behaviour of the enzyme in an actual wastewater be characterized to understand how all the components together impact enzymatic decolourization. Comparing laccase kinetics in buffer and in wastewater may help to identify other inhibitors and knowledge of its behaviour over time will allow us to develop better strategies to maintain long term enzyme stability. Furthermore, the assessment of the enzyme's stability in wastewater must be conducted before the steady-state kinetic studies in a wastewater samples. Once a kinetic rate and enzyme deactivation model are obtained, an enzyme reactor can be sized and tested for the decolourization of an industrial textile wastewater.

10.4 Study the impacts of factors like salts and pH on the interaction of Mersol and Reactive blue 19

The nature of the interaction(s) between the anthraquinone dye, Reactive blue 19, and Mersol should be investigated since the presence of a surfactant like Mersol can negatively affect decolourization. Knowledge of the effects of pH, temperature and common textile salts on the binding of Reactive blue 19 to Mersol may allow us to develop strategies to minimize these influences. Furthermore, it should be determined whether other classes of textile dyes will bind to Mersol in a similar manner.

Appendix A

Statistical analysis of the difference between the dissociation constants estimated from binding and kinetic assays

The t-test is conducted to determine whether the difference between the equilibrium dissociation constants for the Merpol-Reactive blue 19 interaction. The hypothesis (H_1) is that the K_d estimated by saturated equilibrium binding is statistically different than estimated from the steady-state kinetic analysis. The null hypothesis (H_0) is

H_0 : The values are distinct

H_1 : The values are not distinct

H_0 is rejected if $t_{calculated} < t_{table}$

$$K_{d,1}(x_1) = 44.1, \frac{s_1}{\sqrt{n_1}} = 10.1, n_1 = 81$$

$$K_{d,2}(x_2) = 38.3, \frac{s_2}{\sqrt{n_2}} = 3.4, n_2 = 672$$

$$t = \frac{x_1 - x_2}{\sqrt{\frac{s_1^2}{n_1} + \frac{s_2^2}{n_2}}} = \frac{44.1 - 38.3}{\sqrt{10.1^2 + 3.4^2}} = 0.544$$

$$\text{degree of freedom (d.o.f.)} = \frac{\left(\frac{s_1^2}{n_1} + \frac{s_2^2}{n_2}\right)^2}{\frac{\left(\frac{s_1^2}{n_1}\right)^2}{n_1 - 1} + \frac{\left(\frac{s_2^2}{n_2}\right)^2}{n_2 - 1}} = \frac{10.1^2 + 3.4^2}{\frac{10.1^4}{81 - 1} + \frac{3.4^4}{672 - 1}} = 99$$

The p-value for $t_{\text{calculated}} = 0.544$ is 0.294 for a 1 sided-test. The value of $t_{\text{tabulated}}$ with a p-value of 0.294, a significance level $\alpha=0.05$, and a degree of freedom of 99 is 1.055. Since $t_{\text{calculated}} < t_{\text{tabulated}}$, the null hypothesis is rejected. The K_d values are not statistically different.

Appendix B

Derivation of the rate equation for the hyperbolic mixed inhibition

B.1 Rate equation for the general mixed inhibition

Consider the following hyperbolic mixed inhibition scenario (Figure B.1) where the enzyme-inhibitor, EI, is allowed to bind the substrate and to generate a product. The bound inhibitor can affect the enzymes affinity for the substrate by factor α . The parameter β is the fractional effectiveness for the complex ESI to generate the product. The rapid equilibrium rate equation for the mixed-type inhibition is derived as follow:

1. Mass balance for the enzyme species

$$[E]_t = [E] + [ES] + [EI] + [ESI] \quad (\text{B.1})$$

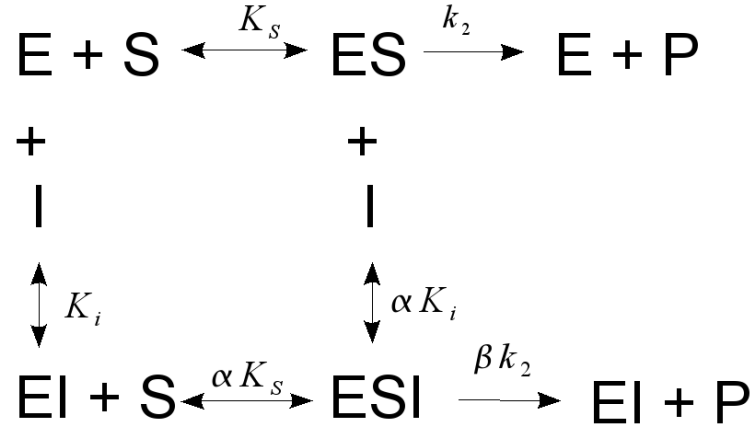


Figure B.1: General partial mixed inhibition (hyperbolic)

2. Rate equation which is a function of the enzyme-substrate complex

$$v = k_2[ES] + \beta k_2[ESI] \quad (\text{B.2})$$

3. Divide the rate equation (B.2) by the mass balance (equation B.1)

$$\frac{v}{[E]_t} = \frac{k_2[ES] + \beta k_2[ESI]}{[E] + [ES] + [EI] + [ESI]} \quad (\text{B.3})$$

4. Express the concentration of each enzyme species in terms of free E and free S at equilibrium

$$\frac{v}{[E]_t} = \frac{k_2 \frac{[E][S]}{K_S} + \beta k_2 \frac{[E][S][I]}{\alpha K_S K_i}}{[E] + \frac{[E][S]}{K_S} + \frac{[E][I]}{K_i} + \frac{[E][S][I]}{\alpha K_S K_i}} \quad (\text{B.4})$$

5. Cancel [E] and rearrange

$$\frac{v}{[E]_t} = \frac{k_2 \frac{[S]}{K_S} + \beta k_2 \frac{[S][I]}{\alpha K_S K_i}}{1 + \frac{[S]}{K_S} + \frac{[I]}{K_i} + \frac{[S][I]}{\alpha K_S K_i}} \quad (\text{B.5})$$

$$\frac{v}{[E]_t} = \frac{k_2[S] + \beta k_2 \frac{[S][I]}{\alpha K_i}}{K_S + [S] + \frac{K_S[I]}{K_i} + \frac{[S][I]}{\alpha K_i}} \quad (\text{B.6})$$

$$v = \frac{k_2[E]_t[S] \left(1 + \frac{\beta[I]}{\alpha K_i}\right)}{K_S \left(1 + \frac{[I]}{K_i}\right) + [S] \left(1 + \frac{[I]}{\alpha K_i}\right)} \quad (\text{B.7})$$

B.2 Derivation of the rate equation for the parabolic mixed inhibition

Parabolic inhibition occurs when more than one inhibitor binding site exist and is usually complete, i.e. no product can be generate by the enzyme when all inhibitor sites are occupied by the inhibitor. Consider the following parabolic inhibition kinetic scheme

where the inhibitor (I) can bind two independent sites with the same affinity, i.e., the inhibition constant, K_i , is identical for both inhibitor binding sites. The α factor indicates that binding of the inhibitor affects the binding of the substrate S. The enzyme-substrate with one inhibitor molecule can generate the product by a fraction β of k_2 but it cannot when two inhibitor molecules are bound. The rate equation for this kinetic scheme is derived as follow

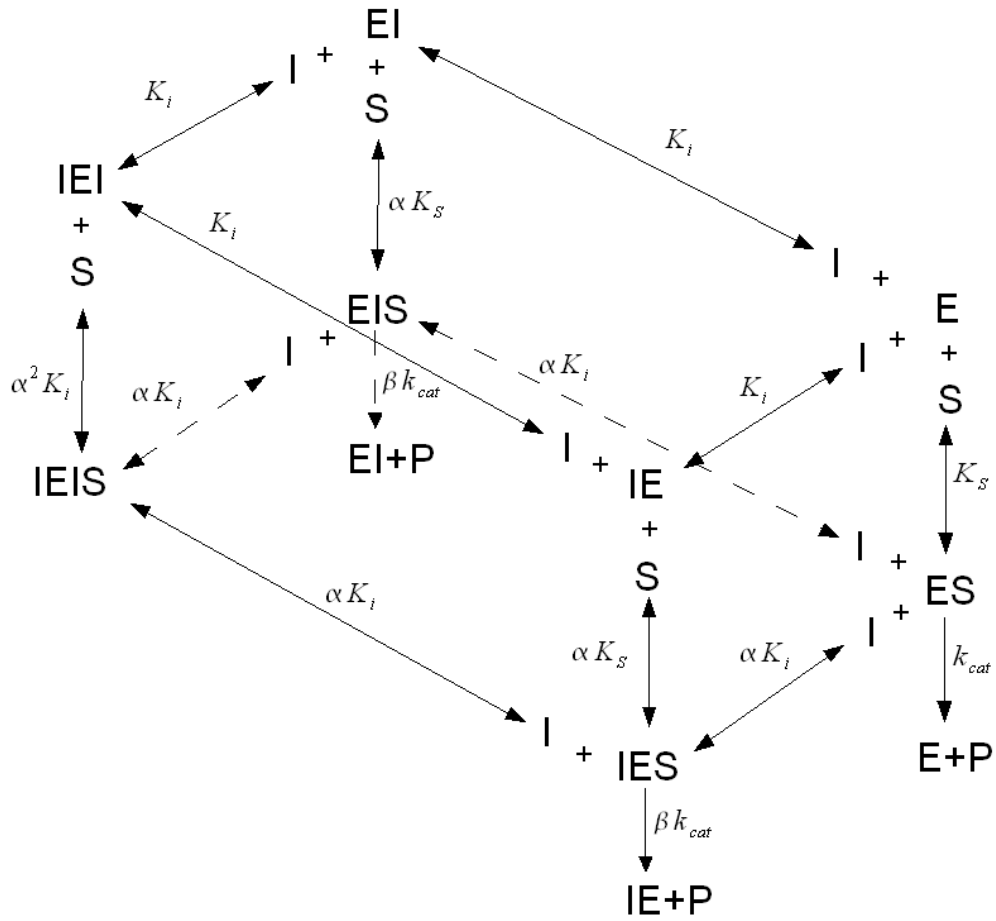


Figure B.2: Parabolic two-site mixed inhibition

1. Write the velocity equation divided by the enzyme conservation equation

$$\frac{v}{[E]_t} = \frac{k_2[ES] + 2\beta k_2[ESI]}{[E] + [ES] + [EI] + [IE] + [ESI] + [IES] + [IEI] + [IEIS]} \quad (\text{B.8})$$

2. Express each enzyme complex species by its equilibrium dissociation relationship

$$\frac{v}{[E]_t} = \frac{k_2 \left(\frac{[E][S]}{K_S} + 2\beta \frac{[E][S][I]}{\alpha K_S K_i} \right)}{[E] + \frac{[E][S]}{K_S} + \frac{[E][I]}{K_i} + \frac{[I][E]}{K_i} + \frac{[E][S][I]}{\alpha K_S K_i} + \frac{[E][S][I]}{\alpha K_S K_i} + \frac{[E][I]^2}{K_i^2} + \frac{[E][S][I]^2}{\alpha^2 K_S K_i^2}} \quad (\text{B.9})$$

3. Eliminate [E]

$$\frac{v}{[E]_t} = \frac{k_2 \left(\frac{[S]}{K_S} + 2\beta \frac{[S][I]}{\alpha K_S K_i} \right)}{1 + \frac{[S]}{K_S} + \frac{2[I]}{K_i} + \frac{2[S][I]}{\alpha K_S K_i} + \frac{[I]^2}{K_i^2} + \frac{[S][I]^2}{\alpha^2 K_S K_i^2}} \quad (\text{B.10})$$

4. Multiply the numerator and denominator by K_S and rearranging

$$\frac{v}{[E]_t} = \frac{k_2[S] \left(1 + \frac{2\beta[I]}{\alpha K_i} \right)}{K_S + [S] + \frac{2[I]K_S}{K_i} + \frac{2[S][I]}{\alpha K_i} + \frac{K_S[I]^2}{K_i^2} + \frac{[S][I]^2}{\alpha^2 K_i^2}} \quad (\text{B.11})$$

$$v = \frac{k_2[E]_t[S] \left(1 + \frac{2\beta[I]}{\alpha K_i} \right)}{K_S \left(1 + \frac{2[I]}{K_i} + \frac{[I]^2}{K_i^2} \right) + [S] \left(1 + \frac{2[I]}{\alpha K_i} + \frac{[I]^2}{\alpha^2 K_i^2} \right)} \quad (\text{B.12})$$

Appendix C

Calculation of reaction rates

C.1 Initial rates

In chapter six and seven, the initial rate was determined by calculating the slope of the tangent at the onset of the reaction or progress curve so that the points considered did not exceed 10 % conversion as shown in Figure C.1).

C.2 Calculation of average reaction rates and of rate constants from the immobilized laccase reactor

For dye decolourizations conducted with the CPC-silica-laccase packed bed, the reactor inlet and outlet concentration were monitored and recorded (Figure C.2 and C.3). The rate of decolourization in the packed bed was calculated as follow:

The rate of decolourization in the reactor was calculated as follow

- $C_{inlet} = 17.59 \text{ mg/l}$
- $C_{outlet} = 7.36 \text{ mg/l}$

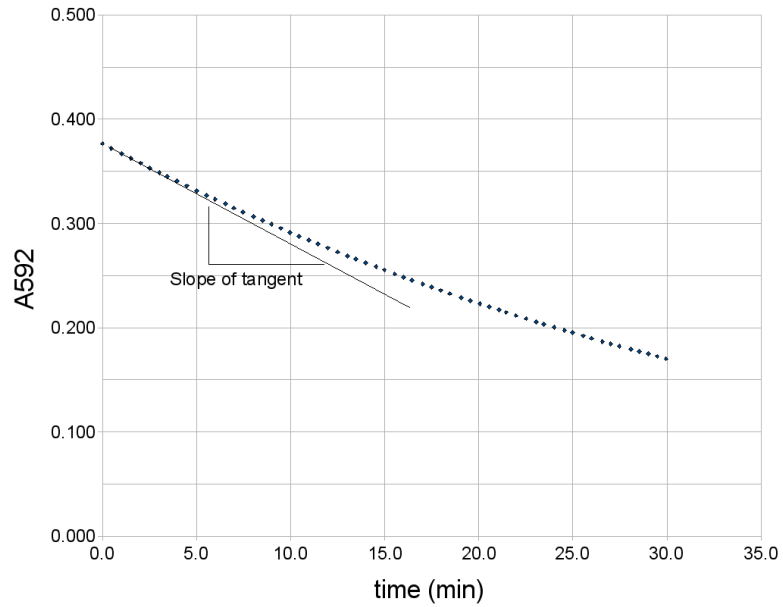


Figure C.1: Example time course curve return by the software SOFTmax PRO (Molecular Devices, Sunnyvale CA,USA)

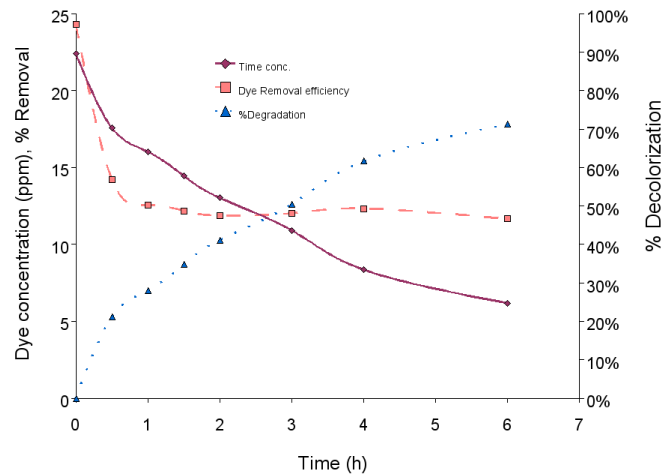


Figure C.2: Concentration profile of Reactive blue 19 decolorization by immobilized laccase.

Time (h)	RBBR reactor inlet (ppm)	RBBR reactor outlet (ppm)	Removal efficiency (%)	%Degradation
0	22.39	0.25	98.88%	0.00%
0.5	17.59	7.36	58.15%	21.10%
1	16.03	7.80	51.36%	27.95%
1.5	14.47	7.24	49.99%	34.79%
2	13.04	6.68	48.80%	41.10%
3	10.92	5.49	49.70%	50.41%
4	8.36	4.06	51.48%	61.64%
6	6.18	3.12	49.48%	71.23%

Figure C.3: Table of measured concentrations, calculated 1-reactor volume removal efficiency in (%) with time

- $V_{reactor,void} = 1.6 \text{ ml}$
- flowrate = $4.15 \frac{\text{ml}}{\text{min}}$
- hydraulic retention time (HRT) = 0.385 min

$$\text{rate} = \frac{C_{inlet} - C_{outlet}}{HRT} = \frac{(17.59 - 7.36) \frac{\text{mg}}{\text{l}}}{0.385 \text{ min}} \text{ mg/l} = 26.6 \frac{\text{mg}}{\text{lmin}}$$

The removal efficiency of the reactor is equal to

$$\% \text{removal} = \frac{C_{inlet} - C_{outlet}}{C_{inlet}} \times 100 = \frac{17.6 - 7.36}{17.6} \times 100 = 58.2\%$$

The rate constant (k) was calculated as follow:

$$k = \frac{\text{decolourizationrate}}{C_{inlet}} = \frac{26.6 \frac{\text{mg}}{\text{lmin}}}{17.6 \text{ mg/l}} = 1.51 \text{ min}^{-1}.$$